Modeling Aviation's Global Emissions, Uncertainty Analysis, and Applications to Policy

by

JOOSUNG JOSEPH LEE

B.S. Mechanical Engineering
University of Illinois at Urbana-Champaign, 1998

S.M. Aeronautics and Astronautics
S.M. Technology and Policy Program
Massachusetts Institute of Technology, 2000

Submitted to the Department of Aeronautics and Astronautics
in Partial Fulfillment of the Requirements for the Degree of

DOCTOR OF PHILOSOPHY

at the

MASSACHUSETTS INSTITUTE OF TECHNOLOGY

February 2005

© 2005 Joosung Lee All rights reserved

The author hereby grants to MIT permission to reproduce and to distribute publicly paper and electronic copies of
this thesis document in whole or in part.

Signature of Author...
Department of Aeronautics and Astronautics
December 17, 2004

Certified by...
Ian A. Waitz
Professor and Deputy Head of Department of Aeronautics and Astronautics
Thesis Supervisor

Certified by...
John-Paul B. Clarke
Associate Professor of Aeronautics and Astronautics

Certified by...
David H. Marks
Morton and Claire Goulder Family Professor of Civil and Environmental Engineering and
Engineering Systems

Certified by...
Gregg G. Fleming
Volpe National Transportation Systems Center

Accepted by...
Jaime Peraire
Professor of Aeronautics and Astronautics
Chair, Committee on Graduate Students
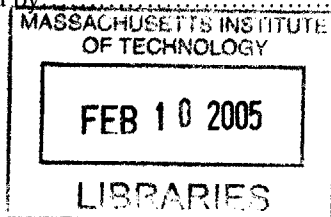
Modeling Aviation's Global Emissions, Uncertainty Analysis, and Applications to Policy

by

Joosung Joseph Lee

Submitted to the Department of Aeronautics and Astronautics
in Partial Fulfillment of the Requirements for the Degree of
Doctor of Philosophy
at the Massachusetts Institute of Technology

December 17, 2004

ABSTRACT

Air travel continues to experience fast growth. Although the energy intensity of the air transport system continues to improve, aviation fuel use and emissions of many pollutants have risen.

This thesis focuses on developing, assessing and applying a system model to evaluate global aircraft fuel consumption and emissions, and to examine technological and operational measures to mitigate these emissions. The model is capable of computing how much emissions are produced on a flight-by-flight, fleet and global basis and where in the atmosphere the emissions are deposited. These are important questions for aviation environmental policy-making.

Model development was followed by a comprehensive uncertainty analysis. It involved comparisons of reported versus modeled results at both the modular and system levels. On average, the aggregate-level composite fuel burn results showed about -6% difference from reported fuel burn data. A statistical analysis showed that this mean shift was a combined contribution of the key uncertainties in aircraft performance and operations.

A parametric study followed to rank-order the effects that the key modeling uncertainties had on estimates of fuel burn and emissions. Statistical methods were developed to analyze both the random and systematic errors of the modeling tools.
The analyses showed that the uncertainties in engine and aerodynamic performance had the largest impact on system errors, accounting for around 60-70% of the total variance in full-mission fuel burn results. The uncertainties in winds aloft and take-off weight explained another 20-25%. LTO procedures, which consist of engine throttle setting, rate of climb/descent and flight speed, were the most influential uncertainties that drove the variance in fuel burn results below 3000 ft. For emissions, the emissions indices were the most influential uncertainties for the variance in model outputs.

By employing the model, this thesis examined three policy options for mitigating aviation emissions. More stringent engine certification standards, continuous descent approach procedures, and derated take-off procedures were analyzed. Uncertainties of the model were carefully accounted for in the fuel burn and emissions scenarios of the policy options. The considered policy options achieved roughly 10-30% reductions in NOx emissions. However, HC and CO emissions rather increased due to higher emissions production rate for the CDA and derated take-off. In addition, the NOx emissions reductions in some cases were not statistically significant given the uncertainty in the modeling tool.

Thesis Supervisor: Ian A. Waitz
Professor and Deputy Head
Department of the Aeronautics and Astronautics

ACKNOWLEDGEMENTS

I thank Professor Earll Murman for being my General Examiner, Professor Karen Willcox for being my Thesis Reader and having given several advices at research meetings, and Professor Daniel Hastings for being my Minor Advisor.

I am obliged for the love of my church friends and MIT-Korea Program committee members. We had so much fun together and they often expressed their care for me by asking how I was doing on my thesis. At the same time, so many elderly people, friends and relatives prayed for me from Georgia, Illinois and Korea.

My father, mother, brother, sister-in-law, my nephew Abraham, brother-in-law, sister, my nephew Timothy and niece Elizabeth are all my beloved supporters. I thank them and miss them. I also cannot forget to thank my father-in-law, mother-in-law and brother-in-law to be. I feel very lucky that my family size has tripled since I first came to MIT.

I thank God for His never-changing grace. May all glory be to Him.

I dedicate this thesis to Kyungmi, my fiancée, the October Bride. Throughout the years, she has been with me and given me the courage to go on.

CONTENTS

7

A-3 SAGE Inventory of Commercial Jet & Turboprop Global Activity for Calendar Year 2002

LIST OF FIGURES

LIST OF TABLES

NOMENCLATURE

Roman

Adjusted R^2	R^2 adjusted by the degrees of freedom of both the numerator and the denominator
C_{D0}	parasitic drag coefficient
C_{D2}	induced drag coefficient
C_{f1}	1st fuel flow coefficient in BADA
C_{f2}	2nd fuel flow coefficient in BADA
C_{f3}	1st descent fuel flow coefficient in BADA
C_{f4}	2nd descent fuel flow coefficient in BADA
C_L	lift coefficient
C_{TDES_AP}	approach thrust coefficient in BADA
C_{TDES_LD}	landing thrust coefficient in BADA
C_{TDES_LOW}	low altitude descent thrust coefficient in BADA
D	aerodynamic drag force
dBA	A-weighted decibel
E_I	energy intensity
EI	emissions index
EICO	Emissions Index for CO
EIHC	Emissions Index for HC
EINOx	Emissions Index for NOx
E_{TO}	SAGE AIR 1845 corrected net thrust at zero speed
F	engine thrust
F	F-statistic (for the regression result to be significant)
F_{max}	maximum thrust
ft	feet
F_{TO}	SAGE AIR 1845 speed adjustment coefficient
g	gravitational acceleration constant
G_{A_TO}	SAGE AIR 1845 altitude adjustment coefficient
G_{B_TO}	SAGE AIR 1845 altitude-squared adjustment coefficient

h	altitude
H	humidity factor
H_{TO}	SAGE AIR 1845 temperature adjustment coefficient
L/D	lift-to-drag ratio
m	aircraft mass
n	number of subjects of number of iterations
NM	nautical miles
p	p-value (probability for the regression result to be false)
R^2	the coefficient of determination
REICO	Referred Emissions Index for CO
REIHC	Referred Emissions Index for HC
REINOx	Referred Emissions Index for NOx
S	wing area
Std. Err.	standard deviation of the estimated coefficient or relationship
T	ambient temperature
V	flight speed
V_2	take-off speed at the end of run way
V_{CAS}	calibrated airspeed
V_{zf}	zero flap minimum safe maneuvering speed
W_{ff}	corrected fuel flow rate
x	subject variable
Δh	change in flight altitude
Δt	change in time

Greek

B (Beta)	standardized regression coefficient
δ	pressure ratio (ambient to sea-level)
ε	error
Θ	temperature ratio (ambient to sea-level)
ρ	air density
σ	standard deviation

GLOSSARY

AERO	Aviation Emissions and Evaluation of Reduction Options
ANCAT	Abatement of Nuisances Caused by Air Transport
ASM	Available Seat Miles
ASQP	Airline Service Quality Performance
BADA	Base of Aircraft Data
BM2	Boeing Method 2
CAEP	Committee on Aviation Environmental Protection
CDA	Continuous Descent Approach
CFDR	Computer Flight Data Recorder
DLR	Deutsches Zentrum für Luft- und Raumfahrt
EC	European Commission
EDMS	Emissions and Dispersion Modeling System
EPA	Environmental Protection Agency
ETMS	Enhanced Traffic Management System
FAA	Federal Aviation Administration
FESG	Forecasting Economic Support Group
GC	Great Circle
ICAO	International Civil Aviation Organization
IPCC	Intergovernmental Panel on Climate Change
ISA	International Standard Atmosphere
LTO	Landing and Take-off
NASA	National Aeronautics and Space Administration
OAG	Official Airline Guide
RPK	Revenue Passenger Kilometers
RPM	Revenue Passenger Miles
SAE AIR	Society of Automotive Engineers Aerospace Information Report
SAGE	System for Assessing Aviation's Global Emissions
SFC	Specific Fuel Consumption
TL	Technology Level

TOGW   Take-off Gross Weight

CHAPTER 1

INTRODUCTION

Air travel continues to experience a fast, 4-5% growth each year. Although the energy intensity[1] of the air transport system continues to decline, aviation fuel use and emissions of many pollutants have risen. This trend, which represents a conflict between industry growth and environmental impact, has motivated the aircraft manufacturing and airline industries, the scientific community, and governmental bodies to evaluate a variety of methods for emissions mitigation.

This thesis focuses on developing, assessing and applying a system model to evaluate global aircraft fuel consumption and emissions. It examines technological and operational measures that mitigate aviation emissions to support policy decision-making. Uncertainties of the model are analyzed in detail and carefully accounted for in the policy scenarios considered. This chapter provides an overview on the topic of aviation and the atmospheric environment. A discussion of uncertainties and use of the model in a policy scenario analysis will follow.

1.1 AVIATION ENERGY USE

Since passenger aircraft were introduced for large-scale commercial services in the 1950s, there has been fast growth in aviation as a form of mobility and consequently significant growth in energy use. In 2002, aviation accounted for 3 trillion revenue passenger-kilometers (RPKs), approximately 10% of world RPK's traveled on all transportation modes, and 40% of the value of world freight shipments [ICAO, 2002]. Demand for air travel has grown fastest among all modes of transport. Note that subsequent to the events of September 11, 2001, total RPKs fell by 8% and fuel burn by 16%, comparing 2-year averages before and after. In addition, the percentage of the commercial fleet parked increased from 6% to 13% [Waitz et al., 2004]. However,

---

[1] A measure of aircraft fuel economy on a passenger-kilometer basis. It is denoted by energy used per unit of mobility provided (e.g. fuel consumption per passenger-kilometer).

future projections estimate a resumption of the long-term growth trend within the next several years. Worldwide growth is anticipated to continue at around 4-5% per year [FAA, 2004; Boeing, 2004].

Aviation fuel consumption today corresponds to 2% to 3% of the total fossil fuel use worldwide, more than 80% of which is used by civil aviation operations [Schafer and Victor, 1999]. Energy use in the production of aircraft is relatively minor in comparison to that consumed in their operation. While the majority of air transportation demand is supplied by large commercial aircraft, defined as those aircraft with a seating capacity of 100 or more, smaller regional aircraft have emerged as an important component of both demand and energy use within air transportation. For example, in the United States, although regional aircraft currently perform under 4% of domestic RPK's, they account for almost 7% of jet fuel use and for 40% to 50% of total departures. Future growth in demand for regional aircraft RPK's could be up to double the rate for large commercial aircraft [Babikian et al., 2002; Lee et al., 2004]. Cargo operations account for some 10% of total revenue ton-kilometers and fuel use within the aviation sector. Economic activity, as measured by world GDP, is the primary driver for air cargo industry growth. World air cargo traffic is expected to grow at an average annual rate of over 6% for the next decade [Boeing, 2004].

1.2 AVIATION'S IMPACT ON GLOBAL ATMOSPHERE AND LOCAL AIR QUALITY

The growth in air transportation volume has important environmental impacts associated with climate change and stratospheric ozone reduction on a global scale. On local to regional scales, noise, decreased air quality related primarily to ozone production and particulate levels, and other issues, such as roadway congestion related to airport services and local water quality, are all recognized as important impacts. This section focuses on emissions-related impacts and provides some additional detail on the aviation role in climate change, which, along with regional/local air quality, is the primary motivation for the work of this thesis.

Because the majority of aircraft emissions are injected into the upper troposphere and lower stratosphere (typically 9-13 km in altitude), resulting impacts on the global environment are unique among all industrial activities. The fraction of aircraft emissions that is relevant to atmospheric processes extends beyond the radiative forcing[2] effects of CO_2. The mixture of exhaust species discharged from aircraft perturbs radiative forcing 2 to 3 times more than if the exhaust was CO_2 alone. In contrast, the overall radiative forcing from the sum of all anthropogenic activities is estimated to be a factor of 1.5 times CO_2 alone. Thus the impact of burning fossil fuels at altitude is approximately double that due to burning the same fuels at ground level. The enhanced forcing from aircraft compared with ground-based sources is due to different physical (e.g. contrails[3]) and chemical (e.g. ozone formation/destruction) effects resulting from altered concentrations of participating chemical species and changed atmospheric conditions. However, many of the chemical and physical processes associated with climate impacts are the same as those that determine air quality in the lower troposphere [Penner *et al.*, 1999].

Estimates of the radiative forcing by various aircraft emissions for 1992 offered by the Intergovernmental Panel on Climate Change (IPCC) and projections for the year 2050 (see Penner *et al.* 1999) are shown in Figure 1.1. Note that the bar for CO_2 represents instantaneous radiative forcing from the cumulative effects of all historical CO_2 emissions from aviation, while those for contrails and cirrus represent the instantaneous radiative forcing without any atmospheric accumulation. Further, different gases have a range of different lifetimes in the atmosphere. For example, the CO_2 has an effect long into the future, while the contrails do not [Penner *et al.*, 1999]. The estimates translate to 3.5% of the total anthropogenic forcing that occurred in 1992 and to an estimated 5% by 2050 for an all-subsonic fleet. Associated increases in ozone levels are expected to decrease the amount of ultraviolet radiation at the surface of the earth. Future fleet composition also impacts the radiative forcing estimate. A supersonic aircraft flying at

---

[2] A measure of the change in Earth's radiative balance associated with atmospheric changes. Positive forcing indicates a net warming tendency relative to pre-industrial times.
[3] The moist, high temperature air in the jet exhaust condenses into particles in the atmosphere when it mixes with the ambient cold air and saturation occurs. The result is a condensation trail, or contrail.

17-20 km would have a radiative forcing 5 times greater than a subsonic equivalent in the 9-13 km range. It is important to note that these estimates are of an uncertain nature [Penner *et al.*, 1999].
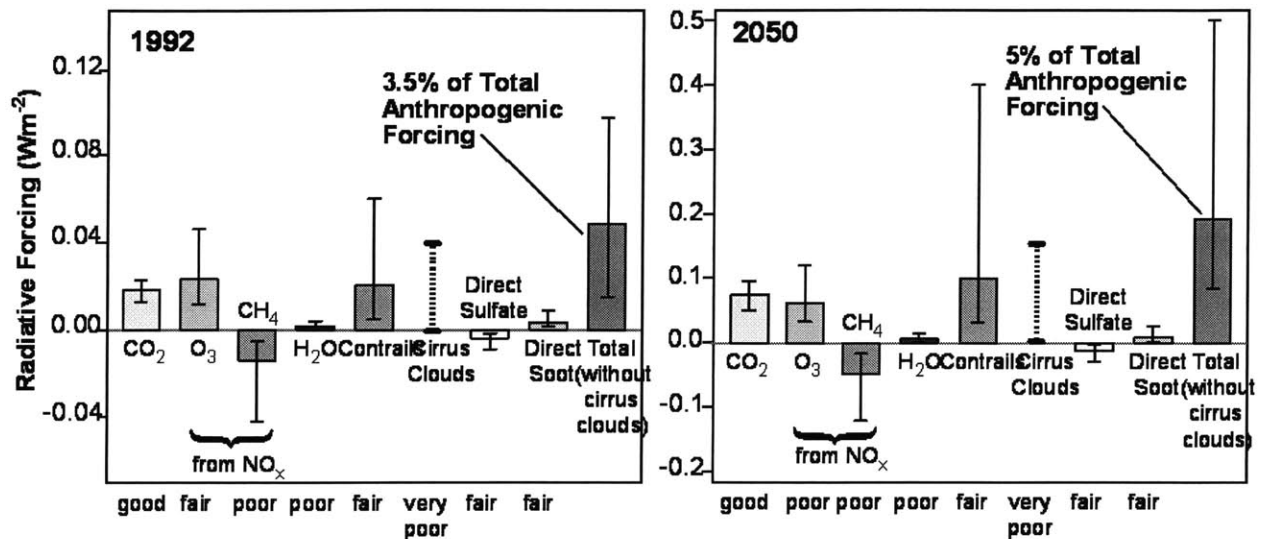
Figure 1.1 Radiative forcing estimated for 1992 (0.05 W/m^2 total) and projected to 2050 (0.19 W/m^2 total) [Penner *et al.*, 1999]. Note differences in scale. Note also that the heavier dashed bar for aviation-induced cirrus cloudiness describes the range of estimates, not the uncertainty. The level of scientific understanding of this potential impact is very poor and no estimate of uncertainty was made. Cirrus clouds are not included in the total radiative forcing estimate.

While broadly consistent with these IPCC projections, subsequent research reviewed by the Royal Commission on Environmental Protection (RCEP) in U.K. has suggested that the IPCC reference value for the climate impact of aviation is likely to be an underestimate. In particular, while the impact of contrails is probably overestimated in Figure 1.1, aviation-induced cirrus clouds could be a significant contributor to positive radiative forcing, NOx-related methane reduction is less than shown in Figure 1.1, reducing the associated cooling effect, and growth of aviation in the period 1992-2000 has continued at a rate larger than that used in the IPCC reference scenario [RECP, 2002].

In addition to how much emissions are produced, where the emissions are deposited is equally important. Figure 1.2 shows the radiative imbalance as a function of latitude. The middle latitudes of the Northern Hemisphere experience a severe radiative imbalance, which could have global climate importance. The region with the stronger radiative forcing would be expected to suffer larger local climate change [Rogers et al., 2002]. Therefore, it is important to understand the geographical distribution of aviation traffic and subsequent emissions. This is one motivation for the development of a tool like the System for Assessing Aviation's Global Emissions (SAGE) described in this thesis.
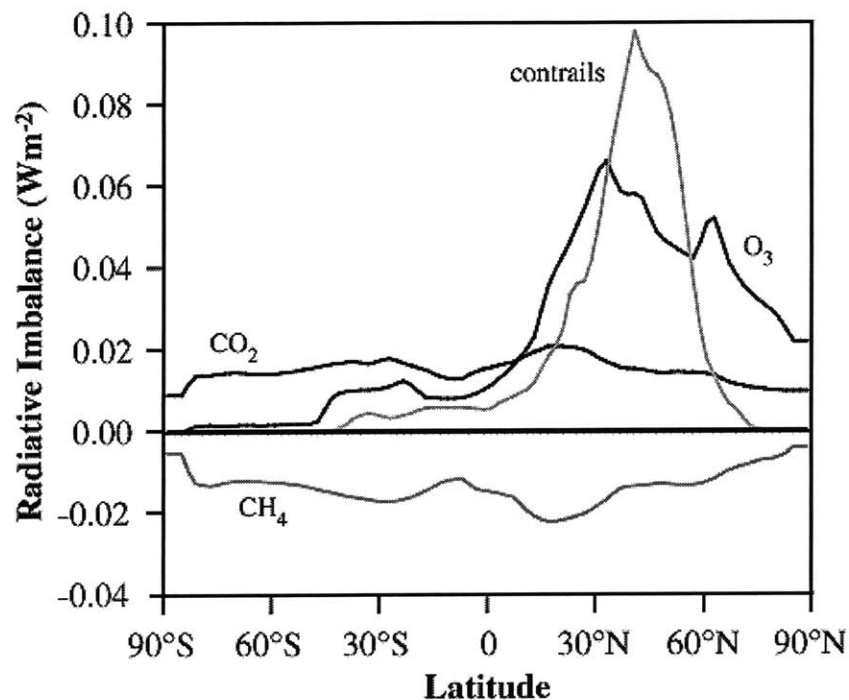
Figure 1.2 IPCC calculation of the aviation induced 1992 radiative imbalance at the tropopause in Watts per square meter as a function of latitude [Penner et al., 1999]

1.3 TRENDS IN ENERGY USE

Fuel efficiency gains due to technological and operational change can mitigate the influence of growth on total emissions. Increased demand has historically outpaced

these gains, resulting in an overall increase in emissions over the history of commercial aviation. The figure of merit relative to total energy use and emissions in aviation is the energy intensity (E_I). When discussing energy intensity, the most convenient unit of technology is the system represented by a complete aircraft. In this section, trends in energy use and E_I are elaborated. It also discusses the relation of E_I to the technological and operational characteristics of an aircraft.

Reviews of trends in technology and aircraft operations undertaken by Lee *et al.* [2001] and Babikian *et al.* [2002] indicate that continuation of historical precedents would result in a future decline in E_I for the large commercial aircraft fleet of 1.2% to 2.2% per year when averaged over the next 25 years and perhaps an increase in E_I for regional aircraft as regional jets use larger engines and replace turboprops in the regional fleet. When compared with trends in traffic growth, expected improvements in aircraft technologies and operational measures alone are not likely to offset more than one-third of total emissions growth. Therefore, effects on the global atmosphere are expected to increase in the future in the absence of additional measures. A variety of industry and government projections are in general agreement. Compared with the early 1990s, global aviation fuel consumption and subsequent CO_2 emissions are expected to increase three- to seven-fold by 2050, equivalent to a 1.8% to 3.2% annual rate of change [Penner el al., 1999]. In addition to the different demand growth projections entailed in such forecasts, variability in projected emissions also originates from different assumptions about aircraft technology, fleet mix, and operational evolution in air traffic management and scheduling.

Figures 1.3a and 1.3b show historical trends in E_I for the U.S. large commercial and regional fleets. Year-to-year variations in E_I for each aircraft type, due to different operating conditions, such as load factor[4], flight speed, altitude, and routing controlled by different operators, can be ±30%, as represented by the vertical extent of the data symbols [Lee *et al.*, 2001; Babikian *et al.*, 2002].

---

[4] Fraction of passengers per available seats
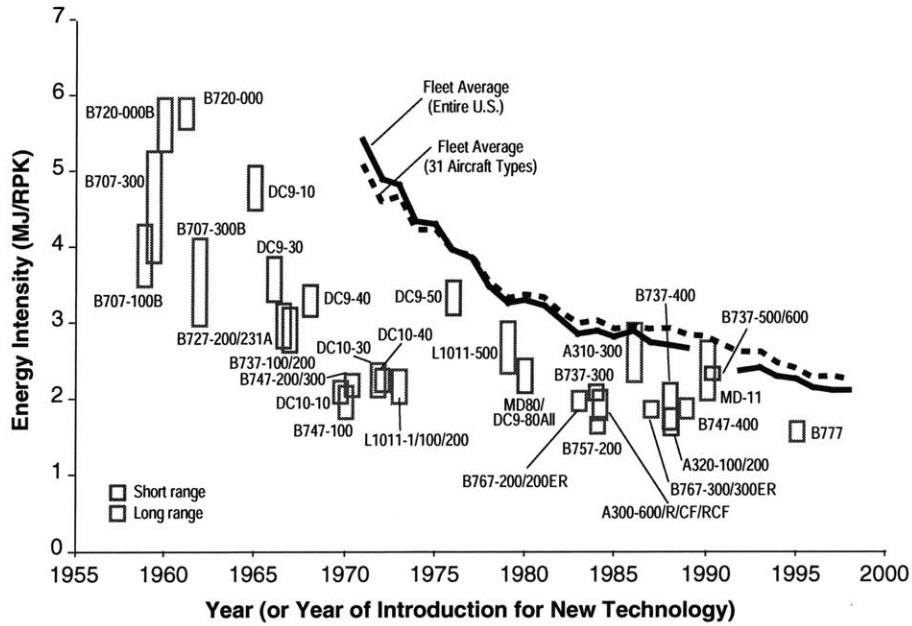
Figure 1.3a Historical trends in energy intensity of the US large commercial fleets. Individual aircraft EI based on 1991–1998 operational data with the exception of the B707 and B727, which are based on available operational data prior to 1991. Fleet averages were calculated using a RPK weighting [Lee *et al*., 2001].
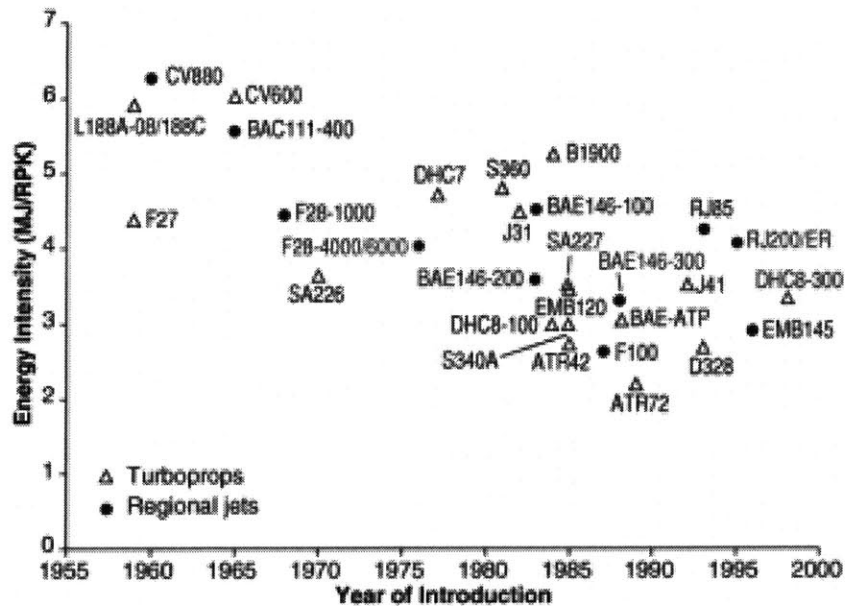
Figure 1.3b Historical trends in energy intensity of the US regional fleets [Babikian *et al*., 2002]

For large commercial aircraft, a combination of technological and operational improvements have led to a reduction in E_I of the entire US fleet of more than 60% between 1971 and 1998, averaging about 3.3% per year. In contrast, total RPK has grown by 330%, or 5.5% per year over the same period. Long-range aircraft are ~5% more fuel efficient than short-range aircraft because they carry more passengers over a flight spent primarily at the cruise condition [Lee, 2000]. Regional aircraft are 40% to 60% less fuel efficient than their larger narrow- and wide-body counterparts, while regional jets are 10% to 60% less fuel efficient than turboprops. Importantly, fuel efficiency differences between large and regional aircraft can be explained mostly by differences in aircraft operations, not technology [Babikian et al., 2002].

Reductions in E_I do not always directly imply lower environmental impact. For example, the prevalence of contrails is enhanced by greater engine efficiency that leads to lower exhaust gas temperature per unit of water emissions. NOx emissions also become increasingly difficult to limit as engine temperatures and pressures are increased—a common method for improving engine efficiency. These conflicting influences make it difficult to translate the expected changes in overall system performance into air quality impacts. Historical trends suggest that fleet-averaged NOx emissions per unit thrust during landing and take-off (LTO) cycles have seen little improvement and total NOx emissions have increased. However, HC and CO emissions have been reduced since the 1950's [Waitz et al., 2004]. Reductions in emissions are also hindered by the relatively long lifespan and large capital and operating costs of individual aircraft and the inherent lag in the adoption of new technologies throughout the aviation fleet as a result. Further, the impact of any efficiency improvements is diminished by fuel expended in airborne or ground travel delays or in flying partially empty aircraft.

1.4 PREVIOUS WORK ON AVIATION EMISSIONS INVENTORIES

Three-dimensional global inventories of civil aircraft fuel burned and emissions have been developed by NASA/Boeing for the years 1976, 1984, and 1992, and the European Abatement of Nuisances Caused by Air Transport (ANCAT)/European

Commission (EC) Working Group and the Deutsches Zentrum für Luft- und Raumfahrt (DLR) for 1991/92. For 1992, the three inventory results are in good agreement. Total fuel used by aviation was calculated to be 129.3 Tg (DLR), 131.2 Tg (ANCAT), and 139.4 Tg (NASA). Total calculated emissions of NOx (as NO_2) in 1992 ranged from 1.7 Tg (NASA) to 1.8 Tg (ANCAT and DLR) [Penner et al., 1999].

All of these models compile an aircraft movement database with aircraft/engine combinations. They then calculate fuel burned and emissions along great-circle paths between origin-destination cities. A similar approach is taken by Eurocontrol and the Dutch Aviation Emissions and Evaluation of Reduction Options (AERO) in developing a model to simulate technology and policy scenarios. Relative to these models, the distinguishing features of SAGE include the use of radar-recorded aircraft trajectory data. This not only enables more accurate aircraft movement and performance modeling but also provides a basis for accounting for canceled and unscheduled flights. In addition, flight-by-flight fuel burn data are available from a major US air carrier so that SAGE outputs are directly compared to the reported airline data. This allows for examining model fidelity in greater detail and provides a basis for assessing the parametric and model uncertainties in fuel burn and emissions estimates made by SAGE.

To assess the air quality impacts of proposed airport development projects, the Emissions and Dispersion Modeling System (EDMS) was developed in the mid-1980s under the auspices of the Federal Aviation Administration (FAA). EDMS is capable of assessing various airport emission sources, which consist of aircraft, auxiliary power units, ground support equipment, passenger access vehicles and stationary sources. It includes emissions and dispersion calculations, the aircraft engine emission factors from the International Civil Aviation Organization (ICAO) Engine Exhaust Emissions Data Bank [2000], vehicle emission factors from the Environmental Protection Agency's (EPA) MOBILE5a, and EPA-validated dispersion algorithms.

For cruise operations, a simple method for estimating NOx, CO, and HC emissions has been developed based on engine performance and emissions data obtained via full-scale engine tests at ground-level. It uses ICAO certification fuel flow versus emissions data taken at sea level as the basis for correcting emissions results for ambient and flight conditions. To report the emissions data, the emissions index (EI) in units of grams of species per kilogram of fuel burned (g species/kg fuel) is mostly used. The method proposed by Boeing, known as Boeing Method 2 (BM2), is currently used in SAGE Version 1.

1.5 USE OF MODELS AND SIMULATIONS TO SUPPORT POLICY DECISION-MAKING

While models are often employed to analyze policy options, the lack of understanding of the uncertainties in them is an increasing concern of policy makers [Cipra, 2000]. For instance, radically different estimates that arise from large uncertainties in different computer models are fueling much of the global climate change debate [Cipra, 2000; Jacoby and Prinn, 1994]. For local air quality regulations, computer models such as EDMS are frequently used. However, the uncertainties in these models have not been extensively quantified or considered for either global climate change or local air quality policies.[5]

For policy makers, it is important to know how uncertain outcomes change with different policy options and if the outcomes can be distinguished given the uncertainties of the computer models used. Policy makers need to know where models disagree and the modeling assumptions that cause the differences [Webster, 1996]. They also desire as small output variability as possible in order to ensure "robustness" of their policy design. Therefore, establishing and communicating model fidelity is an important task, which must parallel model development efforts. Identifying the uncertainty associated with model assumptions as modeling goes on is important because improving assumptions can improve model performance as well [Cipra, 2000; IPCC, 2001].

---

[5] Boeing has conducted a validation study for its 1992 aircraft emissions inventories [Daggett *et al.*, 1999].

It should be noted that non-model uncertainties can also be large. They include technological, economic, social, and political uncertainties that impact any environmental policy making [Jacoby and Prinn, 1994]. This thesis, however, focuses on treatment of model uncertainties that are most relevant to the models and scenarios considered in the subsequent chapters.

As a method to treat model uncertainties, uncertainty analysis allows one to obtain the mean, variance, and probability distributions of the model output, and also conduct variance analysis to quantify the contribution of an uncertain parameter to variance in the output. Uncertainty analysis can also capture the relative likelihood that different outcomes will occur [Morgan and Henrion, 1990]. There are two types of measurable uncertainty in physical sciences. One is parametric uncertainty, and the other is model uncertainty.[6] Parametric uncertainty results from individual parameter values used in the model [Taylor 1999; Webster, 1996]. For example, if engine thrust is used to determine fuel flow rate, both thrust and fuel flow are parameters that have uncertainty in their estimated values. Parametric uncertainties are often interlinked because one parameter is used as input to determine other parameters.

Model uncertainty, also known as structural uncertainty, originates from biases in the methods used to approximate the real world phenomena. It is harder to measure because quantifying the uncertainty associated with the structure of the model is often impossible [Webster, 1996]. The Aerospace System Design Laboratory (ASDL) led by Mavris at Georgia Institute of Technology has applied robust design techniques for a system design. This has provided the assessment of the impact of disciplinary uncertainty (i.e. parametric and model uncertainties) on the confidence in the design solution [Mantis, 2002].

---

[6] Researchers including Mavris uses the terms, *aleatory* and *epistemic* uncertainties [Oberkampf *et al.*, 2004]. According to Mavris, "aleatory uncertainty is random and irreducible and generally due to the variability in nature...Epistemic uncertainty, on the other hand, is due strictly to a lack of knowledge and is generally considered to be reducible uncertainty since, as knowledge is gained, the uncertainty is reduced."

This thesis will assess both parametric and model uncertainties in the model introduced. Various statistical techniques will be employed to analyze uncertainties in a way that is most appropriate to communicating model fidelity and examining policy applications in this thesis.

1.6 THESIS OBJECTIVES

The Federal Aviation Administration's Office of Environment and Energy and a team comprised by Volpe National Transportation Systems Center, Massachusetts Institute of Technology (MIT) and Logistics Management Institute have begun developing the System for Assessing Aviation's Global Emissions (SAGE). SAGE is envisioned to be an internationally accepted computer model that can be used for predicting and evaluating the effects of different policy and technology scenarios on aviation-related emissions and aircraft performance.

The work in this thesis is closely tied to the development, assessment and use of the model. The objectives of this thesis are to:

1. Develop fuel burn and emissions sub-models that describe the performance of current fleets
2. Perform a comprehensive uncertainty analysis of the model
3. Recommend steps that guide future development of SAGE
4. Apply SAGE in analyzing important policy questions

By delivering on these objectives, this thesis makes several contributions for the aviation sector. First, a major contribution is made to develop SAGE, a tool to be used by the FAA for international policy-making. The fuel burn and emissions modules developed in this thesis are the core elements of the SAGE model. Further, this thesis assesses the uncertainty in the fuel burn and emissions predictions of SAGE. It details parametric and model uncertainties and quantifies their impacts on mean shift and variance in final model results.

This thesis employs the SAGE model and airline data to assess the benefits of three different emissions mitigation options under conditions of uncertainty. These options are technological and operational measures that are currently being considered for implementation. Lastly, the methodology presented in this thesis for assessing the uncertainty of a modeling tool and its impact on policy scenario analysis provides a framework that can be applied in support of other policy analyses.

1.7 ANALYSIS APPROACH AND DATA

The fuel burn and emissions module, the key component of SAGE, is based on simplified principles of flight physics and operations. This simplicity is necessary for two reasons, one for clarity for international acceptance and the other to reduce computational complexity due to the large number of flights (i.e. more than 30 million flights a year) to process.

SAGE has unique data sources for assessing the veracity of the model outputs. In particular, flight-by-flight fuel burn data and computer flight data recorder (CFDR) information were available from a major U.S. airline and the National Aeronautics and Space Administration (NASA). Various statistical techniques were employed to establish the uncertainty estimates of the model and understand the effects of key model assumptions on model behavior.

More detailed modeling and analysis procedures as well as data sources used are presented in the main body of the thesis.

1.8 ORGANIZATION OF THE THESIS AND CONTRIBUTIONS

Chapter 2 presents an overview of the model and key results. Specific performance goals for SAGE, modeling methods and assumptions are discussed. Global aviation fuel burn and emissions results are also included.

Chapters 3 and 4 discuss an uncertainty assessment of the SAGE model at both modular and system levels. Chapter 3 provides comparisons of reported versus modeled results. Chapter 4 analyzes the effects that the key uncertainties have on estimates of aggregate, fleet-level fuel burn and emissions. Statistical techniques are employed to quantify the unique contribution of each key uncertainty to the variance and mean of total error.

Chapter 5 presents three case studies analyzing one technological and two operational policy scenarios that are of immediate interest to the aviation community today. New NOx stringency measures, Continuous Descent Approach (CDA) procedures and derated take-off procedures are analyzed with a research version of SAGE. The research version of SAGE is capable of parameter and equation modifications that are needed to examine these various policy scenarios. Uncertainties in model outputs are considered in presenting the results and making recommendations for policy. A successful outcome of this thesis is to help evaluate technological and operational solutions that mitigate aviation's global emissions.

Research conclusions and recommendations for future development of SAGE are summarized in Chapter 6.

CHAPTER 2

OVERVIEW OF SAGE MODEL

SAGE is intended to be an internationally accepted model used for estimating aircraft fuel burn and emissions and evaluating the effects of different policy and technology scenarios on aircraft performance, aviation-related emissions, costs and industry responses. From an aircraft level to airport, regional and global levels, the model is capable of various analyses such as:

- Implementation of new aircraft technology
- Improvements to air traffic control/airspace capacity
- Enhancements to airport infrastructure
- Improvements in aircraft operations

The performance objectives for SAGE Version 1 are to compute aircraft performance, fuel burn and emissions of CO_2, H_2O, NOx, HC and CO at each point along the flight trajectory. The results are aggregated and fuel burn and emissions inventories are constructed on 1 ° by 1 ° by 1 km world grids.

This chapter presents an overview of the SAGE model structure and results.

2.1 MODEL STRUCTURE

As shown in Figure 2.1, SAGE is composed of four basic computational modules—1) aircraft movements, 2) capacity and delay, 3) fuel burn and emissions, and 4) forecasting. The following section presents excerpts from the *SAGE Detailed System Architecture and Design Specification* [FAA, 2002].
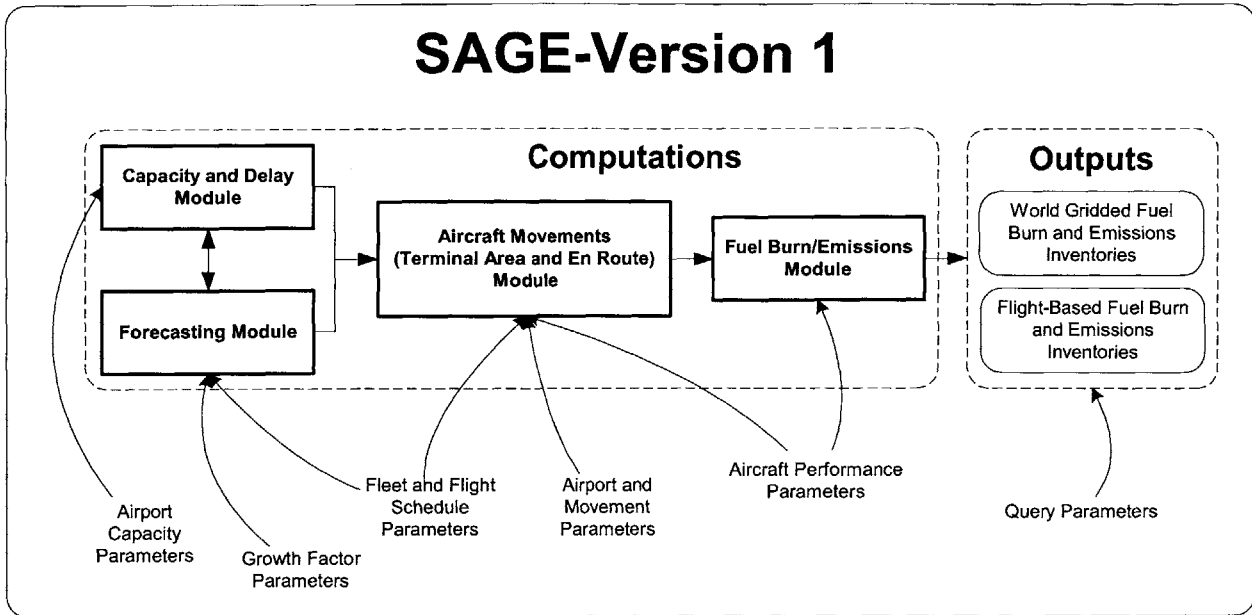
Figure 2.1 SAGE-Version 1 model structure

2.1.1 Aircraft Movements

Aircraft movements data used in SAGE for past-year estimates are a mix of radar data and flight schedule-generated trajectories. For SAGE-Version 1, radar data are from the Enhanced Traffic Management System (ETMS), which mainly cover North America and Western Europe. In addition to using a portion of radar data directly, thousands of ETMS flights were statistically analyzed. The results of these analyses were used to develop a vertical and horizontal flight track dispersion model that was used in place of the traditional Great Circle[7] and nominal altitude model for each origin-destination (OD) pair in the Official Airline Guide (OAG) schedules.

The SAGE movements database includes commercial flights worldwide and the associated global fleet mix for each of the past years that are modeled. Among the total flights modeled in determining global fuel burn and emissions for the year 2000, ETMS and OAG flights comprised 17% and 83%, respectively. Because of the reliance on the OAG schedules for regions outside of the U.S. and parts of Western Europe where

---

[7] Great circle distance is the minimum distance between two points on the surface of a sphere.

ETMS data are not available, some unscheduled and cancelled flights are not accounted for in SAGE-Version 1. Efforts are currently underway to acquire additional radar-based data, similar to ETMS data, which is also radar-based.

Aircraft movements data in SAGE can be separated into three basic categories—1) ground, 2) take-off/climb-out and near-terminal approach, 3) and en route cruise. For SAGE Version 1, the ground movements are represented as a combination of taxi and ground delay times. Taxi time statistics are extracted from the Airline Service Quality Performance (ASQP) On-Time Performance Data, which are directly applicable to the major airports in the U.S. and applied to other airports worldwide. Taxi times for major airports in Europe are obtained from the Eurocontrol Central Flow Management Unit (CFMU). Ground delays are obtained from WWLMINET. WWLMINET it is a queuing model that runs the flight demand through a network of queues and outputs the delays associated with serving the demand level [Long *et al.*, 1998]. LTO trajectories are modeled through a combination of using the methodologies and data from the Society of Automotive Engineers (SAE) Aerospace Information Report (AIR) 1845 and the Eurocontrol Base of Aircraft Data (BADA) [Bishop, 1992; SAE, 1986; Eurocontrol, 2000]. Airborne approach delays are also modeled and obtained from WWLMINET.

The SAE AIR 1845 provides engine and aerodynamic performance equations and coefficients for standard LTO procedures. Its database offers a pre-computed static set of aircraft profiles that describe departure and arrival performance of over 9000 unique aircraft/engine combinations. All of the engine types in the ICAO emissions data bank are included. For each aircraft type, there are up to seven take-off weight classes based on stage lengths [SAE, 1986].

BADA provides a set of performance and operating procedure modules (equations and coefficients) for 186 different aircraft types. They include those used to calculate drag, thrust and fuel flow and those used to specify nominal cruise, climb and descent speeds. More details on individual BADA modules are presented below.

2.1.2 Aircraft Performance, Fuel Burn and Emissions
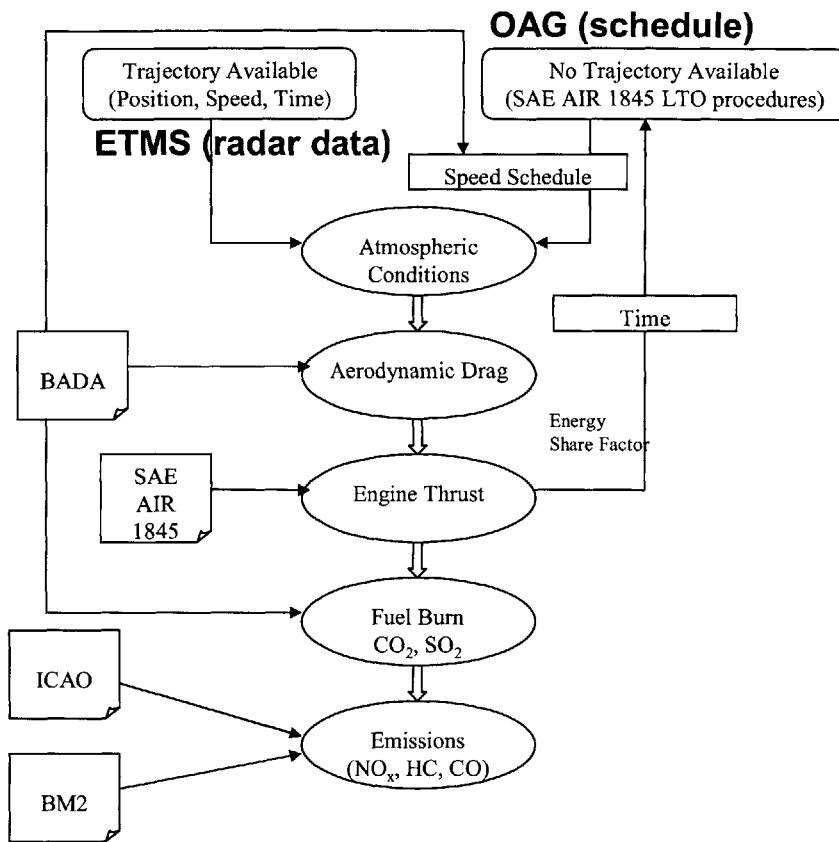
Figure 2.2 SAGE fuel burn and emissions components

Figure 2.2 shows the structure of the fuel burn and emissions components. For SAGE Version 1, an International Standard Atmosphere (ISA) with no wind is assumed. Take-off gross weight (TOGW) must also be assumed. Stage-based TOGW information from SAE AIR 1845 is used. From the ETMS or OAG-based trajectory data, the atmospheric module computes ambient temperature, pressure, density, and speed of sound. The lift coefficient (C_L) is calculated using Equation 2.1. Drag coefficients (C_{D0} and C_{D2}) are available from BADA and used to compute drag force for each aircraft type using Equations 2.2 and 2.3. Note that the drag coefficients are mode-specific, meaning that each of take-off, climb-out, cruise, approach and landing configurations has a unique set of C_{D0} and C_{D2} values.

$$C_L = \frac{2 \cdot m \cdot g}{\rho \cdot V^2 \cdot S} \qquad (2.1)$$

where:

m = aircraft mass

g = gravitational acceleration constant

ρ = air density

V = flight speed

S = wing area

$$C_D = C_{DO} + C_{D2} \cdot (C_L)^2 \qquad (2.2)$$

$$D = C_D \frac{\rho \cdot V^2 \cdot S}{2} \qquad (2.3)$$

where:

D = aerodynamic drag force

Engine thrust at a particular point on a flight mission can then be computed using Equation 2.4. Specifically, the excess power of the aircraft (from thrust minus drag) is set equal to the time rate of change in potential energy (proportional to the rate of change in height) plus the time rate of change in kinetic energy (proportional to the rate of change in speed). Equation 2.4 is a scalar equation and thus must include all of the components of velocity and the forces resolved in the direction.

$$(F - D) \cdot V = mg \frac{\Delta h}{\Delta t} + mV \frac{\Delta V}{\Delta t} \qquad (2.4)$$

where:

F = engine thrust

Δh = change in flight altitude

Δt = change in time

In some cases (e.g. near terminal area) where there is no trajectory data available, landing and take-off (LTO) profiles are created using standard LTO procedures specified in SAE AIR 1845 as below:

1. Take-off and climb at V_2+10 knots to 1000 ft. Take-off flap and thrust.
2. Accelerate 10 knots.
3. Intermediate flap. Thrust cutback.
4. Accelerate to zero flap minimum safe maneuvering speed, V_{zf}.
5. Clean flap. Climb at V_{zf} to 3000 ft.
6. Accelerate to 250 knots at max climb thrust.
7. Climb out to 10,000 ft at 250 knots.

BADA provides values for V_2 and V_{zf}. For landing, $3°$ descent for jets and $5°$ descent for turboprops are used.

The SAE AIR 1845 thrust model is employed to generate thrust force and complete the LTO trajectory information. In SAE AIR 1845, the maximum thrust for jet aircraft is determined using a quadratic expression that is a function of height and flight speed with coefficients that are corrected for temperature effects as shown in Equation 2.5. For descent modes (approach and landing), the maximum thrust is scaled down by corresponding thrust coefficients (C_{TDES_LOW}, C_{TDES_AP} and C_{TDES_LD}) in BADA.

$$F_{\max} = \left(E_{TO}+F_{TO}\cdot V_{CAS} + G_{A\_TO}\cdot h + G_{B\_TO}\cdot h^2 + H_{TO}\cdot T\right)\times \delta \qquad (2.5)$$

where:

F_{max} = maximum thrust

E_{TO}, F_{TO}, G_{A_TO}, G_{B_TO}, H_{TO} = SAGE AIR 1845 thrust coefficients

V_{CAS} = calibrated airspeed

h = altitude

T = ambient temperature

δ = pressure ratio (ambient to sea-level)

Once thrust is determined, the rate of climb ($\Delta h/\Delta t$) can be calculated from Equation 2.4, which then provides change in time (Δt) for calculating the subsequent fuel burn and emissions below.

Total fuel burn is estimated from the thrust specific fuel consumption (SFC), thrust (F) calculated and Δt as in Equation 2.6.

$$Fuel\,Burn = SFC \times F \times \Delta t \qquad (2.6)$$

BADA provides a linear expression for SFC as a function of flight speed as shown in Equation 2.7. A thrust reduction factor is applied to this expression during cruise.

$$SFC = C_{f1} \cdot \left(1 + \frac{V}{C_{f2}}\right) \qquad (2.7)$$

where:

C_{f1}, C_{f2} = BADA SFC coefficients

If the calculated thrust falls below 7% of max thrust during descent, an SFC expression for minimum fuel flow is used from BADA. Equation 2.8 shows that the BADA minimum fuel flow associated with low engine power settings is only a function of altitude, the simplicity of which causes inaccuracies during the idle and taxi modes.

$$\text{For minimum fuel flow, } SFC = C_{f3} \cdot \left(1 - \frac{h}{C_{f4}}\right) \qquad (2.8)$$

where:

C_{f3}, C_{f4} = BADA SFC coefficients

Emissions of CO_2, H_2O, and SO_2 are then calculated from a mass balance of the chemical species in the fuel and the exhaust as shown in Equations 2.9 to 2.11.

$$CO_2 = 3.155 \times Fuel\ Burn \qquad (2.9)$$

$$H_2O = 1.237 \times Fuel\ Burn \qquad (2.10)$$

$$SO_2 = 0.8 \times Fuel\ Burn \qquad (2.11)$$

To determine NOx, HC and CO emissions, SAGE uses Boeing Method 2 (BM2). BM2 is a simplified method developed based on engine performance and emissions data obtained via full-scale engine tests at ground level. It uses ICAO certification fuel flow versus emissions data taken at sea level as the basis for correcting emissions indices (EI) for installation effects, ambient conditions and flight Mach number. In SAGE, Equation 2.12 corrects the BADA fuel flow (SFC x F) to account for ambient temperature, pressure and flight Mach number. The corrected fuel flow gets correlated with referred emissions indices (REINOx, REIHC and REICO), which are then "unreferred" to account for ambient conditions as in Equations 2.13 to 2.15.

$$W_{ff} = \frac{SFC \times F}{\delta} \theta^{3.8} e^{0.2(Mach\ Number)^2} \qquad (2.12)$$

where:

W_{ff} = corrected fuel flow rate

Θ = temperature ratio (ambient to sea-level)

$$EINO_x = REINO_x \cdot e^H \cdot \left(\frac{\delta^{1.02}}{\theta^{3.3}} \right)^{1/2} \qquad (2.13)$$

where:

EINOx   = Emissions Index for NOx

REINOx = Referred Emissions Index for NOx

H = humidity factor

$$EIHC = REIHC \frac{\theta^{3.3}}{\delta^{1.02}} \qquad (2.14)$$

where:

EIHC = Emissions Index for HC

42

REIHC = Referred Emissions Index for HC

$$EICO = REICO\frac{\theta^{3.3}}{\delta^{1.02}}$$ (2.15)

where:

EICO = Emissions Index for CO

REICO = Referred Emissions Index for CO

To compute total emissions amounts, the corrected emissions indices are multiplied by fuel burn results as in Equation 2.16 to 18.

$$NO_X = EINO_X \times Fuel\ Burn$$ (2.16)

$$HC = EIHC \times Fuel\ Burn$$ (2.17)

$$CO = EICO \times Fuel\ Burn$$ (2.18)

During all taxi operations, a throttle setting of 7% of maximum thrust is assumed, from which fuel burn and emissions are computed using the procedures shown above.

2.2 GLOBAL FUEL BURN INVENTORIES

Figure 2.3 shows the year 2000 output of fuel burn in two-dimensional grids. These data are saved in 1-degree latitude by 1-degree longitude resolution. Note that altitude information is also preserved within the SAGE database in 1-kilometer altitude increments.

43

Fuel Burn in Kg

1 - 301303	5796607 - 7221067	24754156 - 30094182	94836412 - 114316137
301304 - 765743	7221068 - 8785072	30094183 - 35872533	114316138 - 138347798
765744 - 1309661	8785073 - 10465616	35872534 - 42006373	138347799 - 168835275
1309662 - 1929457	10465617 - 12425310	42006374 - 48942779	168835276 - 223229244
1929458 - 2652601	12425311 - 14804738	48942780 - 56401812	223229245 - 286140963
2652602 - 3507676	14804739 - 17513384	56401813 - 66039702	286140964 - 401889224
3507677 - 4543627	17513385 - 20685480	66039703 - 78750965	401889225 - 595284398
4543628 - 5796606	20685481 - 24754155	78750966 - 94836411	> 595284398

Figure 2.3 SAGE global 2000 fuel burn plot

(1 ° by 1 ° all altitudes aggregated)

The SAGE global, aggregate fuel burn inventories for the years 2000, 2001 and 2002 are shown in Figure 2.4, along with some results of previous studies. For all turbojet- and turboprop-powered commercial flights worldwide, the global fuel consumption is computed by SAGE to be 179.6Tg, 159.3Tg, and 159.8Tg for the years above, respectively. Neither general/military aviation nor piston-driven aircraft are included in the inventory. As shown, the SAGE values follow the general trend of the previous inventory results from Boeing and several other European studies. The increasing trend in annual fuel burn reflects the growth in air traffic over the past 30 years with the expected decreases in 2001 and 2002 due to the effects of September 11, 2001.
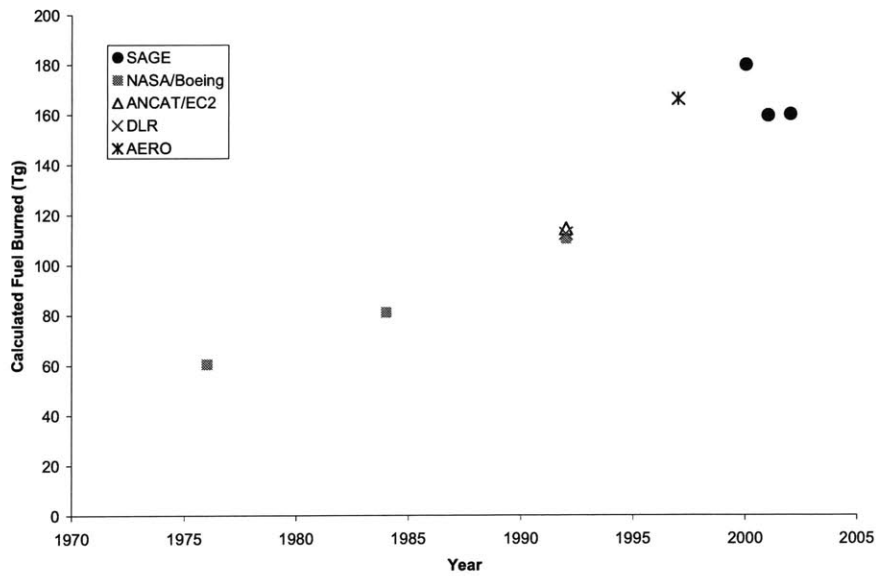
Figure 2.4 SAGE global fuel burn inventories for 2000, 2001 and 2002 and comparison to previous studies

Data from the inventories have also been aggregated by mode: ground (based on origin and destination airport elevation), above ground-to-3000 feet, above 3000 feet, and total. Figure 2.5 shows a comparison of results by year and mode for fuel burn. Most of the global aviation fuel is consumed above 3,000 ft or during cruise.
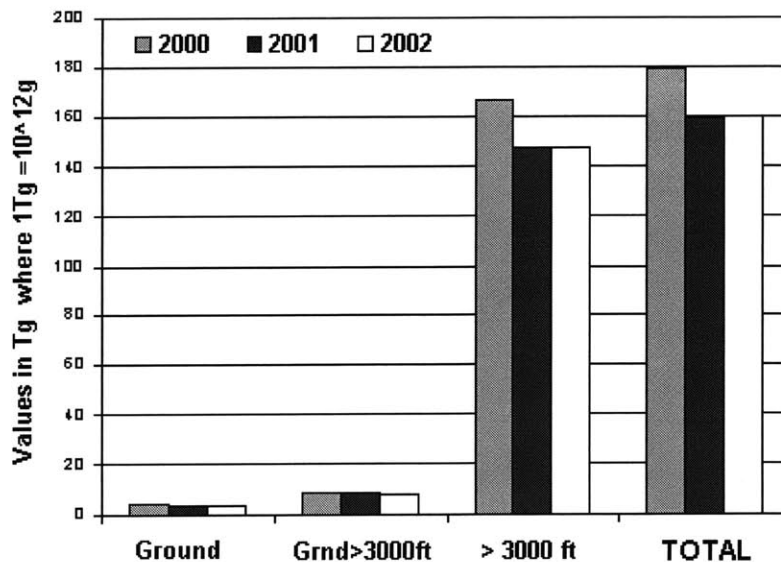
Figure 2.5 SAGE global fuel burn results for 2000, 2001 and 2002

Global fuel burn results can be separated into regions based on the geographic coordinates of the origin and destination airports. Detailed results are shown in Appendix A. Figure 2.6 depicts fuel burn from flights originating in one region but terminating in another region. Note that the term, bunker fuel (or bunker emissions) is used to account for emissions from fuel used by aircraft flown in international transport.
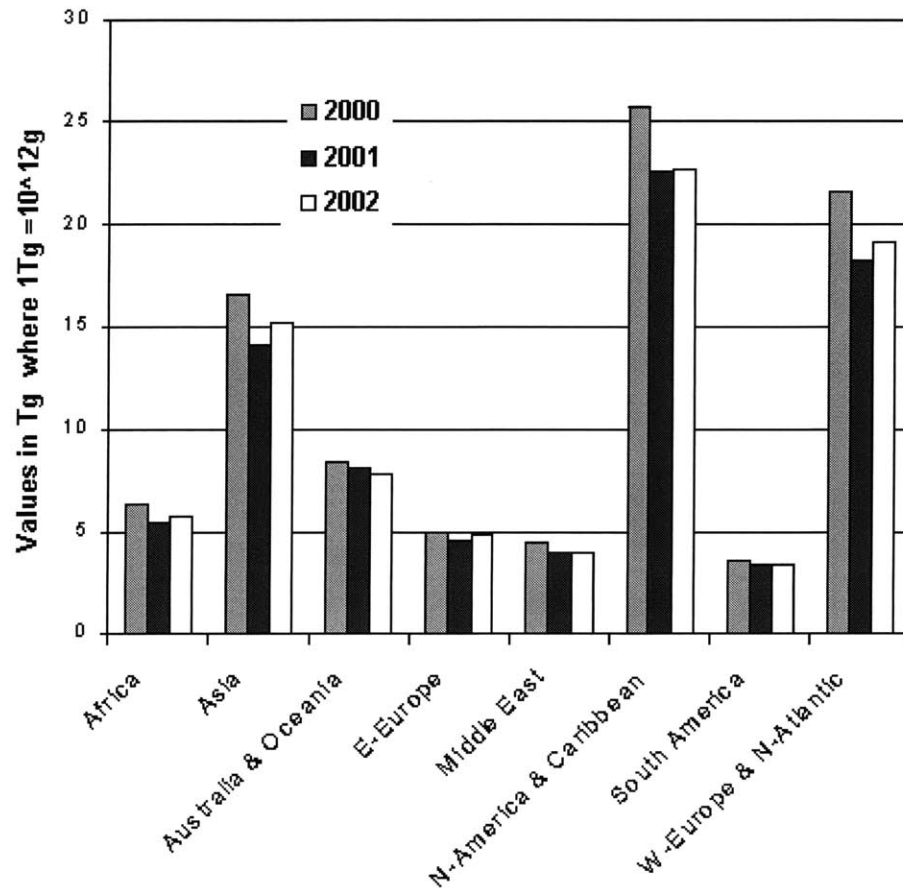
Figure 2.6 Bunker fuel burn by global regions

Table 2.1 shows a comparison of SAGE total fuel burn results with U.S. DOT Form 41 data for 10 major U.S. carriers. For year 2000, the sum of the major passenger carriers' fuel consumption calculated by SAGE is 49.2 billion kg, almost identical to the reported value in Form 41 data. Boeing has made the same comparison for its 1992 emissions inventory that is based on GC trajectories and found an under prediction of 17%

[Daggett *et al.*, 1999]. The difference between SAGE and Boeing emissions results are probably largely caused by the use of different types of trajectories (i.e. ETMS data and OAG-based dispersion tracks) in SAGE. GC distance is the shortest distance on a sphere between two points. Therefore, Boeing's GC trajectories model only the shortest distances between origin-destination pairs. As a result, it has been found that the GC distance is 4.6% smaller than actual distance on average for the 747-400 flights flown in February 1997 [Daggett *et al.*, 1999]. On the other hand in SAGE, horizontal dispersion from the GC distance is determined via a statistical analysis of ETMS data. This provides an estimate for actual distance traversed.

Table 2.1 Total fuel burn comparison for 10 major US carriers for year 2000

Carrier	FORM41 reported (Tg)	SAGE calculated with OAG schedule (Tg)
United Air Lines	9.31	9.90
American Airlines	9.14	8.96
Delta Air Lines	8.23	7.87
Northwest Airlines	6.34	6.37
Us Airways	4.66	3.60
Continental Air Lines	4.48	4.47
Southwest Airlines	3.04	3.60
Trans World Airways	2.00	2.11
America West Airlines	1.27	1.32
Alaska Airlines	0.91	0.98
Total	49.4	49.2

Note also that Boeing consistently underestimates fleet fuel burn by about 16-17% for all 10 major US carriers [Daggett *et al.*, 1999]. On the other hand, SAGE fleet fuel burn errors range around ±25%. Unscheduled and cancelled flights, which are not modeled in SAGE, are believed to be the main reason for this trend (see Section 3.3.1.2).

This chapter has presented an overview of the SAGE model and results. SAGE has been used to compute aviation's global fuel burn and emissions for the years 2000, 2001 and 2002. The results are consistent with prior studies given assumed increases

in fuel usage. A detailed uncertainty assessment of the model assumptions and results is presented in the next two chapters.

CHAPTER 3

UNCERTAINTY ANALYSIS I: MODEL VALIDATION

This chapter quantifies the uncertainties in SAGE model inputs and outputs. While the focus is on uncertainties in fleet-level outputs, consideration is also given to uncertainties in flight segments below 3,000 ft and relative uncertainties of different individual aircraft types. These results help establish the fidelity and applicability of SAGE-Version 1 for evaluating aviation's global fuel burn and emissions. Future work to improve the model is also identified as a result of these uncertainty assessments.

The first half of the uncertainty assessment discussion involves comparisons of reported versus modeled results at both the modular and system levels. Data from government and industry sources are used in the analyses. Modular evaluations mainly involve the use of aircraft performance and fuel burn-related data. In contrast, system evaluations involve the use of aggregate flight level fuel burn information, which takes into account the complete movement (e.g. trajectory) for each flight.

The second half of the uncertainty assessment discussion is a parametric study. It is presented in the following chapter. It includes an investigation into the sensitivity of the model to key input parameters. Using statistical techniques, the uncertainties in the key parameters are aggregated to explain the variability in calculated fuel burn and emissions error. This then helps to identify the parameters that have the largest influence on model accuracy and behavior.

The modeling assumptions and assessment data used are first described below.

3.1 MODELING ASSUMPTIONS

Table 3.1a Detailed assumptions for SAGE modeling

Category	Assumption	Uncertainty (1 Sigma)	Assessment Source	Impact on System Output
Trajectory and Schedules	Dispersion track assigned for OAG flights	5% of flight time	Volpe	Large on OAG flights
	Constant cruise altitude assumed for OAG flights	3000 ft for stage >= 500 nmi, 1500 ft for stage < 500 nmi	Volpe	Large on OAG flights
	Unscheduled flights not modeled for OAG flights	4% of total flights in the U.S.	Form 41	Significant on global inventory
	Some flights discarded due to outlying position data	1% of flights not flown	Volpe	Small
	Pressure altitude assumed for ETMS trajectories	100 ft	Clarke, MIT	Relatively small
Atmospheric Conditions	ISA temperature	3.3 K at cruise conditions	Boeing	Potentially large
	No head or tail wind	12.5 m/s	Boeing	Large
	No crosswind	Small	Boeing	Small
	Relative humidity of 60%	Less than 0.1% at cruise conditions	WG3, CAEP and Lukachko, MIT	Small
Performance	Airframe/engine assignments based on BACK database and expert judgment	Small (less than 10% of fleet fuel burn) because airframe/engine assignments are made by tail number for most flights	Volpe	Small
	BADA aerodynamic coefficients	14% when compared to manufacturer's L/D data	Manufacturer data	Significant
	SAE AIR 1845 engine thrust model for LTO chords	2500 lbs underprediction	Page, Wyle	Significant for LTO emissions
	BADA fuel flow model	11% when compared to published SFC data	Jane's	Significant
	No aging effects in aircraft performance or weight	2% increase in thrust specific fuel consumption at 5000 cycles and -1% to 4% change in average EINOx	Manufacturer data and Lukachko, MIT	Small and can be included in the aerodynamic, engine and weight data uncertainties
Operations	SAE AIR 1845 takeoff weight based on stage length	13%	Major carrier	Large
	Fuel tankering not modeled	4%	Boeing	Potentially large on individual flights
	Aircraft weight is assumed to remain constant for a chord element and gets debited by the amount of fuel burned after each chord	Chord fuel burn is a very small fraction of aircraft weight, and overpredictions and underpredictions add up to cancel	Major carrier	Small on aggregate
	SAE AIR 1845 takeoff ground roll distance where balanced field length is not considered	Takeoff distance differences between full power takeoff and less than full power takeoff can be as much as 5000 ft.	Va Tech	Small on aggregate but important on ground emissions
	SAE AIR 1845 takeoff procedure	10% of takeoff/climb time	Major carrier	Potentially large for LTO emissions
	3 degree descent slope for jets and 5 degree for turboprops	25% of approach/landing time	Major carrier	Potentially large for LTO emissions

50

Table 3.1a Detailed assumptions for SAGE modeling (continued)

Category	Assumption	Uncertainty (1 Sigma)	Assessment Source	Impact on System Output
Operations	Landing stop distance which includes thrust reverser not modeled	Thrust reverser uses about 60% engine power setting for a few seconds	MIT	Small
	BADA speed schedule for LTO chords where speed is not specified by SAE AIR 1845	5% of flight speed	Major carrier	Small
	Constant BADA cruise speed if no ETMS data is available	5%	Major carrier	Important
	Full power takeoff	10% of rated output	Major carrier	Important for LTO emissions
	Reduced climb power as specified in BADA	5% of max output	Clarke, MIT	Small
	BADA speed schedule for LTO segments	10 to 20 knots for 12,000 ft and below	Analysis of major carrier's data	Potentially large for LTO emissions
	No head or tail wind for LTO segments	4 m/s for 5000 ft and below	Clarke, MIT	Potentially large for LTO emissions
	Landing gear deployment at 3000 ft above the airport elevation	1800 ft +/- 600 ft	Analysis of major carrier's data	Can be significant
	7% power setting for taxing	Operations data show 5% power setting on average	Major carrier	Significant for ground emissions
	Average taxi-out times for each airport based on the analysis of ASQP data	10 minutes	Analysis of ASQP data	Significant for ground emissions
	Average taxi-in times for each airport based on the analysis of ASQP data	5 minutes	Analysis of ASQP data	Significant for ground emissions
Emissions	BM2 applied to ICAO EI database for HC, CO, and NOx emissions	Agreement between P3-T3 method and fuel flow correlations (i.e. BM2) to within a standard deviation of 6%	IPCC	Significant
		Schumann's hybrid method had average variability of +/- 18% for NOx at altitude	Lukachko, MIT	Significant
	Fuel flow capped at 7% to prevent very low fuel flow that causes extremely large HC and CO emissions	Small because flight idle power is usually higher than 7% ground idle power	Clarke, MIT	Small
	Combustor efficiency not considered	Dopelheuer and Lecht found as much as 50% error for CO and probably HC if change in droplet evaporation time is not considered at cruise conditions	Lukachko, MIT	Can be significant
	Variability in the fleet not accounted for in ICAO EI database	Would be approximately +/-16%, +/-23%, +/-54% for EINOx, EICO, and EIHC at 2σ level, respectively, based on historical experience with engine testing and the compliance factors analyzed by FAA	Lukachko, MIT	Significant
	Transient engine operation (e.g. engine start-up, power change, etc.) not accounted for in ICAO EI database	Transient operation can increase CO, HC, and particulate emissions temporarily far beyond levels suggested by steady-state measurements	Lukachko, MIT	Can be significant for ground and LTO emissions
	100% fuel combustion with corresponding conversion of fuel into CO_2, H_2O, and SO_2 based on BM2	Less than 5% for CO_2 and H_2O but can be very high (~30%) for SO_2	Kim, Volpe and Lukachko, MIT	Can be significant

51

Table 3.1a shows the large number of assumptions made in SAGE modeling. There are five categories of assumptions – atmospheric conditions, trajectory and schedules, operations, performance and emissions. Each assumption has a certain level of uncertainty which contributes to the total error in SAGE. This uncertainty level has been determined using the assessment sources discussed below. Note that the various methods within the model also represent assumptions (e.g. Boeing Method 2 to model emissions). These component assumptions are listed because they impact model uncertainty as well.

Table 3.1b highlights the key uncertainties that have a major influence on predicting aircraft performance, fuel burn and emissions. These are preliminary determinations based on a literature review of previous aircraft emissions inventory studies [Baughcum et al., 1996; Penner et al., 1999]. The key uncertainties are introduced by the use of OAG-based flight trajectories, use of standard day ambient temperature, not correcting for winds aloft, uncertain aerodynamic and engine performance, and simplified assumptions about aircraft take-off weight, and flight speed. Note that in the emissions category, there are several assumptions that can cause significant uncertainty in SAGE emissions prediction. However, they will be considered on a limited basis because of the lack of data sources for assessment.

Table 3.1b Major assumptions for SAGE modeling

Category	Assumption
Trajectory	Radar flight trajectories for ETMS flights
	Dispersion flight tractories for OAG flights
	Constant cruise altitude for OAG flights
Atmospheric Conditions	ISA temperature, pressure and density
	No head or tail wind
	No crosswind
Performance	Airframe/engine assignment based on BACK database
	BADA aerodynamic performance data
	BADA fuel flow model
Operations	SAE AIR 1845 takeoff weight based on stage length
	SAE AIR 1845 takeoff and landing procedure
	Constant BADA cruise speed if no ETMS data is available
	Full power takeoff
	7% power setting for taxing
	Average taxi times for each airport based on the analysis of ASQP data
Emissions	Boeing Method 2 applied to ICAO EI database for HC, CO, and NOx emissions

3.2 DATA SOURCES FOR MODEL ASSESSMENT

Several sources and types of data were used for uncertainty assessment of SAGE.
They are described below.

3.2.1 Major United States (US) Carrier

The data provided by a major US carrier include both aggregate flight level fuel burn
and detailed computer flight data recorder (CFDR) information. The aggregate data
cover all carrier flights for the month of October 2000. The CFDR data include the
following eight aircraft types: B737-800, B767-200, B777-200, MD80, MD83, F100, and
A300-600. The data are high resolution, recorded every 8 seconds for take-off and
landing segments and every 256 seconds for the cruise segment. The database covers
gate-to-gate movement data, including taxi-out, take-off, climb-out, cruise, descent,
approach, landing, and taxi-in. For each aircraft type, six flights of data were available.
The data cover the full range of movement (i.e. taxi, take-off, cruise, and approach).
The parameters provided in the CFDR data are engine throttle setting, engine spool
speeds, engine pressure ratio, fuel flow rate, exhaust gas temperature, ambient
temperature, wind magnitude and direction, flap and landing gear settings, pressure
altitude, calibrated air speed, latitude/longitude and aircraft gross weight.

3.2.2 Major European Carrier

Data from a major European Carrier were similar in form, but less detailed than the
CFDR data from the US Carrier. Only the cruise portion of B747-400 flights from
October 2000 is included.

3.2.3 National Aeronautics and Space Administration (NASA)

The data from NASA are very high resolution, 10-second time-step CFDR data obtained from their B757-200 test aircraft. The data cover 20 flights and the full range of movement from varying times of the year in 2000.

3.2.4 Form 41 Schedule T-2

Maintained by the U.S. Department of Transportation's (USDOT) Bureau of Transportation Statistics (BTS), this databank contains detailed traffic data for all aircraft operated on US and international routes by major US carriers since 1968. Schedule T-2 reports various traffic statistics including Revenue Passenger Miles (RPM), Available Seat Miles (ASM), airborne hours, block hours (timed from when the blocks are removed from behind the wheels prior to taxiing to when they are replaced after the flight), and fuels issued. Based on this information, further operating statistics, such as load factor and fleet size, can be calculated [USDOT, 2002].

3.3 MODULAR ASSESSMENT

Modular validation involves the assessment of individual sub-models to gauge their accuracies and uncertainties. The following sections discuss important uncertainties in each assumption category. Then for each of these uncertainties, the net impact on global emissions and flight-by-flight emissions will be analyzed in subsequent discussions of system assessment and parametric uncertainty analysis.

3.3.1 Trajectory and Schedules

3.3.1.1 OAG-Based Trajectories

In the SAGE databases, trajectory data exist in two forms: ETMS trajectories and OAG-derived trajectories. The latter type is created by a trajectory generator developed from analyzing thousands of ETMS flights. The analysis involves the determination of offsets (or dispersion) from the Great Circle (GC) route based on total flight distance (stage)

categories. By using these offsets and the associated distributions, the trajectory generator mimics the characteristics of real radar data on an aggregate level. The offsets also represent a significant portion of the differences that may be seen between SAGE results and any studies conducted using GC trajectories such as those by Boeing. Boeing used GC trajectories for all worldwide flights, and estimated to have under-predicted fuel burn by 17% as a result of the GC assumption and flight schedules modeled [Daggett et al., 1999].

Using OAG-based trajectories rather than ETMS trajectories introduces additional uncertainty into fuel burn and emissions calculated by SAGE. The main uncertainties are associated with assuming constant cruise altitude derived from a statistical analysis of ETMS data and constant cruise Mach number available from BADA. In practice, airlines often change cruise altitude as well as cruise speed to achieve minimum total operating cost (i.e. fuel cost and crew cost in particular). On a long flight, airplanes typically perform step climbs. As fuel is burned and the weight of the airplane becomes lighter, the pilot chooses to climb higher to save on fuel if the fuel consumption rate at the next higher flight level is lower [Personal communication, 2003a; Padilla, 1996]. As altitude increases, the combined effects of increased induced drag and decreased parasitic drag shift the minimum drag condition to a point that corresponds to a higher cruise speed. This is why airplanes tend to increase cruise Mach number with increasing cruise altitude. For the case of maintaining constant cruise altitude, the cruise speed for minimum drag scales with the square root of aircraft weight, which continues to decrease along the flight path.

An analysis of both ETMS data and the European carrier's CFDR information has shown cruise altitude variability of ±3000 ft (1σ). Analyzing the same data for cruise speed has shown variability of Mach ±0.02 (1σ). The impact of cruise altitude and speed uncertainties on fuel burn and emissions estimates is assessed in the next chapter. The assumptions regarding take-off and landing trajectories will be discussed in Section 3.3.4.2 below.

3.3.1.2 Schedules

Unscheduled flights and canceled flights, which are not included in SAGE emissions inventories, are a significant source of modeling bias. A comparison between OAG schedules and ETMS records has indicated that unscheduled flights are around 20% of total ETMS flights and cancelled flights are around 4% of total OAG flights [Malwitz, 2004]. This could explain the high variance in comparing the SAGE results to the Form 41 data for the US airlines in the previous chapter. It is, however, necessary to conduct a more rigorous comparison of ETMS and OAG flights within the Form 41 data to confirm some airlines have more unscheduled flights and/or cancellations than others.

3.3.2 Atmospheric Conditions

3.3.2.1 Ambient Temperature

Table 3.2 shows seasonal variations in ambient temperature at typical cruise altitude on a US transcontinental route [Baughcum et al., 1996]. On average, the ambient temperature at cruise altitude is only 1.1 K higher than the ISA temperature. This increase is higher during summer times. Similar data for North Pacific, North Atlantic, and North-South routes show typical temperature increases above ISA values to be less than 5 K with an average increase of 1.6 K.

Table 3.2 Temperature variation on a US transcontinental route [Baughcum et al., 1996]

	ISA	Annual temps	Spring temps	Summer temps	Autumn temps	Winter temps
Approximate Delta T (K)	0	1.1	0.6	2.2	1.1	0.6

As ambient temperatures increases, the density of air decreases. The aircraft then must fly at a higher lift coefficient (thus a higher drag coefficient) to make the same lift. This causes increased aerodynamic drag. Boeing analysis shows that the increase of 2.8 K over the ISA temperature results in an increased fuel burn by 0.55%. Of this increase, about 0.15% would be the result of the larger aerodynamic drag, and the

balance would be due to reduced engine performance [Baughcum et al., 1996]. Therefore, the ambient temperature uncertainty of 5 K may not have a major impact on the system-level performance of SAGE.

3.3.2.2 Winds Aloft

Table 3.3 shows seasonal variations in winds aloft at typical cruise altitudes on a US transcontinental route. Depending on the season, winds at cruise altitude range from 16.5 m/s to 29.3 m/s. An average wind for all US transcontinental, North Pacific, North Atlantic, and North-South routes is calculated to be 18.8 m/s (~37 knots), and a standard deviation is estimated to be 12.5 m/s (~20 knots) [Baughcum et al., 1996].

Table 3.3 Wind variation on a US transcontinental route [Baughcum et al., 1996]

	No wind	Annual winds	Spring winds	Summer winds	Autumn winds	Winter winds
Approximate winds (m/s)	0	23.1	24.2	16.5	23.1	29.3

Fuel burn for a round trip flight with a constant wind magnitude and direction is not equivalent to a round trip with no wind. The Boeing analysis shows that adding a wind component increases the round trip fuel burn on average by approximately 1-2% [Baughcum et al., 1996]. This is due to increased time and energy spent flying against the headwind relative to the reduced time and energy spent flying with the tailwind. In North America, eastbound flights mostly benefit from a tailwind while westbound flights see a strong headwind and burn more fuel. A strong directionality in winds aloft is a source of model uncertainty that can systematically bias SAGE fuel burn and emissions results.

3.3.3 Performance

The aerodynamic component and the fuel flow component for cruise were assessed using proprietary industry data and CFDR information from NASA. The lift-to-drag ratio[8] (L/D) was used as a measure of aerodynamic performance. It was shown that the industry-validated data were within ±14% of the SAGE-generated L/D values with 1σ confidence. The thrust specific fuel consumption (SFC) [9] was used as a measure for assessing the fuel flow component. The published SFC data were within ±11% of those generated by SAGE with 1σ confidence. These flight-by-flight uncertainties in aerodynamic and engine performance are quite substantial; however, their effects become smaller when propagated through to a fleet level. A more detailed discussion is presented below.

3.3.3.1 Aerodynamic Component
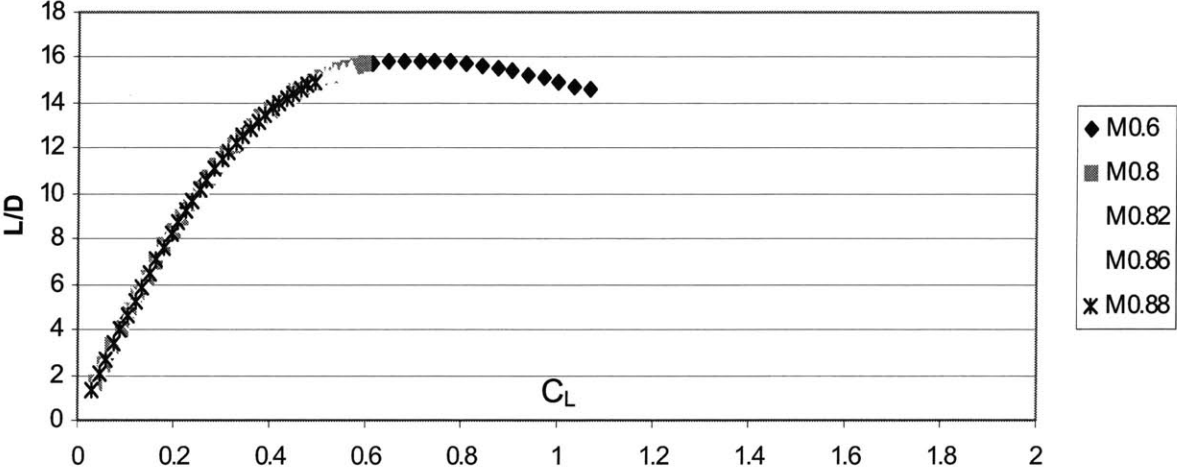
Figure 3.1 SAGE aerodynamic component assessment of B747-400 at 35,000 ft

Figure 3.1 shows a SAGE (as obtained from BADA) L/D curve as a function of the lift coefficient (C_L) for a B747-400 at cruise altitude of 35,000 ft. When compared with published data shown in Figure 3.2, the BADA lift curve is insensitive to flight altitude or speed changes. This is due to the fact that BADA has only a fixed set of drag

---

[8] A measure of aerodynamic efficiency, the ratio of lift force generated to drag experienced by the aircraft
[9] A measure of engine efficiency as denoted by the rate of fuel consumption per unit thrust (e.g. kg/s/N)

coefficients, which are mainly tuned for best cruise performance. To simulate flight altitude and speed effects more accurately, it will be necessary to introduce a correction factor for BADA drag coefficients in a future version of SAGE.
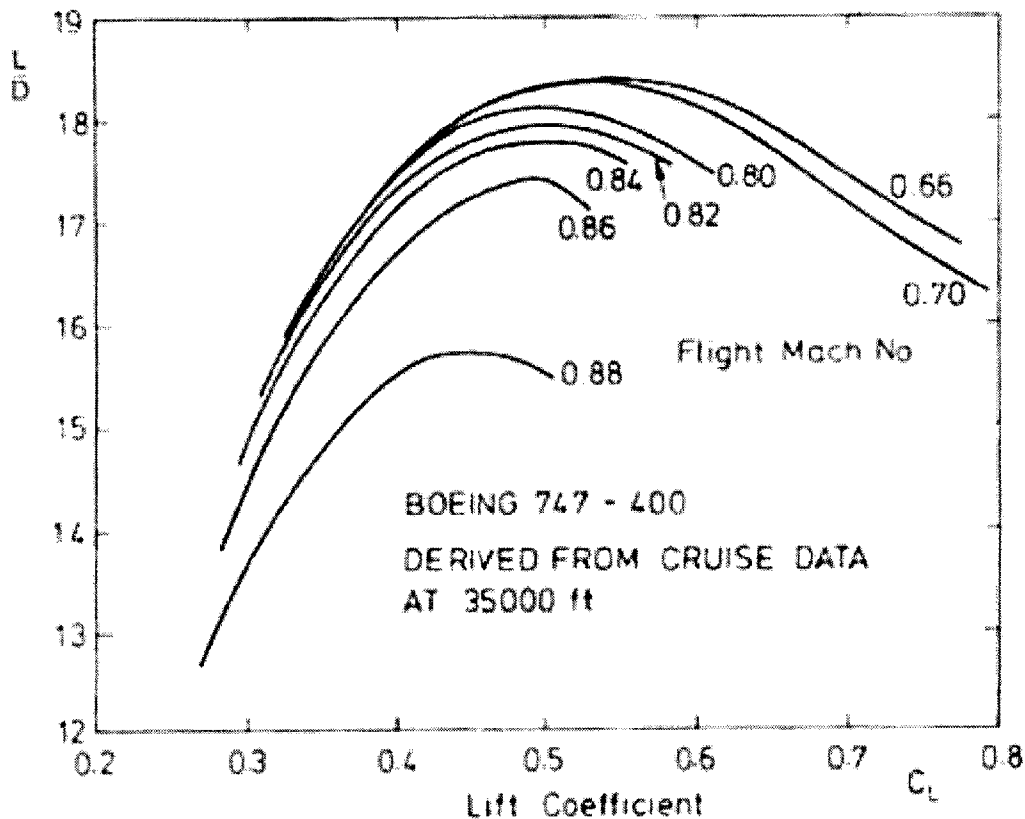
Figure 3.2 Lift-to-drag ratio versus lift coefficient for various Mach numbers
[Cumpsty 1997]

A comparison of the L/D values for various aircraft types used in SAGE versus NASA-industry provided data [see Lee *et al.*, 2001] are shown in Figure 3.3. Analysis of the data shows that the SAGE-generated L/D values are within ±14% of the NASA-industry provided data with 1σ confidence.
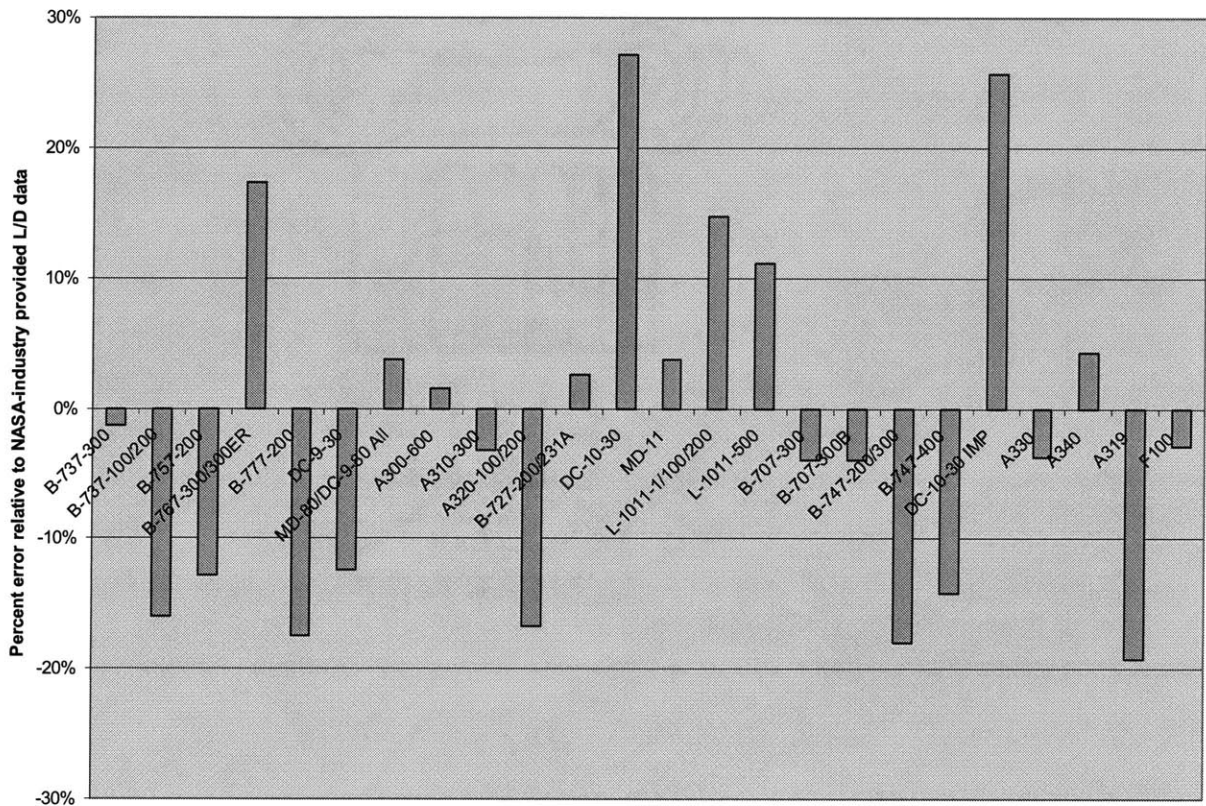
Figure 3.3 Comparison of BADA L/D values to NASA-industry provided data

3.3.3.2 Fuel Flow Component

Figure 3.4 shows a comparison of fuel flow rate between reported and SAGE-predicted values for six MD80 flights. High fuel flow rates (around 3 kg/s) correspond to take-off conditions while low fuel flow rates (below 0.5 kg/s) are associated with approach and ground idle conditions. Most data points appear in between 0.5 kg/s and 1 kg/s at cruise conditions. In general, the SAGE fuel flow values agree reasonably well with the reported fuel flow values with less than 5% error on average. For altitudes greater than 10,000 ft, the agreement is quite favorable where the standard deviation of fuel flow errors is calculated to be about 17%. For altitudes below 10,000 ft, the errors become larger where the standard deviation of errors is as high as 40%. These results are consistent with the technological and operational uncertainties of the aircraft types modeled in SAGE as shown in the next chapter. In particular, fuel flows at low engine

power settings (e.g. idle and taxi) are not as well predicted. This is because the BADA minimum fuel flow associated with low engine power settings is only a function of altitude, the simplicity of which causes the inaccuracies during the idle and taxi modes.
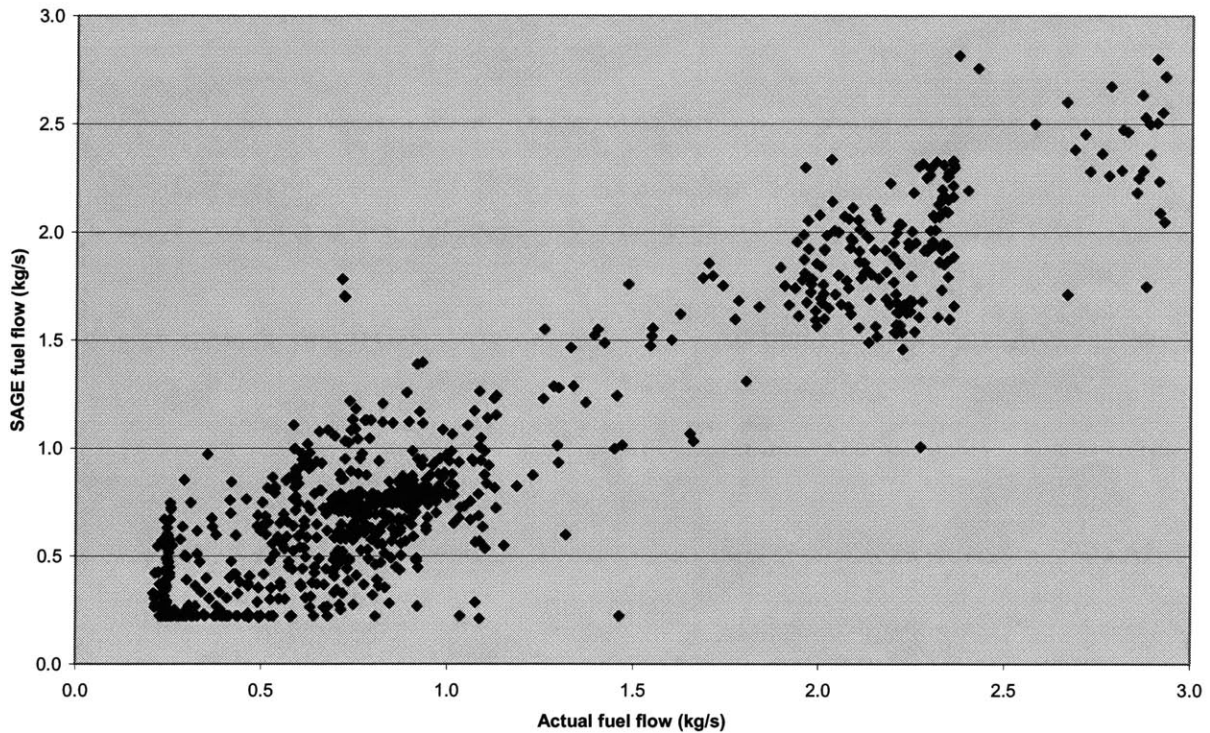
Figure 3.4 SAGE Fuel flow component assessment for the MD80

A more systematic investigation of the fuel flow component involves analyzing the cruise SFC data used in SAGE. Figure 3.5 shows a plot of the SAGE cruise SFC values versus those obtained from Jane's Aero-Engines [Gunston, 2000]. The engine types shown essentially cover over 75% of those used in the world fleet. Analysis of the data shows that the SFC values generated by SAGE are within ±11% of the published values with 1σ confidence. It should be noted that the lack of proper dependence of BADA SFC model on altitude and Mach number may be a cause of the differences here.
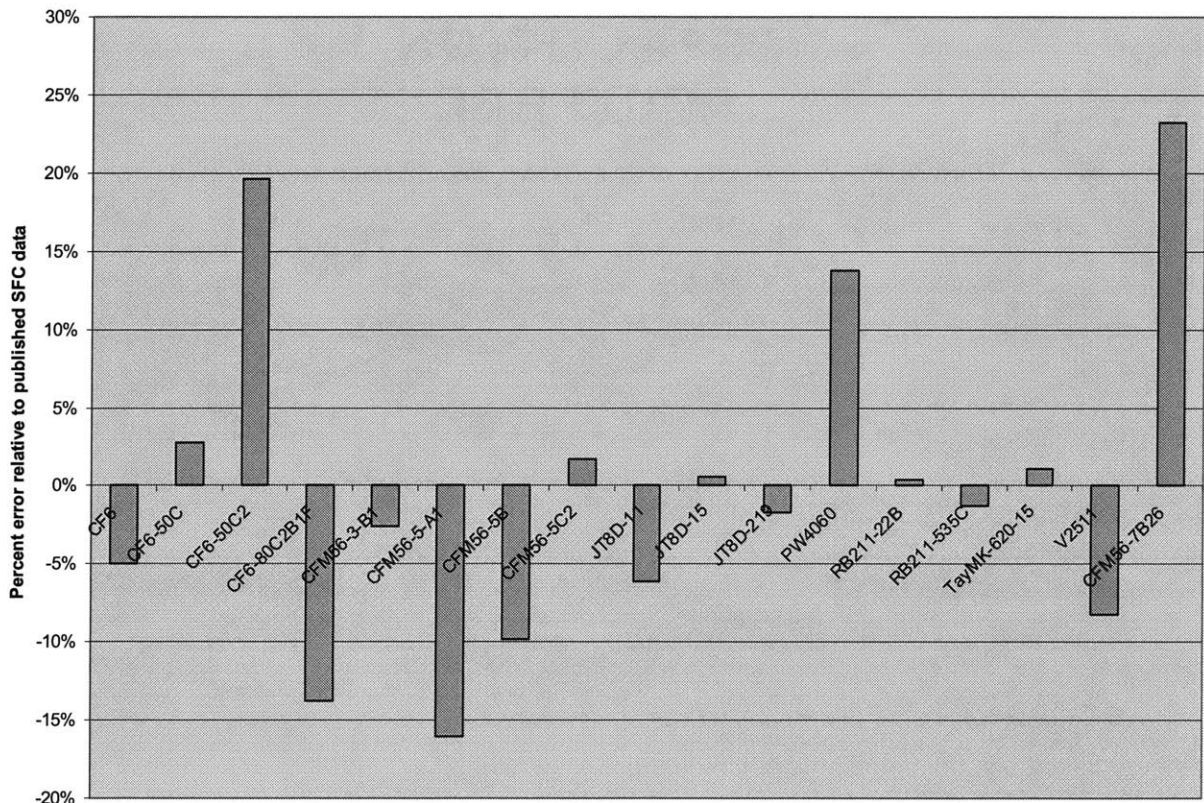
Figure 3.5 Comparison of BADA SFC values to published data in Gunston [2000]

3.3.3.3 Airframe-Engine Combinations

The BACK fleet database contains a list of all registered aircraft in the U.S. and other parts of the world. This allows for an identification of aircraft and engine types. When these data are not available for a particular airline, the BACK database is analyzed to develop distributions of aircraft and engines for the top 50 airlines from one year's worth of flight schedules. Counts of different aircraft and engine types in each of the airline categories serve as the basis for the distribution.

Once the airframe-engine combinations are made, airframe data (i.e. aerodynamic performance) and engine SFC data come from the BADA database. Engine thrust and emissions data are obtained from the FAA's Integrated Noise Model (INM) [Bishop, 1992] and ICAO/EDMS, respectively. If a particular airframe or engine type is not

available from the corresponding databases above, a substitution is made. For example, the MD90 is not available in the BADA database, so the MD80 is used in its place.

The substitutions generate additional uncertainty in the aerodynamic and engine performance. Based on the U.S. data [USDOT, 2002], the substituted aircraft-engine types account for less than 10% of the total fuel consumed for major US carriers. Given the uncertainties in the airframe and engine performance data (i.e. 14% and 11%, respectively) as assessed above, the aggregate effects of the airframe-engine substitutions are estimated to cause around 1% error for total SAGE results. Therefore, further treatment of this uncertainty is not addressed in this thesis.

3.3.4 Operations

3.3.4.1 Aircraft Take-off Gross Weight (TOGW)

Uncertainties in TOGW are dictated by the uncertainties in payload and fuel on board. Payload and fuel together typically account for 25-50% of TOGW, depending on the size and load factor of the airplane. The heavier the TOGW, the more fuel the airplane burns. Boeing [1996] analysis shows that increasing the load factor from 70% to 75% causes a small 0.80% increase in block fuel for a B747-400 but a large 2.54% increase for a B737-300. This is due to the fact that mission fuel burn is roughly proportional to the sum of operating empty weight plus payload. Thus, increasing payload has a greater impact on the fuel burn of a smaller airplane due to the increased fuel requirement relative to the lower operating empty weight.

The TOGW data used in SAGE are based on stage length flown as determined by the SAE AIR 1845. The longer the stage length, the heavier the TOGW to account for the increased fuel requirement. Figure 3.6 shows a comparison between SAGE take-off weights versus CFDR-reported values for 17 flights. It shows that the stage-based take-off weights in SAGE are within ±7% of the reported values with 1σ confidence.

The take-off weights of short-haul flights tend to be overestimates while those of long-haul flights are underestimates. It is necessary to obtain more CFDR data to examine this trend and estimate the uncertainty in SAE AIR 1845 take-off weights with increased confidence. Due to the lack of further assessment sources at present, a conservative estimate of ±10% (1σ) uncertainty is assumed for take-off weight in the subsequent analyses of this thesis.
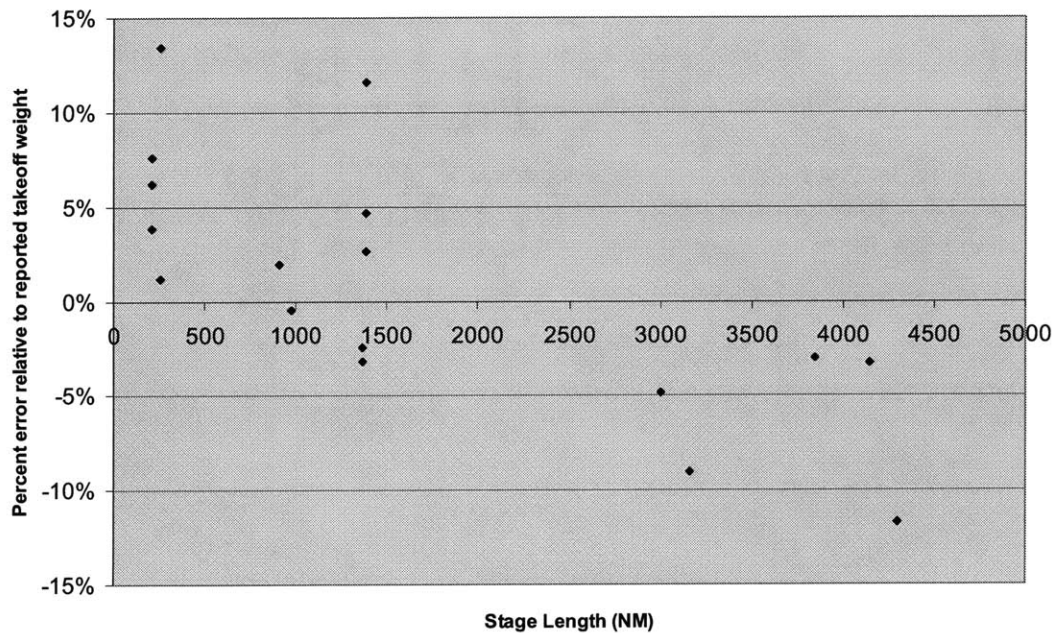
Figure 3.6 Comparison of SAE AIR 1845 take-off weights to CFDR-reported values

3.3.4.2 Landing and Take-off (LTO) Procedure

For the LTO modes, the SAE AIR 1845 procedure and engine thrust data have been implemented in SAGE. This is the same methodology employed in the FAA's Integrated Noise Model (INM) [Bishop, 1992]. It is an internationally recognized and accepted methodology that has been extensively validated [Flathers, 1982]. Note, however, that SAE AIR 1845 assumes full power take-off. According to a major airline, the number of de-rated take-off operations is increasing annually. They are performed between 67% and 95% of the time depending on aircraft type and weight, runway length, and weather conditions. Typical de-rates range from 5% up to 25% [Personal

communication, 2003b]. Since aircraft emissions are highly sensitive to engine power settings, the full power take-off assumption may have a significant impact on LTO emissions predicted by SAGE.

Although the SAE AIR 1845 methodology has been implemented in SAGE, there are some slight differences. Figure 3.7 shows LTO profiles generated for a B727-200. For take-off, SAGE produces a slightly faster climb (i.e. steeper curve). This is mainly due to the energy share factor used. The energy share factor is how the excess power generated by aircraft engines is allocated to changing the potential energy versus kinetic energy of the airplane. If the energy share factor is equal to 1, all excess power of the engines goes to changing potential energy. For fast acceleration, it is usually set to around 0.3 which indicates that the majority of the available power is devoted to a change in speed. The energy share factor remains almost constant for the case of SAGE. But for INM, it is programmed to decrease (less energy going into potential energy change) with altitude increase. This is why it takes longer for the INM profile to achieve the same altitude increase. Other differences in take-off performance are attributed to different aerodynamic coefficients (i.e. C_{D0} and C_{D2}) used by the two models. During approach and landing, the SAGE profile precisely overlaps with the INM one because both use a 3-degree gliding slope.
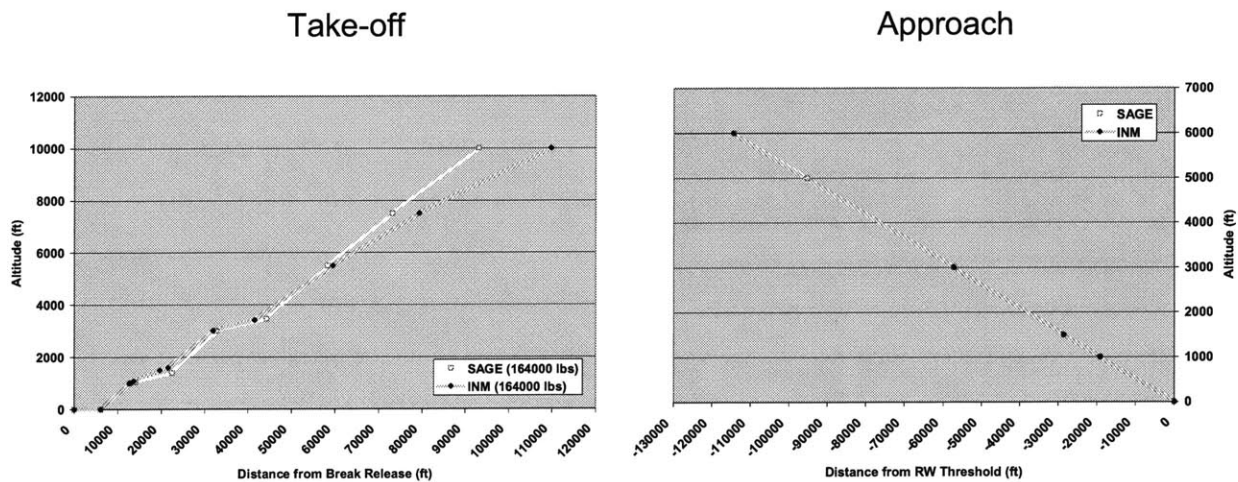
Take-off   Approach

Figure 3.7 SAGE take-off and approach profiles in comparison to SAE AIR 1845 standards for a B727-200

Figure 3.8 shows the horizontal distances traversed during take-off and climb up to 10,000 ft for various aircraft types. The INM and SAGE results agree with 10-20% differences with no apparent bias in either direction. These uncertainties are mainly due to the fact that airlines use slightly different LTO procedures depending on various factors including aircraft types, airport configurations and traffic loads and weather conditions.
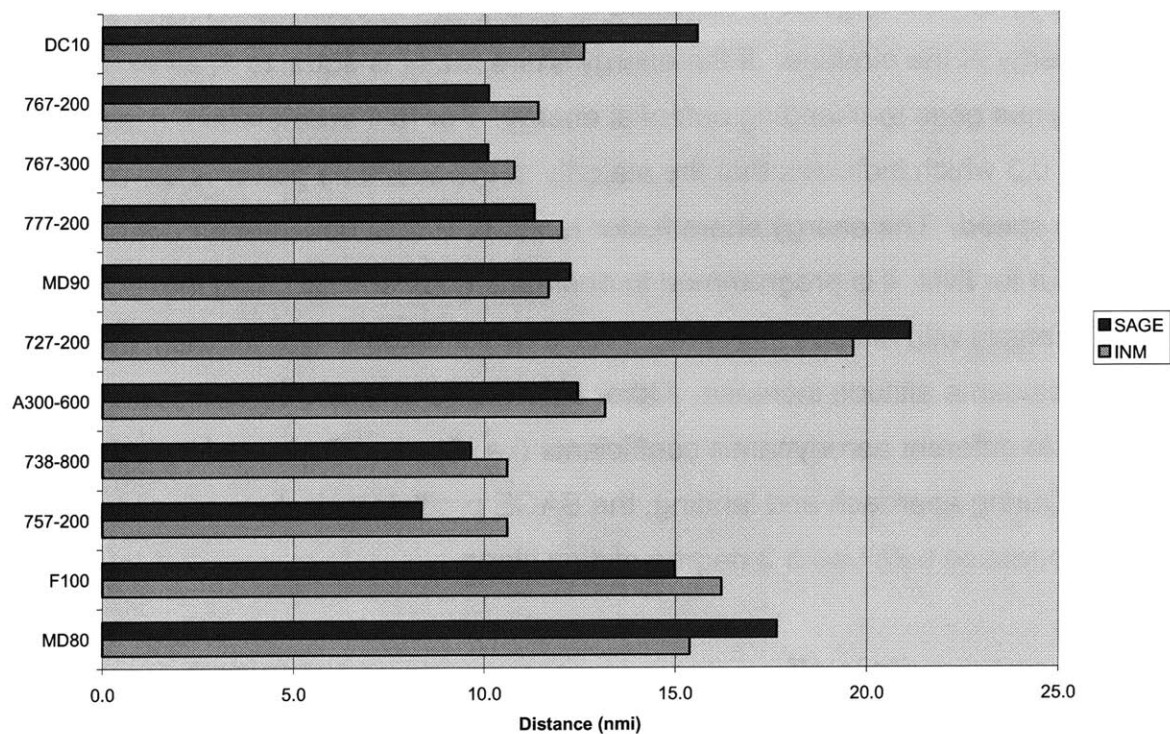
Figure 3.8 Comparison of horizontal distance traversed during take-off and climb

3.3.4.3 Taxiing Operations

SAGE assumes 7% engine power during taxiing. However, airlines use various methods including decreased engine power, single-engine taxiing and tow trucks to reduce ground emissions [Miller, 2001]. Table 3.4 shows typical engine power settings calculated from a major airline's taxiing data for 5 aircraft types, assuming a linear relationship between engine power setting and fuel flow [Personal communication,

2003b]. On average, 5% engine power is used for taxiing in this case. An analysis with SAGE has shown that HC and CO emissions are highly sensitive to throttle settings at low engine power so that they can grow as much as twice if engine power is reduced from 7% to 5%. While the impact of the 7% engine power assumption on global emissions inventory is believed to be small, it is an important area of uncertainty in estimating ground emissions.

Table 3.4 Typical engine power settings for taxiing operations

| Flight No. | Fuel flow rate per aircraft during taxiing (kg/s) | | | | |
	B737-800/JT8D-15A	B757-200/RB211-535C	B767-200/PW4060	B777-200/GE90-76B	A300-600/PW4158
1	0.184	0.217	0.365	0.446	0.366
2	0.189	0.216	0.385	0.478	0.370
3	0.205	0.276	0.370	0.468	
4	0.208	0.293	0.357	0.451	0.339
5	0.200	0.288	0.392	0.486	0.362
6	0.204	0.289	0.368	0.481	0.360
Average ff (kg/s)	0.198	0.263	0.373	0.468	0.360
ICAO idle ff (kg/s)	0.302	0.440	0.469	0.616	0.464
% thrust calculated	4.6%	4.2%	5.6%	5.3%	5.4%

Additional uncertainty exists in taxi times when actual values are not available from Airline Service Quality Performance (ASQP) for flights outside of the U.S. Analysis of annual ASQP data shows that taxi-out times and taxi-in times vary by 10 minutes and 5 minutes, respectively, with 1σ confidence.

3.4 SYSTEM ASSESSMENT

System assessment examines the effects that the uncertainties discussed above have on estimates of aggregate, fleet-level fuel burn and emissions.

3.4.1 Assessment Using Airline Data

SAGE fuel burn results have been computed using 35,359 ETMS and matching OAG flights for October 2000. Errors are computed between SAGE fuel burn outputs and values reported by a major US carrier as shown in Figures 3.9 and 3.10 and summarized in Table 3.5. The mean and standard deviation of errors are -5.7% and

18.7%, respectively, when comparing ETMS flights to reported values, and -1.2% and 17.7% when comparing OAG flights to reported values. Standard errors (estimated standard deviations of the mean) are 0.11% and 0.10%, which confirm that SAGE can predict fleet fuel burn with less than 6% error on average for both ETMS and OAG-based flights. On a fleet total basis (i.e. the fuel burn sum of all 35,359 flights), the ETMS flights underestimate the reported fleet fuel burn by 7.4% and the OAG flights underestimate by 4.4%.
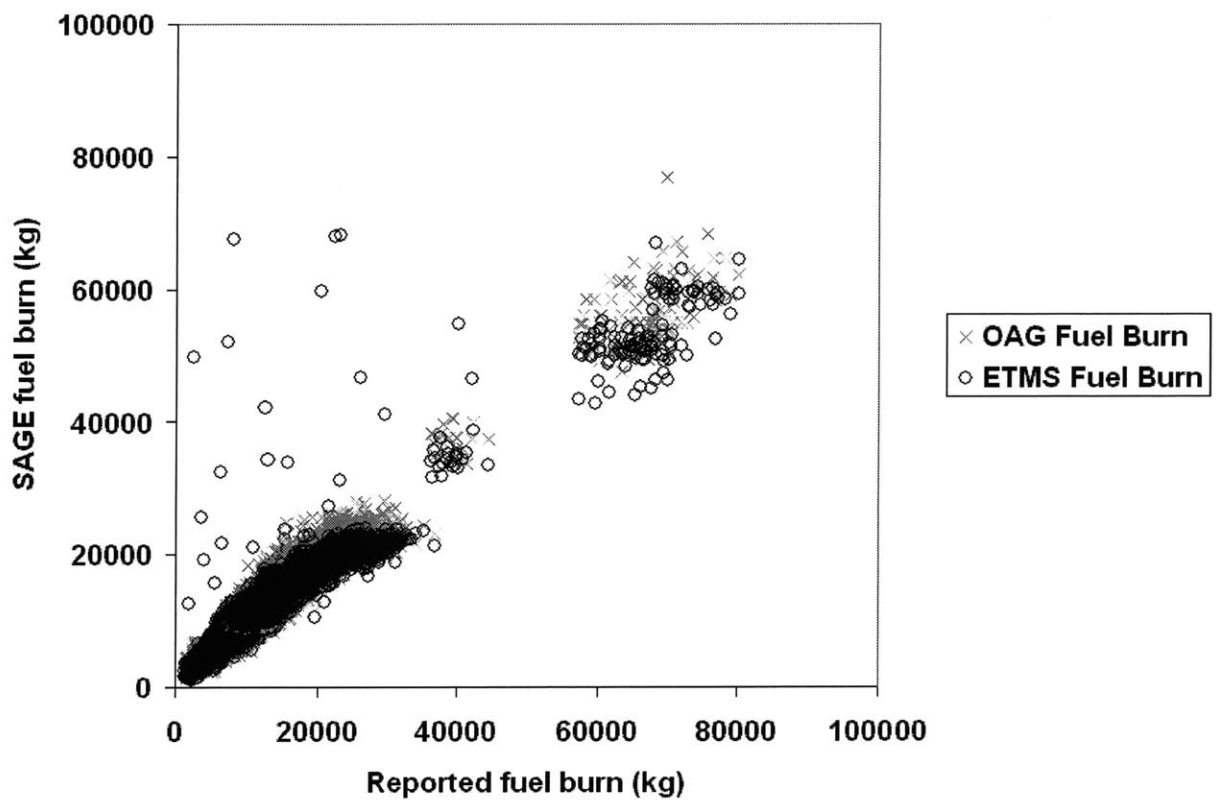
Figure 3.9 SAGE results comparisons to reported fuel burn data of a major airline for October 2000 for 35,356 flights
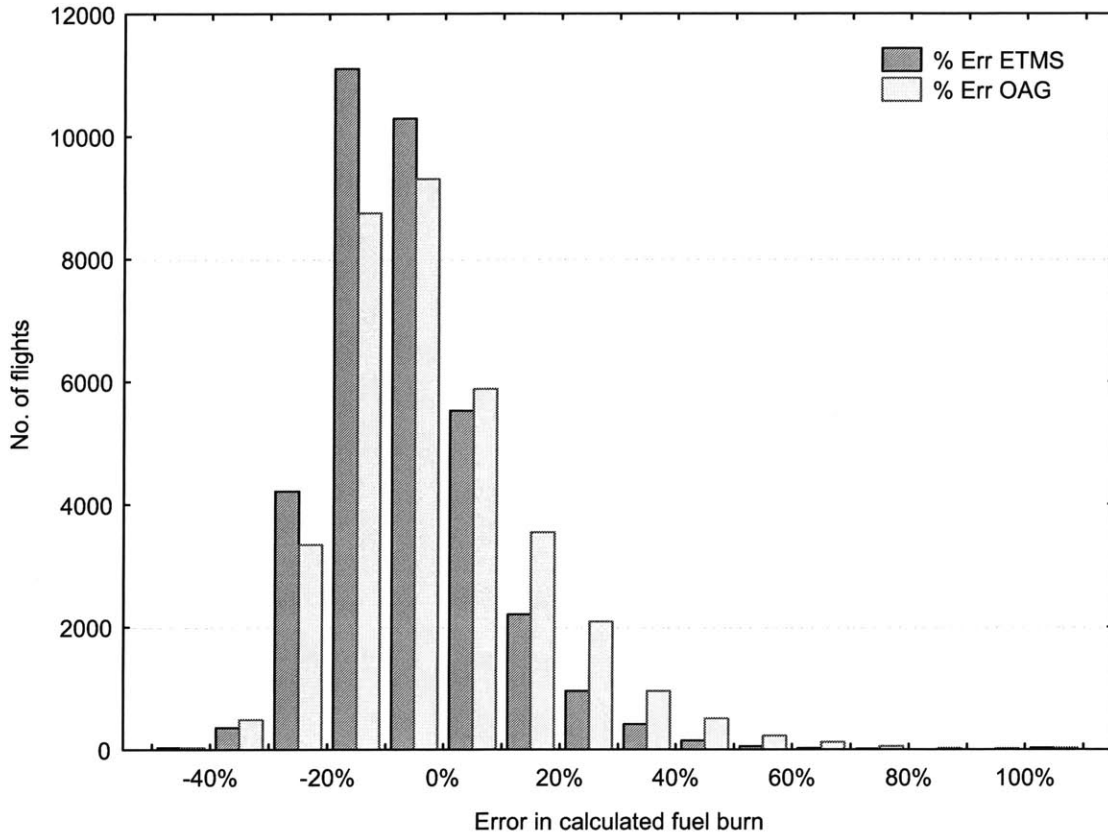
Figure 3.10 Histogram results of SAGE fuel burn comparisons to airline-reported data

Table 3.5 System error statistics for ETMS versus OAG-based flights

		ETMS	OAG
All flights	Mean	-5.7%	-1.2%
	Standard Dev.	18.7%	17.7%
	Standard Error	0.11%	0.10%
	Fleet Error	-7.4%	-4.4%
	Flight counts	35,359	35,359
Flights > 500 NM only	Mean	-5.8%	-6.2%
	Standard Dev.	14.6%	13.5%
	Standard Error	0.089%	0.082%
	Fleet Error	-7.4%	-6.5%
	Flight counts	27163	27163

The results show that the dispersion model in SAGE is effective in predicting total fuel burn for OAG-based flights. However, using a constant cruise speed of around Mach 0.8 for flights on a very short stage (i.e. less 500 NM) with a low cruise altitude (i.e. less than 15,000 ft) causes excessively large fuel burn. Figure 3.11 shows that these short-haul flights are a significant source of bias error for OAG flights. They are also a large source of standard deviation increase for both ETMS and OAG flights. Table 3.5 shows that the mean error in calculated fuel burn becomes around -6% and the standard deviation decreases to less than 15% for both ETMS and OAG flights when the flights on less than 500 NM stage are excluded.
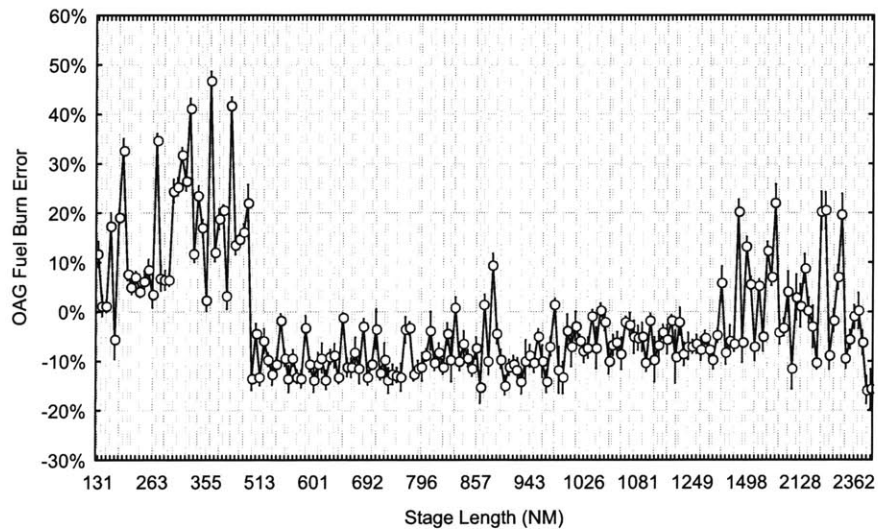
Figure 3.11 OAG fuel burn errors by stage length
(Vertical bars/ranges denote 0.95 confidence intervals of the mean)

The total number of ETMS and OAG flights modeled in determining global fuel burn/emissions for 2000 are 4,524,728 and 21,899,800, respectively. Using the appropriate weighting factors (equivalent to fractions of total flights) of 0.17 and 0.83 for ETMS and OAG flights, respectively, the composite statistics are:

- Composite Mean Error = -2.0%
- Composite Standard Deviation of Errors = 17.9%

Note that the composite mean error of -2.0% has a significant bias due to the large fuel burn errors of short-haul flights as shown in Figure 3.11. Without the short-haul flights, the composite mean error is -6.1%. The negative composite value of mean error indicates that SAGE Version 1 tends to under-predict on average. This is due to several modeling assumptions in SAGE. First, a round trip with a wind component burns 1-2% more fuel over no wind condition [Baughcum et al., 1996]; therefore, the no wind assumption of SAGE results in an underestimation of fuel burn. Second, the INM take-off weights used in SAGE are nominal values. Actual take-off weights distributed normally around the nominal values would lead to burning more fuel. Therefore, not using actual take-off weights results in an underestimation of fuel burn. Other technological and operational assumptions can also cause the under-prediction of fuel burn in SAGE. A quantitative examination of the sources of the variability in mean and standard deviation is possible and will be presented in the next chapter.

Analyzing errors without the OAG-based trajectory uncertainties provides further insight for improvement. Figures 3.12a and 3.12b show errors by stage length and aircraft type for ETMS flight results. Errors are small and relatively insensitive to stage length under 2500 nautical miles. However, for 2500-5000 NM flights, errors are systematically large averaging around -19%. Interestingly, they are all DC10 flights to/from Honolulu. It is clear from Figure 3.12b that fuel burn is systematically underestimated by about 18% for the DC10. So it is Honolulu-related operations and DC10 performance data that cause this error. Since there are only one hundred forty seven DC10 flights in the 2500-5000 NM category, the overall effect on aggregate fuel burn for a month or year is insignificant.

Figure 3.12b also suggests that three other aircraft types with 20% or larger error require further examination. Among them are MD90 and B737-800 for which MD80 and B737-500 performance data have been substituted, respectively. It is clear that the substitutions are not very successful. The B777-200 also requires improved performance data. Cruise fuel burn outputs from SAGE have been also compared to those from a manufacturer's performance model for the following aircraft: B747-400,

B737-300, B737-500, B757-200, B767-300, B777, and B737-800. With two exceptions, the errors were generally within 10%, often within 5%, with no apparent bias either around zero or as a function of other variables (e.g. aircraft weight). The two exceptions were again the B777-200 and the B737-800. For the B777-200, SAGE-predicted fuel burn was about 20% high, and for the B737-800, the fuel burn was about 20-30% high [Personal communication, 2003c]. As the next paragraph will show, aircraft performance data is the primary source of the large error in the B777-200 and B737-800 results.

(a) Stage Length   (b) Aircraft Type
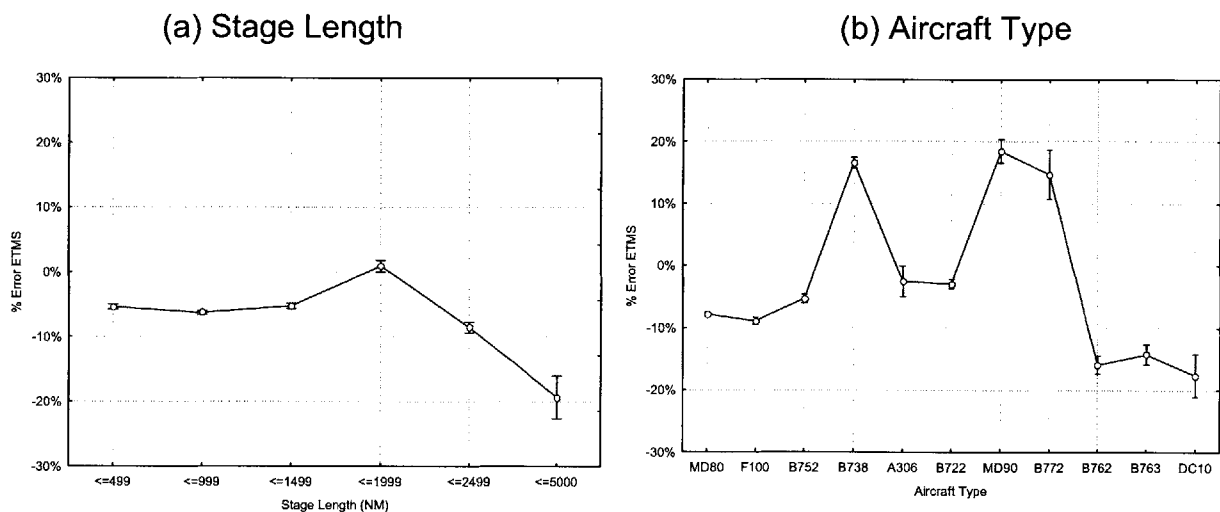
Figure 3.12 SAGE fuel burn errors by (a) stage length and (b) aircraft type for ETMS
(Vertical bars/ranges denote 0.95 confidence intervals of the mean)

An updated version of aerodynamic and engine fuel flow performance data is available through BADA 3.5. Figure 3.13 shows the fuel burn results of B777-200, B767-200, B767-300 and B737-800, the engine and aerodynamic performance data of which are either added or improved in BADA 3.5. It is clear that the errors get reduced to less than 10% for all four aircraft types. This illustrates the need for continuous assessment and improvement in aircraft performance data. In this regard, obtaining data sources for assessing turboprop aircraft performance is also necessary.
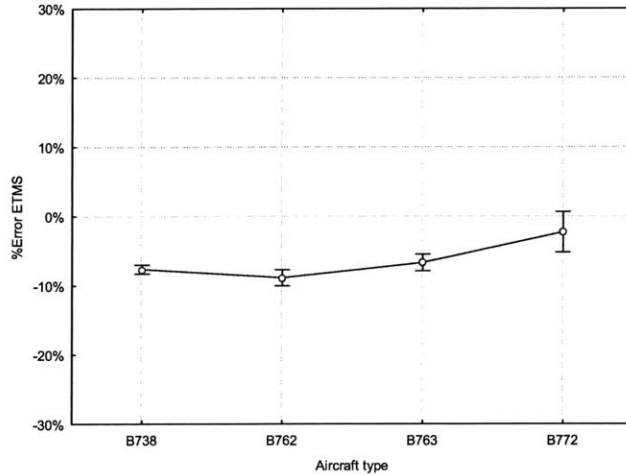
Figure 3.13 New SAGE fuel burn results with BADA 3.5

3.4.2 Assessment of Terminal Area Performance

In order to assess the effects of different LTO procedures (i.e. engine throttle setting, rate of climb/descent and flight speed), the times-in-mode based on the standard SAE AIR 1845 procedure are compared to actual trajectory information in the CDFR data. Figure 3.14 shows that actual time-to-climb from the ground to 3000 ft altitude is about 38% longer than that of the standard procedure when averaged across the six aircraft types examined (MD80, B757-200, B737-800, A300-600, B777-200 and B767-200).

(a)   (b)
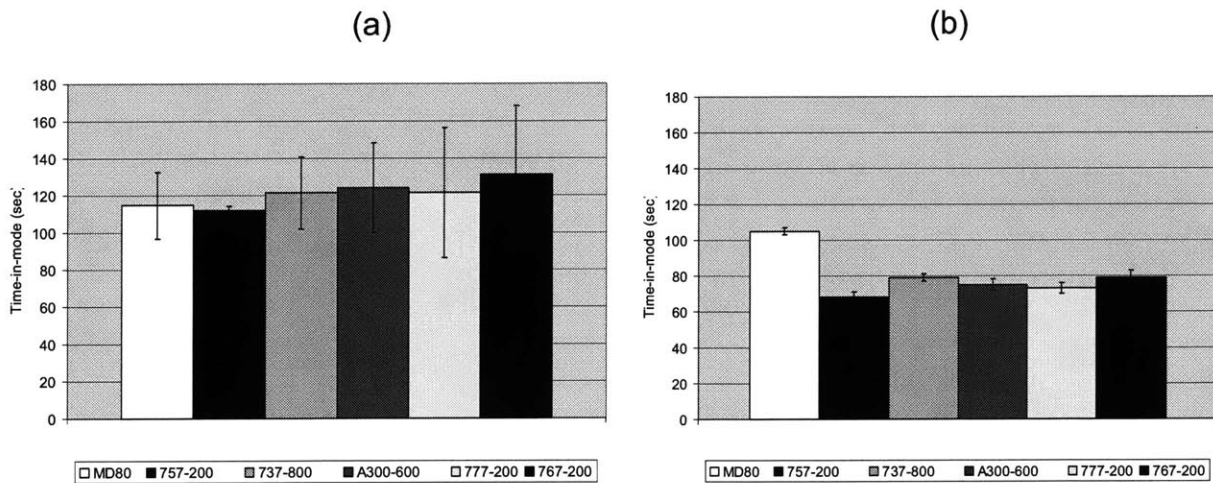
Figure 3.14 Time-to-climb comparisons between (a) reported data and (b) SAGE calculation for the ground-to-3000 ft

For descent, actual time-to-descent from 3000 ft altitude to the ground takes about 28% longer than the standard procedure does as shown in Figure 3.15.

(a)   (b)
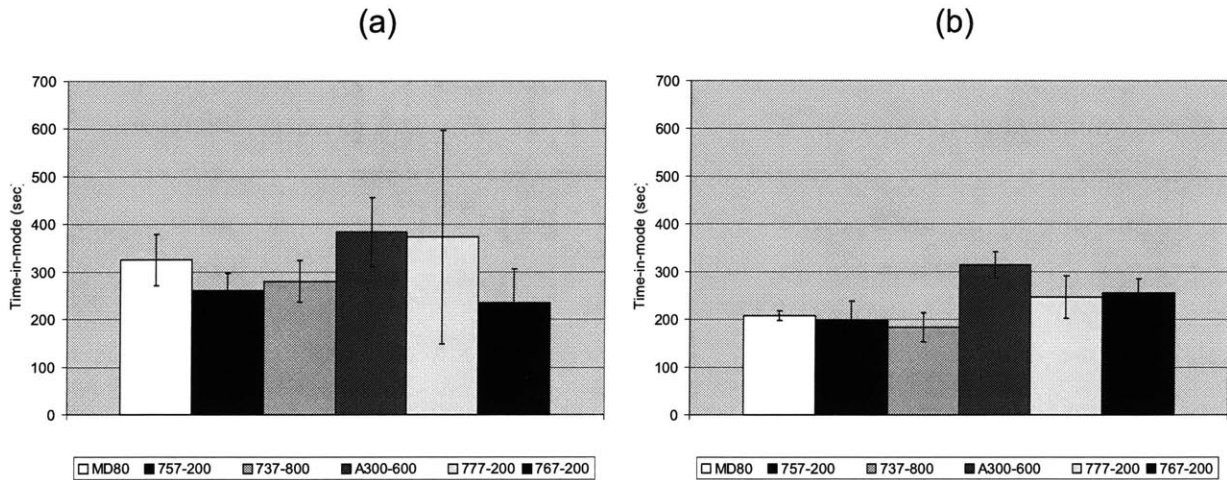
Figure 3.15 Time-to-descent comparisons between (a) reported data and (b) SAGE calculation for 3000 ft-to-the-ground

The fuel burn calculated by the LTO component of SAGE was compared to that obtained from a major US airline's CFDR for 32 flights and 6 aircraft types. Actual flight trajectory, speed, winds aloft and ambient temperature information is fed into SAGE. This comparison then shows the error in the aerodynamic and fuel flow components of SAGE. For the take-off segments (e.g. the ground to 3,000 ft), SAGE over-predicts reported fuel burn by 10% on average with a standard deviation of 12% as shown in Figure 3.16. A large portion of this error is driven by the inaccuracies in the performance data of the B777-200. Using updated performance data (i.e. BADA 3.5) for the B777-200 reduces the calculated fuel burn by about 20% and the subsequent error to less than 5%.

Figure 3.16 also shows the results of BADA 3.5 implementation for B737-800, B777-200 and B767-200. As indicated by the dotted lines, the fuel burn of the take-off segments decreases by 10-20% for these aircraft types which have updated engine and aerodynamic performance coefficients.
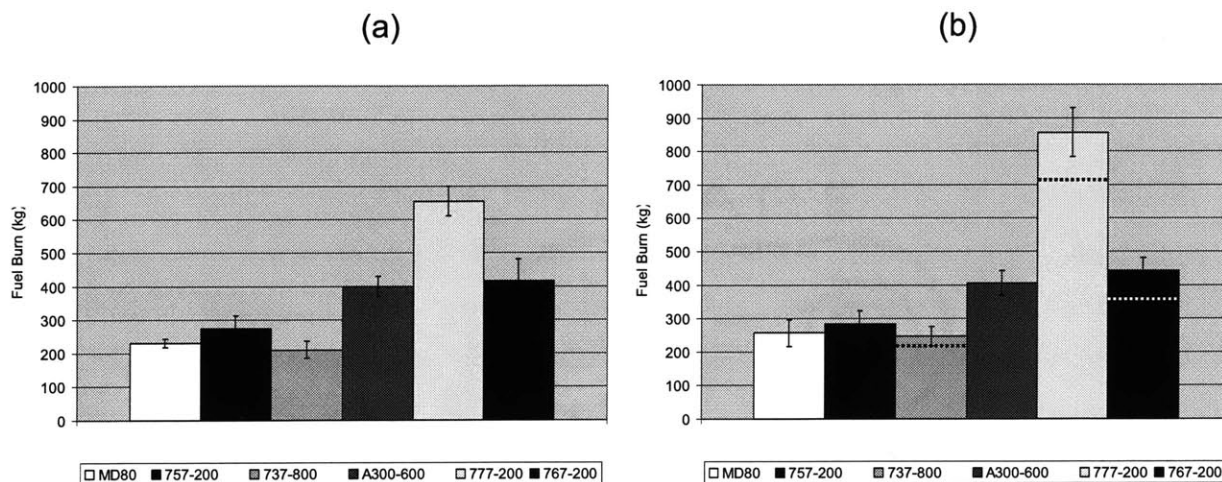
Figure 3.16 Take-off fuel burn comparisons between (a) reported data and (b) SAGE calculation (BADA 3.5 results in dotted line for B737-800, B777-200 and B767-200)

For the descent segments (e.g. 3,000 ft to the ground), SAGE over-predicts reported fuel burn by 8% on average with 42% standard deviation as shown in Figure 3.17. The results of BADA 3.5 implementation for B737-800, B777-200 and B767-200 are also shown with dotted lines. While the fuel burn error is reduced for the B767-200, there is almost no change in the B777-200 results. The discussion below will show that lowering the landing gear extension height improves the B777-200 results.

(a)   (b)
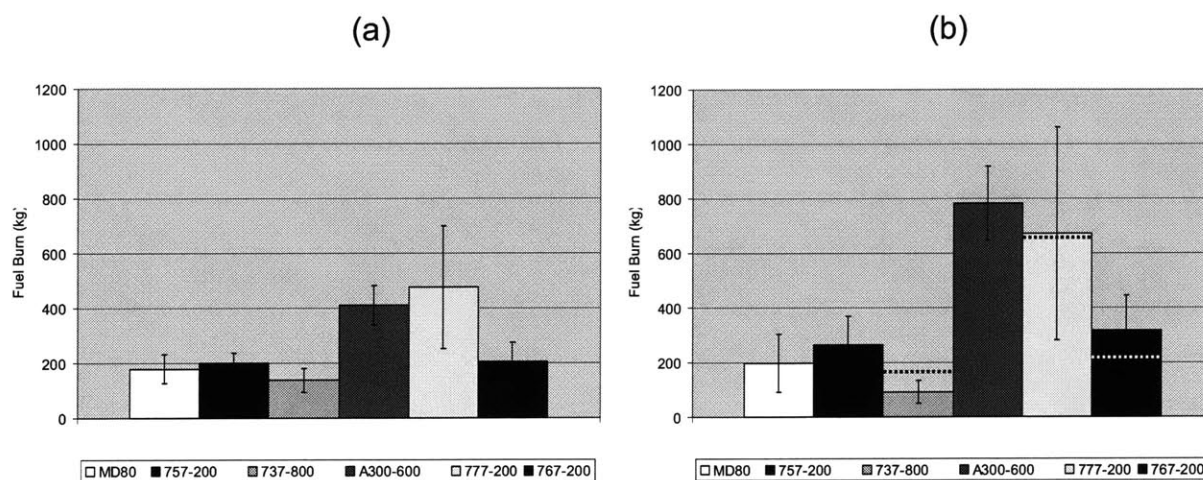
Figure 3.17 Descent fuel burn comparisons between (a) reported data and (b) SAGE calculation (BADA 3.5 results in dotted line for B737-800, B777-200 and B767-200)

To improve the descent fuel burn of SAGE, two modifications have been examined. Currently, if drag coefficients (i.e. C_{D0} and C_{D2}) at take-off, climb-out, approach or landing mode are not available in the BADA database, those at cruise mode are substituted. This assumption leads to an inaccurate representation of C_{D0}. As shown in Figure 3.18, C_{D0} values at take-off, approach and landing modes are 1.5 to 2.5 times larger than those at cruise mode. Therefore, it is necessary to adjust cruise C_{D0} by an appropriate factor and use adjusted C_{D0} values for other modes. In Figure 3.18, C_{D0} values for various turboprop and jet aircraft types are plotted and a second-order polynomial curve is fit through the data points.
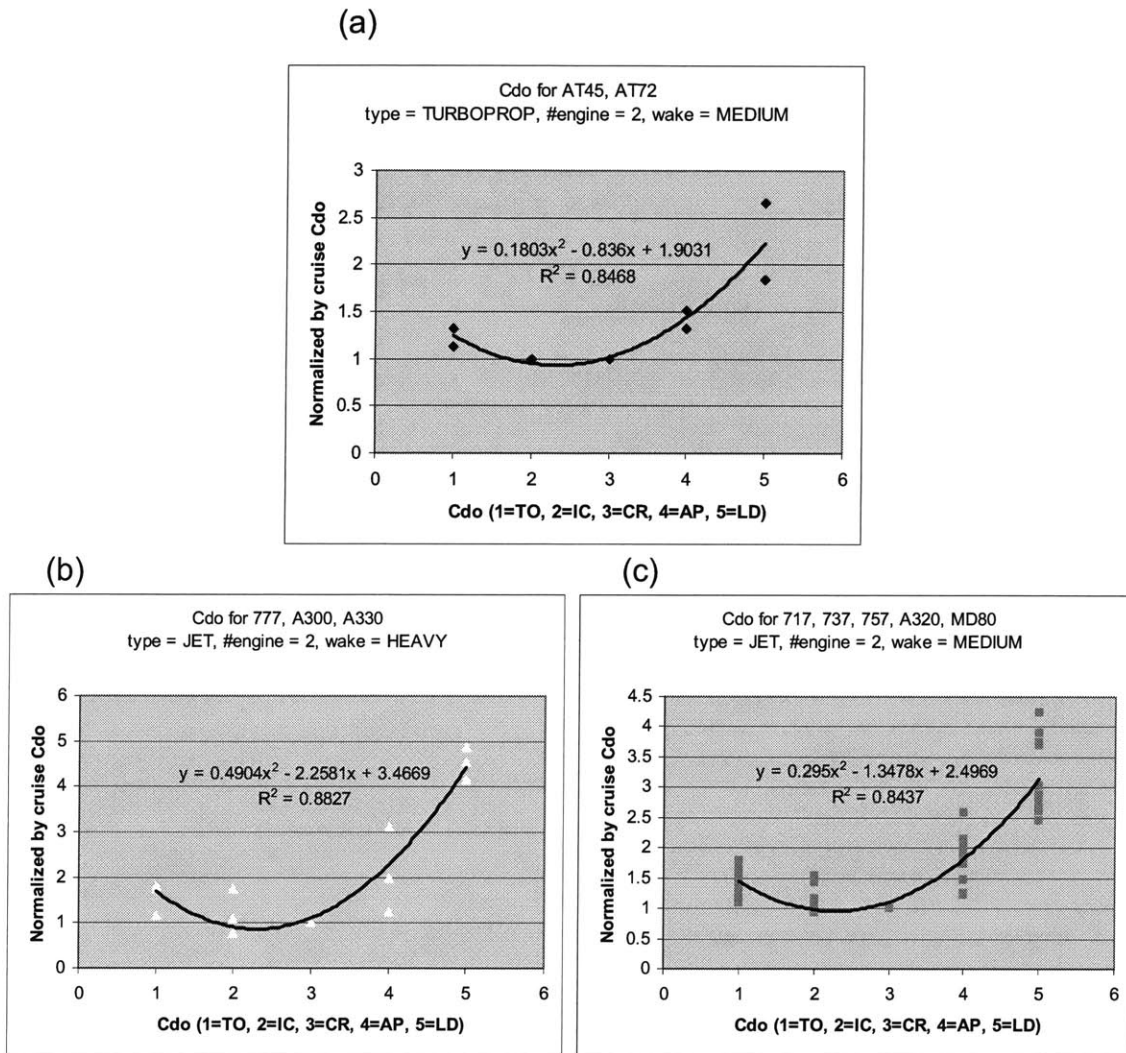
Figure 3.18 BADA C_{D0} values at all modes

Adjusting C_{D0} values based on these curve fits has been shown to reduce over 30% of descent fuel burn error for the A300-600 as shown in Figure 3.19.
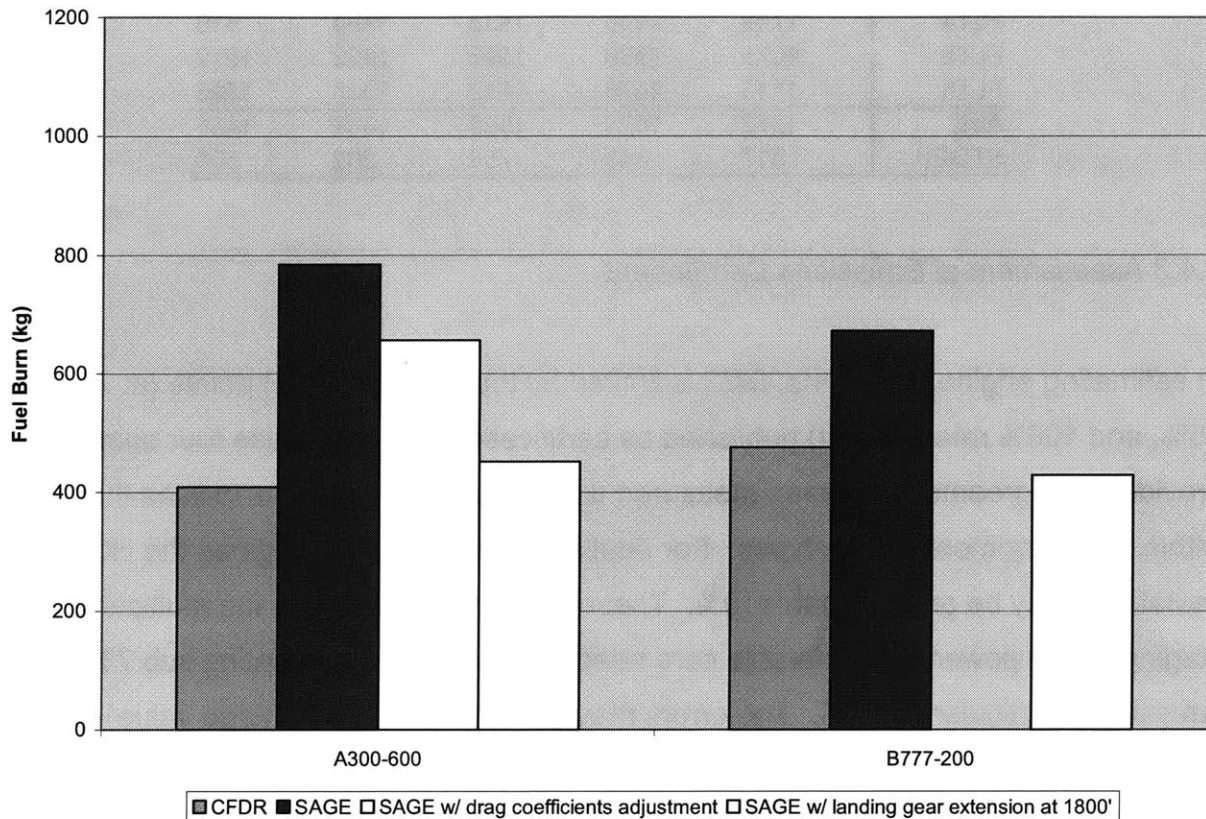
Figure 3.19 Improvements to descent fuel burn modeling

SAGE is also currently programmed to deploy the landing gear and full flaps at 3000 ft above the elevation at the airport. This causes large drag and overestimation of descent fuel burn when compared to CFDR information. Table 3.6 shows reported landing gear extension heights for various aircraft types. On average, the landing gear is extended at 1800 ft above the ground, with a standard deviation of 600 ft. Based on this, lowering the landing gear extension height to 1800 feet has been shown to reduce most of the descent fuel burn error for the A300-600 and the B777-200 as shown in Figure 3.19.

Table 3.6 Landing gear deployment height for various aircraft types

(Source: CFDR of a major US airline)

(in feet)	A300-600	B737-800	B757-200	MD80S	MD83
FLT1	835	1176		1538	1707
FLT2	1371	1173	3319	1660	1390
FLT3	1491	2240	1561	1890	1519
FLT4	1719	1986	1836	1834	516
FLT5	1075	1889	1597	1622	1979
FLT6	1143	2478	1612	1335	1595
AVE	1272	1824	1985	1647	1451
STDEV	317	543	754	202	500

3.4.3 Assessment of Emissions Component

In estimating engine emissions, BM2 is limited by the four, sea-level points (at 7%, 30%, 85%, and 100% rated output) published as certification data. At these four points, BM2 provides an agreement between measured and calculated emissions indices that is within ±10% for most engine types. For dual annular combustor engines the HC deviations may be greater than ±10%. These deviations are due to the multiple fuel staging at low power. Considerable care needs to be taken in estimating sub 7% idle emissions, particularly of HC. The errors may be large (as a percentage value) and tend to be an under-prediction [CAEP, 2004].

The interpolation method (i.e. use of the ICAO emissions indices and curve-fitting between them) is another source of uncertainty. For example, BM2 uses a bi-linear fit on a log-log scale, having a horizontal mean line through the lowest two certification power settings, and then a second line connecting the two highest settings. For NOx, a single best fit line is used on the log-log scale. A comparison undertaken by ICAO [Penner et al., 1999] found agreement between direct measurement and fuel flow correlations using curve-fitted ICAO data to within a standard deviation of 6% and a maximum error of 13%.

Other sources of uncertainty in most emissions data, including certification data, are the variability in emissions inherent among engines in the fleet and aging of the engine

[Fring, 1980; Lukachko and Waitz, 1997; CAEP, 2004]. Engine certification procedures are based on historical experience in engine-to-engine variability [FR 58; FR 251; FR 155]. The resulting compliance factors imply that 67% confidence intervals for EINOx, EIHC and EICO of any engine picked out of a fleet of engines based on a single engine sampled three times would be approximately ±16%, ±54% and ±23%, respectively. These standard deviations measure variability in the fleet based on new, uninstalled engine performance, not the precision error in the measurement of a particular engine, which is typically lower than 1% for all certification measurements [Lukachko and Waitz, 1997]. Note also that the estimated standard deviations are based on studies conducted in the late 1970's. As engines have evolved since then with a significant effort in reducing the variability in performance, these uncertainty estimates may be conservative numbers.

A further source of uncertainty is found in the aging of the engine. The impact of lifecycle deterioration on emissions must be discerned from the baseline of variability in emissions indicated by the scatter in data taken for new engines. Lukachko and Waitz [1997] found a maximum, but partially recoverable (with maintenance) change in average EINOx with aging of between -1% and +4% for typical aging scenarios. The sensitivity of SFC and combustor flow parameters to component aging is enhanced by increases in cycle temperatures and pressures (which are representative of more advanced technology).

Based on all of the above, ±24% uncertainty for EINOx has been conservatively estimated by aggregating the 16% uncertainty incorporated in the engine certification process, adding (using sum of squares) the uncertainty in curve-fitting and BM2 (6% and 10%, respectively) and then accounting for the bias error due to degradation (4%).

The uncertainties in the certification process for EIHC and EICO (54% and ±23%, respectively) have been also aggregated with those in curve-fitting and BM2. As a result, 1σ uncertainty of ±55% has been obtained for EIHC and ±26% for EICO. These

79

estimated uncertainties are to be confirmed by comparing SAGE emissions results to actual emissions data, which are not readily available at present.

In this chapter, SAGE performance has been assessed at both the modular and system levels. On average, SAGE predicts reported fleet fuel burn with less than 6% error. On an individual flight basis, the error can be as large as 18% with 1σ confidence. The next chapter presents a parametric uncertainty analysis that reveals the biggest contributors to fuel burn and emissions errors in SAGE. It summarizes uncertainties at both the modular and system levels as a roadmap for model improvement and a reference for assessing uncertainties in the technology and policy scenarios considered.

CHAPTER 4

UNCERTAINTY ANALYSIS II: PARAMETRIC STUDY

The objective of this chapter is to identify the most influential uncertainties in SAGE and to quantify the magnitude of their impact on system-level performance. The uncertainties that have the largest impact on global fuel burn and emissions estimates are first examined followed by those that impact local air quality. Note that the uncertainties due to unscheduled and canceled flights are not fully addressed in this thesis.

As previously discussed, the most influential uncertainties for global fuel burn results are: use of standard day ambient temperature, not correcting for winds aloft, uncertain aerodynamic and engine performance, and simplified assumptions about aircraft take-off weight and flight speed. Additional uncertainties associated with the use of OAG-based flight trajectories are considered only for OAG flights. Uncertainties in emissions estimated are also significantly influenced by uncertainties in emissions indices.

A sensitivity analysis is performed first to show the effects that the key uncertainties have on estimates of aggregate, fleet-level fuel burn and emissions. In order to quantify the magnitude of their impact on system errors, errors in total fuel burn results are correlated with uncertainties in key input parameters. Monte Carlo simulations are employed to assess the unique contribution of each key input uncertainty to the variance and mean of total error.

4.1 SENSITIVITY ANALYSIS

Figure 4.1 shows changes in SAGE emissions due to 1% increase in specific fuel consumption, aerodynamic drag, take-off weight, flight speed (headwind impact), ambient temperature (in K) and altitude during cruise. The results are based on all aircraft types in SAGE. They were flown under the same cruise conditions—altitude of

35,000 ft at Mach 0.8. Their fuel burn and emissions were then aggregated based on fuel burn weighting. For 1% increase in SFC, fuel burn increases by 1% because it is directly impacted by the SFC increase through higher fuel flow rate. NOx emissions increase by almost 2%, which shows a higher sensitivity to fuel flow change. This is due to the fact that $EINO_x$ increases proportionally with increasing fuel flow so that the overall impact of higher $EINO_x$ and fuel burn is multiplicative. HC and CO emissions decrease by 0.5% and 0.2%. This is because EIHC and EICO are inversely proportional to fuel flow rate so that the net impact of a lower EI combined with somewhat increased fuel flow leads to a relatively smaller increase or even a reduction in total emissions, depending on the sensitivity of EI to fuel flow.
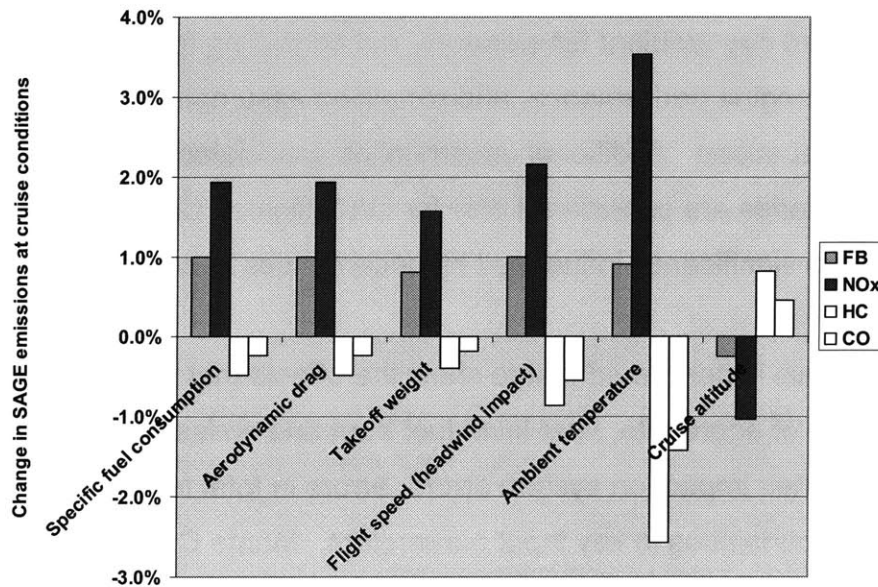
Figure 4.1 Changes in SAGE emissions due to 1% increase in key input variables
(Cruise at 35,000 ft, M0.8, all aircraft types in SAGE)

For 1% increase in aerodynamic drag, fuel burn increases by 1% while NOx emissions increase almost 2%. This is because higher drag requires increased engine power and hence increased fuel flow to keep the airplane at the same cruise speed. Note that the net effect of increased drag is the same as that of increased SFC because thrust is equal to drag during cruise. It should be noted, however, that the SFC and drag effects are not strictly linear. For example, burning more fuel for the same mission (due to

increased SFC or drag) requires that the airplane have a higher take-off weight (due to the added fuel on board). This increased take-off weight then leads to additional fuel burn for the mission [Baughcum *et al.*, 1996]. For the cruise sensitivity study presented here, these effects are not captured and therefore the estimated sensitivities may be an underestimate.

Similar trends are observed with respect to 1% increase in take-off weight as well as flight speed. This is because higher aircraft weight or stronger headwind also impacts fuel flow rate through increased engine power. The fact that all emissions species have a higher sensitivity to flight speed change is also notable. This results from the Mach number correction in BM2 as discussed in Section 2.1.2 above so the higher the change in flight speed, the larger the change in EI's and total emissions.

Figure 4.1 also shows changes in SAGE emissions due to 1% increase in ambient temperature (in K). While fuel burn increases by about 1%, NOx emissions increase by as much as 3.5% and HC and CO emissions decrease about 2.5% and 1.5%, respectively. Higher ambient temperature requires higher engine power through increased aerodynamic drag. In addition, a temperature correction term in BM2 leads to the high sensitivity of emissions species to ambient temperature change. If temperature effects that lower engine fuel flow performance are considered (but not currently modeled in SAGE), they may cause even higher sensitivity.

The most influential uncertainties in SAGE are judged by their impact on SAGE outputs using a "biggest-hitters" analysis. This impact is a result of the multiplicative effects of high uncertainty and high sensitivity. That is, a parameter that has high uncertainty and causes high model sensitivity has the biggest impact on system error. Current SAGE analysis shows that a 3.3 K (1σ uncertainty) increase in ambient temperature results in less than 2% increase in fuel burn. Therefore, ambient temperature may not be major contributor to fleet-level fuel burn errors. Temperature effects, however, can grow much more important on individual flight fuel burn or emissions estimates as illustrated in the

sensitivity analysis. For this reason, the ambient temperature remains in the analyses of the subsequent sections.

Figure 4.1 shows the effect of increased cruise altitude as well. Fuel burn and NOx emissions decrease by 0.2% and 1.0%, respectively. A higher cruise altitude is associated with a lower air density, which reduces the drag on the airplane body. Since this lowers the thrust required and fuel flow rate, the HC and CO emissions increase by 0.8% and 0.4%, respectively.

4.2 INTRODUCTION TO ROLL-UP OF UNCERTAINTIES

% error in fuel burn = -.0127 + .761 * % error in winds aloft
Correlation: r = .874
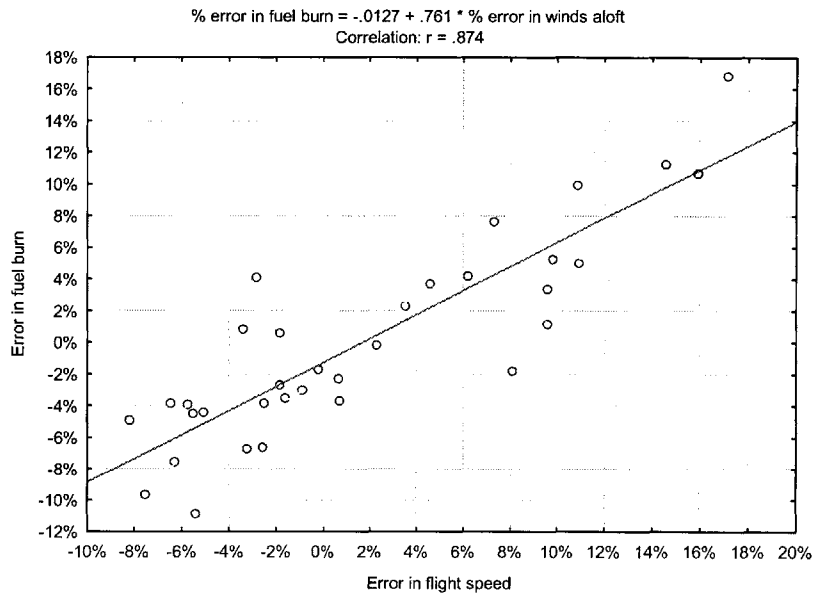
Figure 4.2 Contribution of uncertainty in winds aloft to total error in fuel burn (B747-400)

In this section, the impact of the key input uncertainties on final output error is quantified. For example, a large portion of fuel burn error can be attributed to the fact that SAGE Version 1 assumes no winds aloft. In order to quantify the effects of the no wind assumption, 34 flights from the major European carrier's B747-400 CFDR data in October 2000 were randomly selected. Detailed position, actual TOGW, winds aloft, and ambient temperature information were obtained from the sample. To determine the effects of the no wind assumption, actual position and TOGW were used as input to

SAGE, and errors in flight speed were calculated. Figure 4.2 shows that fuel burn error is highly correlated with flight speed error as indicated by the correlation factor of 0.87.

A more systematic uncertainty roll-up can be performed via Monte Carlo simulation. The key uncertainties are randomly varied according to the mean and standard deviation established in the previous chapter, and a fuel burn calculation is made for each set of randomly varied inputs. This allows for quantifying the unique contribution of each key uncertainty to total error.

4.3 UNCERTAINTY ROLL-UP FOR FULL-MISSION FUEL BURN

4.3.1 Monte Carlo Simulation

Table 4.1 Key input uncertainties for Monte Carlo simulation on SAGE flights
(Dispersion track and cruise altitude applicable to OAG flights only)

Parameters	Uncertainty estimates	Approximated distribution
Dispersion track (OAG only)	±5% of flight time (1σ)	Normal
Cruise altitude (OAG only)	±3000 ft (1σ)	Discrete Normal
Ambient temperature at cruise	3.3 K (1σ)	Normal (one sided)
Winds aloft	±12.5 m/s (1σ)	Normal
Aerodynamic drag	±14% (1σ)	Normal
Engine fuel consumption	±11% (1σ)	Normal
Takeoff weight	±13% (1σ)	Normal

The values for the key uncertainties are randomly generated based on a normal distribution where their default values as used in SAGE are assumed to be the mean. Cruise altitude deviations from the mean altitude are generated using a discrete normal distribution with a 1000 foot increment. Ambient temperature deviations from the ISA temperature are generated using a one-sided normal distribution in between 0K and 3.3K (1σ). This is because the Boeing analysis (see Chapter 3 Section 3.3.2.1) showed that at cruise altitudes, temperature deviations occur only above the standard day temperature [Daggett el al., 1999]. Table 4.1 shows seven key uncertainties with their estimated standard deviations for a simulation on SAGE flights. All 11 aircraft types of

the major US carrier (e.g. B727-200, B737-800, B757-200, B767-200, B767-300, B777-200, A300-600, DC10, MD80, MD90 and F100) are used. Dispersion track and cruise altitude uncertainties are included only with a simulation on OAG flights to account for the additional uncertainty caused by artificial flight trajectories used.

Based on these inputs, 3000 iterations were performed for both sets of ETMS and OAG flights. Figure 4.3 shows the simulation results for the fuel burn of ETMS flights. The difference between the nominal fuel burn (i.e. with mean input values) and mean fuel burn (i.e. average fuel burn for the distribution) was calculated. The difference was -3.9% with standard deviation of 16.5%. This accounts for about 90% of the total variance in ETMS fuel burn errors in SAGE. Figure 4.4 shows the simulation results for the fuel burn of OAG flights where the difference between nominal fuel burn and mean fuel burn was -5.1% and standard deviation was 17.0%. This accounts for about 95% of the total variance in OAG fuel burn errors in SAGE.
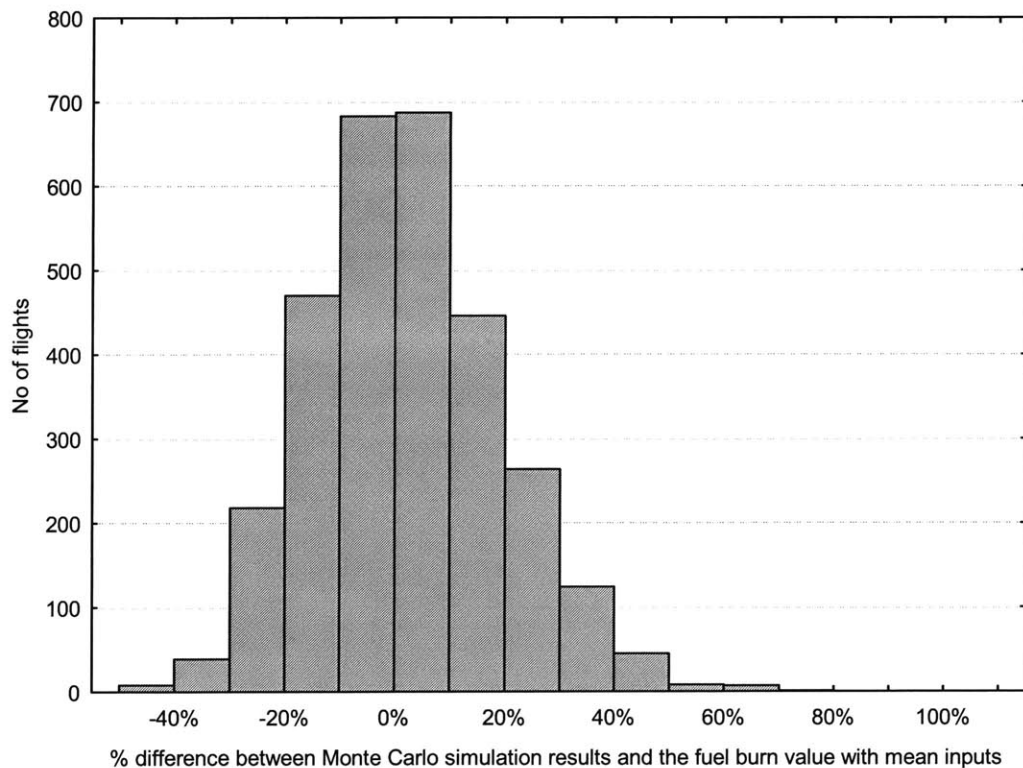
Figure 4.3 Monte Carlo simulation results on ETMS trajectories
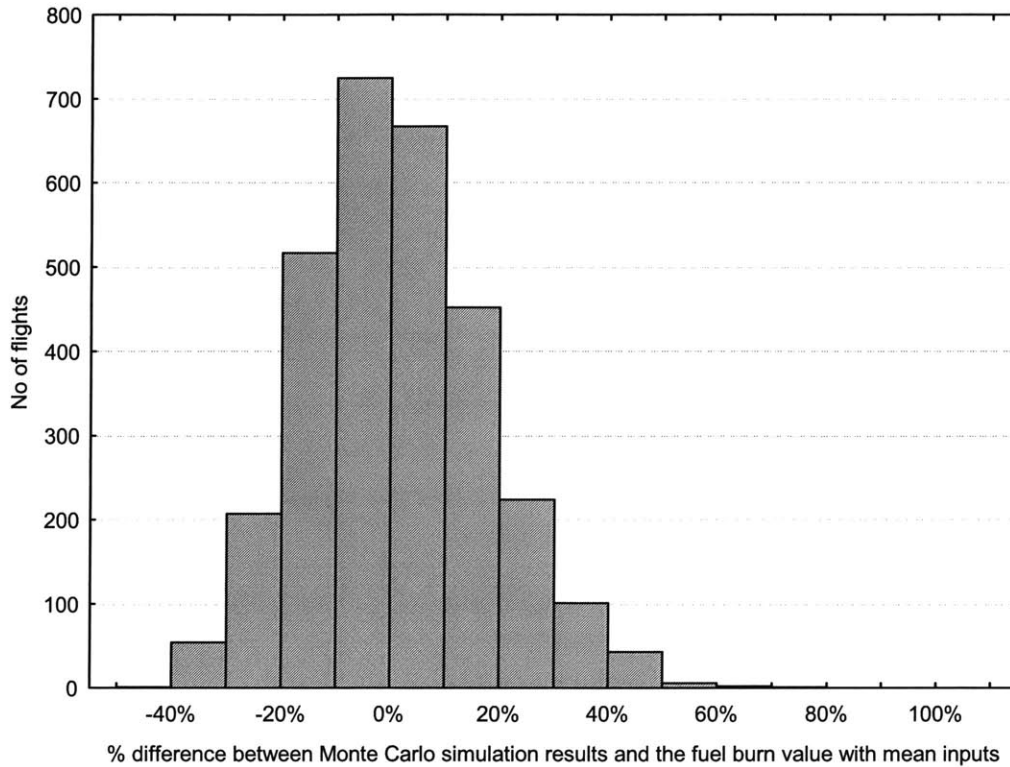
Figure 4.4 Monte Carlo simulation results on OAG trajectories

It is important to check the convergence of the simulation results. The criterion is to examine the total error in the simulation output as following:

Total error, $\varepsilon = \dfrac{3\sigma}{\sqrt{n}}$

where σ = standard deviation of the entire population and n = number of iterations

The standard deviation of the entire population is given by:

$$\sigma = \sqrt{\dfrac{n\sum x^2 - (\sum x)^2}{n^2}}$$

where x = subject variable (fuel burn output in this case)

Figures 4.5 and 4.6 show the convergence history of ETMS and OAG flights, respectively. After 1500 iterations, both ETMS and OAG flights converge with less than 2% error.
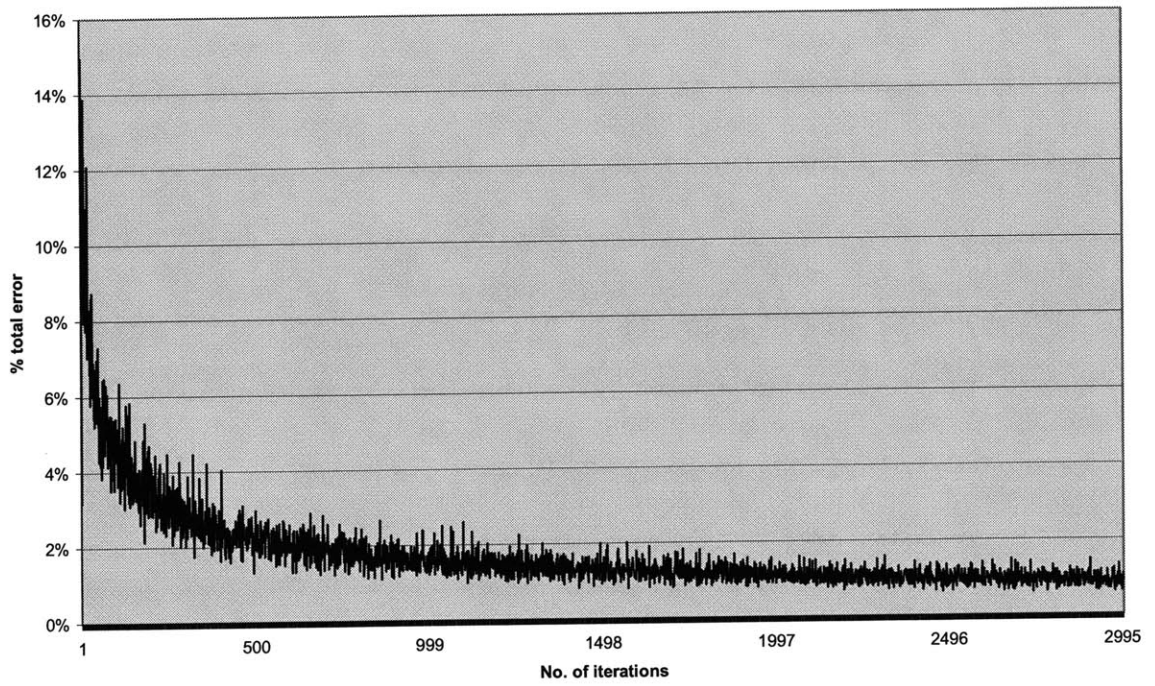
Figure 4.5 Convergence history of Monte Carlo simulation on ETMS trajectories
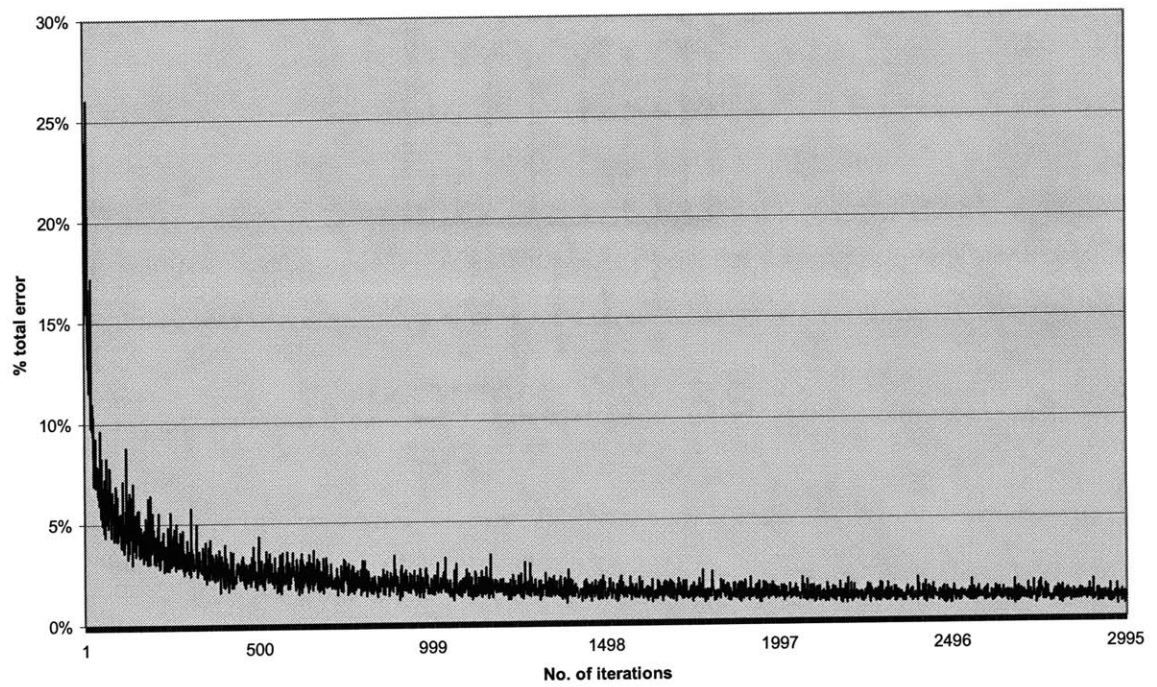
Figure 4.6 Convergence history of Monte Carlo simulation on OAG trajectories

88
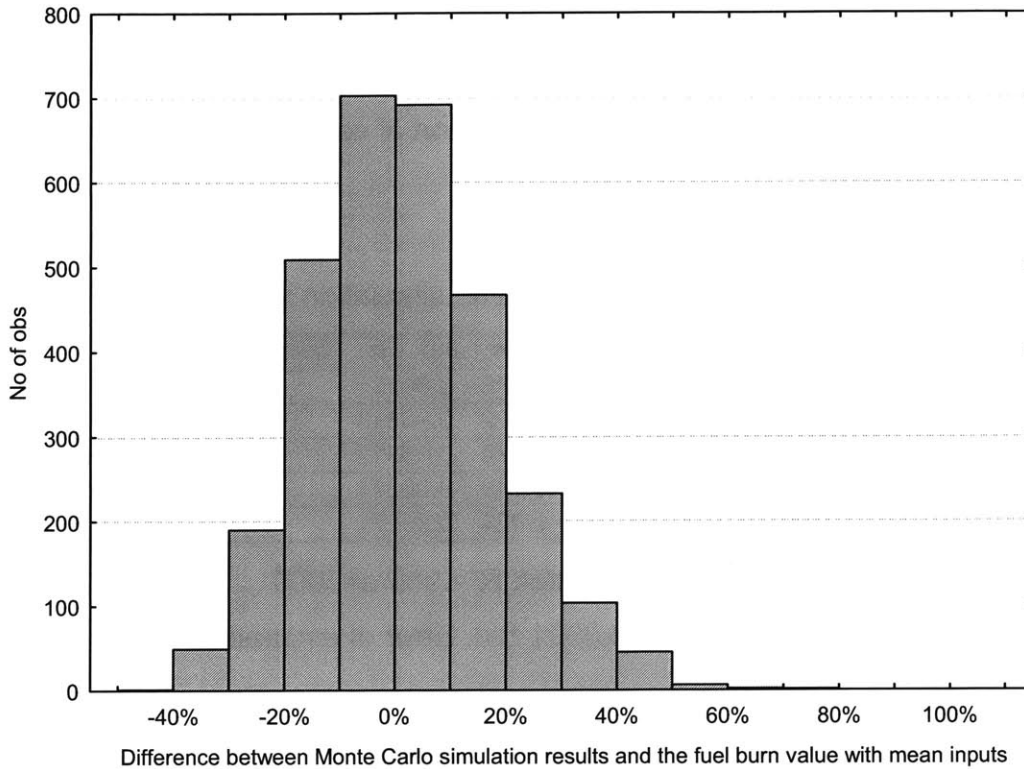
Figure 4.7 Monte Carlo simulation results of all aircraft types in SAGE on OAG trajectories

Simulation results based on 11 aircraft types (B727-200, B737-800, B757-200, B767-200, B767-300, B777-200, A300-600, DC10, MD80, MD90 and F100) were shown to compare directly to the error distribution for the 35,356 flights for a major US carrier. Figure 4.7 shows the same type of uncertainty roll-up for all aircraft types in SAGE. The difference between nominal fuel burn and mean fuel burn is -4.4% with standard deviation of 16.0%. This result shows that the 11 aircraft types represent well the aircraft performance characteristics and associated uncertainties in the full SAGE fleet (359 aircraft types).

4.3.2 Understanding Variance of Error

In order to quantify the unique contribution of the key uncertainties to total error, the fuel burn results of the Monte Carlo simulations are regressed on the input values. Both the input and the output values are standardized (i.e. z-scored) by subtracting the mean

from the respective value and dividing the difference by the standard deviation. Tables 4.2 and 4.3 show the regression results for ETMS and OAG flights. The magnitude of the beta coefficients shows the relative contribution of each key uncertainty in the prediction of fuel burn.

Table 4.2 Regression among the Monte Carlo simulation variables for ETMS flights

	Beta	Std. Err.	Contribution to Var.
Engine fuel consumption	0.480	0.00271	29.4%
Aerodynamic drag	0.592	0.00313	44.7%
Takeoff weight	0.374	0.00312	17.9%
Winds aloft	0.249	0.00271	7.91%
Ambient temperature at cruise	0.024	0.00271	0.075%

$R^2 = .986$ Adjusted $R^2 = .986$ n=3000

$F(5,2994) = 26848.$ $p < 0.0001$ Std. Error of estimate: .12113

where:

Beta = standardized regression coefficient

Standard Error = standard deviation of the estimated coefficient or relationship

R^2 = the coefficient of determination (variance in the dependent variable that is explained by the independent variables)

Adjusted R^2 = R^2 adjusted by the degrees of freedom of both the numerator and the denominator

F = F-statistic (for the regression result to be significant)

p = p-value (probability for the regression result to be false)

Table 4.3 Regression among the Monte Carlo simulation variables for OAG flights

	Beta	Std. Err.	Contribution to Var.
Engine fuel consumption	0.480	0.00271	24.0%
Aerodynamic drag	0.592	0.00313	36.5%
Takeoff weight	0.374	0.00312	14.6%
Winds aloft	0.249	0.00271	6.46%
Ambient temperature at cruise	0.024	0.00271	0.061%
Cruise altitude	-0.111	0.00374	1.28%
Dispersion track	0.406	0.00374	17.1%

$R^2 = .968$ Adjusted $R^2 = .967$ n=3000

$F(7,2992) = 9991.7$ $p < 0.0001$ Std. Error of estimate: .16670

For ETMS flights, the uncertainties in engine and aerodynamic performance are the largest sources of error, together accounting for over 70% of the total variance. The take-off weight and winds aloft uncertainties account for 17.9% and 7.9%, respectively. The ambient temperature uncertainty accounts for less than 1% of the error. However, on an individual flight basis on a specific day or in a region, the ambient temperature uncertainty can be large and therefore become a major source of fuel burn error. For OAG flights, the engine and aerodynamic performance uncertainties also account for the largest fraction of the error, 24.0% and 36.5% each. The take-off weight uncertainty accounts for 14.6% of the error while the winds aloft uncertainty accounts for 6.5%. The uncertainties in dispersion track explain most of the remaining variance, 17.1%. The cruise speed and ambient temperature uncertainties together comprise less than 2% of the total variance.

4.3.3 Understanding Bias Error

In the previous chapter, it was shown that the average fuel burn error was around -6% for both ETMS and OAG flights. This indicates a bias error in SAGE. In order to understand why fuel burn in SAGE is underestimated, another statistical technique (namely "vary all but one") is employed.

Figure 4.8 shows two uncertainty roll-up results. One ("vary all") is the same histogram from the Monte Carlo simulation of the 7 key uncertainties on OAG trajectory with 11 aircraft types as seen before. The other ("vary all but take-off weight") is a result of a Monte Carlo simulation of only 6 key uncertainties on OAG trajectory where take-off weight uncertainty has been frozen. Since there is one less source of uncertainty, the mean and standard deviation of the fuel burn differences change. The magnitude of this mean shift indicates the unique contribution of the respective variable to bias error. In this case, take-off weight is responsible for about 1% mean shift.
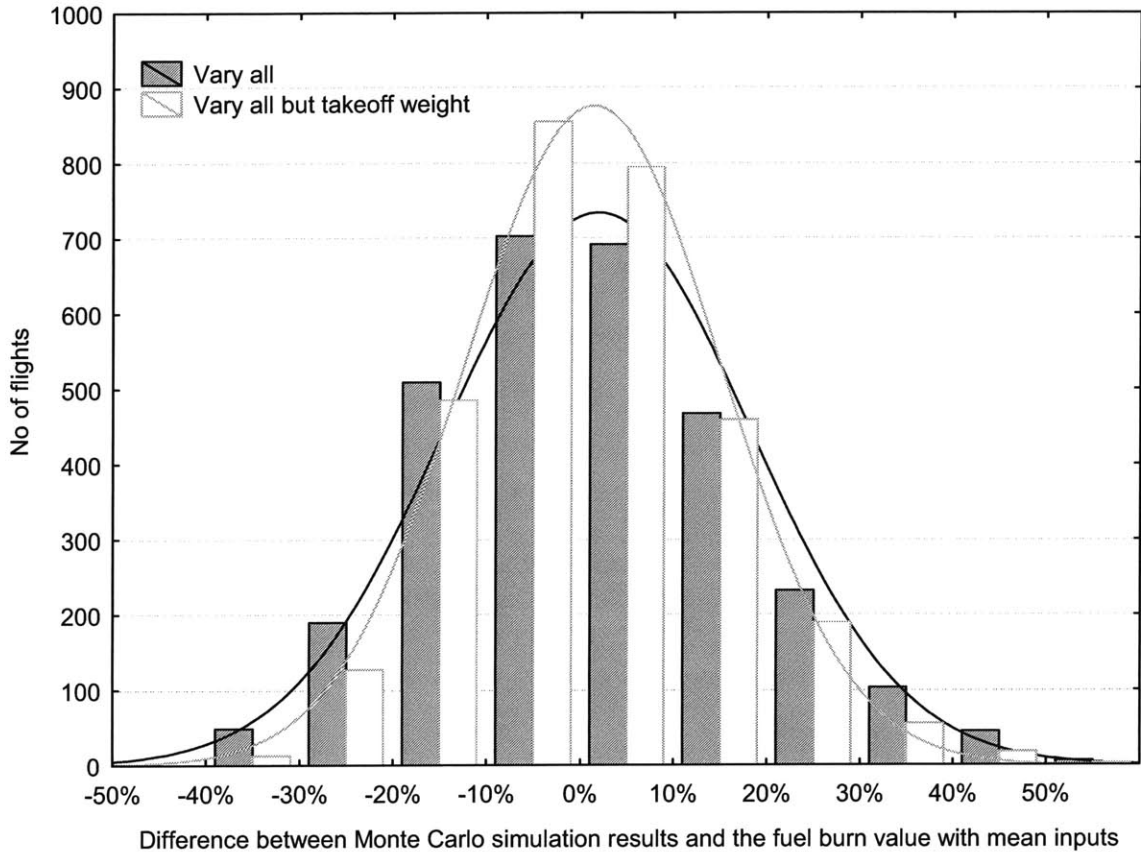
Figure 4.8 Vary-all-but-one technique to understand bias error

By freezing the variability of one source of uncertainty at a time, a complete "vary all but one" analysis for the 7 key uncertainties has been conducted and summarized in Table 4.4. Mean shifts are shown with their confidence intervals. With the exception of dispersion track, all the key uncertainties together cause the mean fuel burn to be shifted by -4% to -5%. As previously noted (see Chapter 3 Section 3.3.2.2), a round trip with a wind component burns 1-2% more fuel than without a wind component. Also, take-off weights distributed normally around a nominal value (as used in SAGE) lead to burning more fuel than for the case of using the single nominal weight. Thus not having a wind component or using a true take-off weight would lead to an underestimation of fuel burn when a large number of flights are aggregated. On the other hand, the large standard errors associated with the estimated mean shifts due to SFC and ambient temperature imply that the mean shifts could occur in the other direction.

OAG flights would have a larger bias due to the additional uncertainty in cruise altitude, which is estimated to cause a mean shift of -1.0%. When the standard errors of the estimated mean shifts are considered, most of the mean error in SAGE fuel burn (-6%) seems to be explained by the key uncertainties examined here. This is also consistent with the 4-5% difference in nominal fuel burn and mean fuel burn described earlier (see Section 4.3.1).

Table 4.4 Estimated contributions of key uncertainties to mean shift

Parameters	Contribution to mean shift
Engine fuel consumption	-0.073% ± 0.36%
Aerodynamic drag	-0.81% ± 0.28%
Takeoff weight	-1.3% ± 0.34%
Winds aloft	-1.8% ± 0.31%
Ambient temperature at cruise	-0.38% ± 0.38%
Cruise altitude	-1.0% ± 0.37%
Dispersion track	0.012% ± 0.38%

4.4 UNCERTAINTY ROLL-UP FOR FUEL BURN BELOW 3000 FEET

Below 3000 ft where aircraft emissions have a greater impact on local air quality, LTO procedures become an important uncertainty. LTO procedures mainly consist of engine throttle setting, rate of climb/descent and flight speed. Based on the previous analysis of the major carrier's CFDR data (see Chapter 3 Section 3.3.4.2), the engine throttle setting at take-off is assumed to have 10% derate with 1σ confidence. The rate of climb/descent and flight speed together are assumed to cause a 30% increase in time-to-climb and time-to-descend with 1σ confidence when compared to SAE AIR 1845's standard procedures (see Chapter 3 Section 3.4.2).

The ambient temperature uncertainty is estimated to be 10K with 1σ confidence, which is larger than for the full-mission uncertainty roll-up. This is because deviations from the standard day temperature are larger (mostly ranging ±20K) near the ground across four seasons. Table 4.5 summarizes these uncertainty estimates for an uncertainty roll-up below 3000 ft.

Table 4.5 Key input uncertainties for Monte Carlo simulation of LTO fuel burn

Parameters	Uncertainty estimates	Approximated distribution
Ambient temperature	±10 K (1σ)	Normal
Winds aloft	±12.5 m/s (1σ)	Normal
Aerodynamic drag	±14% (1σ)	Normal
Engine fuel consumption	±11% (1σ)	Normal
Takeoff weight	±13% (1σ)	Normal
Rate of climb/descent + speed	+30% of flight time (1σ)	Normal (one sided)
Takeoff throttle setting	-10% (1σ)	Normal (one sided)

Based on these inputs, 3000 Monte Carlo runs were performed for the 11 aircraft types flown on OAG trajectories. The mean difference in fuel burn was -1.8% with standard deviation of 46.5%. Table 4.6 shows the results of a regression among the standardized input and output values of the Monte Carlo simulation. The rate of climb/descent and flight speed account for 61.8% of the variance while drag, wind and ambient temperature together account for most of the remaining variance. Note that the increased uncertainty in ambient temperature leads to the larger effect of ambient temperature on the fuel burn results below 3000 ft.

Table 4.6 Estimated contributions of key uncertainties to variance of LTO fuel burn

	Beta	Std. Err.	Contribution to Var.
Ambient temperature	0.295	0.00928	9.15%
Winds aloft	0.316	0.00934	10.5%
Aerodynamic drag	0.404	0.00928	17.1%
Engine fuel consumption	0.090	0.00929	0.852%
Takeoff weight	-0.016	0.00932	0.025%
Rate of climb/descent + speed	0.768	0.00930	61.8%
Takeoff throttle setting	0.075	0.00930	0.583%

$R^2=.915$ Adjusted $R^2=.914$ n=3000

$F_{(7,2992)}=1518.3$ $p<0.0001$ Std. Error of estimate: .29321

4.5 UNCERTAINTY ROLL-UP FOR FULL-MISSION EMISSIONS

In the previous chapter, the uncertainties in emissions indices were estimated to be ±24%, ±55% and ±26% for EINOx, EIHC and EICO, respectively, at 1σ confidence.

Table 4.7 summarizes them along with the key uncertainties for full-mission fuel burn results.

Table 4.7 Key input uncertainties for Monte Carlo simulation of emissions

Parameters	Uncertainty estimates	Approximated distribution
Dispersion track (OAG only)	±5% of flight time (1σ)	Normal
Cruise altitude (OAG only)	±3000 ft (1σ)	Discrete Normal
Ambient temperature at cruise	3.3 K (1σ)	Normal (one sided)
Winds aloft	±12.5 m/s (1σ)	Normal
Aerodynamic drag	±14% (1σ)	Normal
Engine fuel consumption	±11% (1σ)	Normal
Takeoff weight	±13% (1σ)	Normal
EINOx	24% (1σ)	Normal
EIHC	55% (1σ)	Normal
EICO	26% (1σ)	Normal

Based on these inputs, 3000 Monte Carlo runs were performed for the 11 aircraft types flown on OAG trajectories. The standard deviations for NOx, HC and CO were 40.0%, 60.0% and 31.6%, respectively. The differences between the nominal (i.e. with mean input values) and the mean (i.e. average for the distribution) emissions were calculated. The differences were -8.2%, -9.4% and -4.7% for NOx, HC and CO results, respectively. In order to quantify the unique contribution of the key uncertainties to these emissions results, a regression was performed among the standardized input and output values of the Monte Carlo simulation.

Table 4.8 Estimated contributions of key uncertainties to variance of NOx emissions

	Beta	Std. Err.	Contribution to Var.
Engine fuel consumption	0.291	0.00593	11.2%
Aerodynamic drag	0.389	0.00682	20.1%
Takeoff weight	0.252	0.00681	8.45%
Winds aloft	0.202	0.00592	5.43%
Ambient temperature at cruise	0.128	0.00592	2.17%
Cruise altitude	-0.143	0.00592	2.71%
Dispersion track	0.180	0.00609	4.28%
EINOx	0.587	0.00608	45.7%

$R^2 = .930$ Adjusted $R^2 = .930$ n=3000

$F_{(8,2991)} = 3331.9$ $p < 0.0001$ Std. Error of estimate: .26416

Table 4.8 shows the regression results for NOx emissions. EINOx is the biggest hitter accounting for over 45% of the variance. Drag and engine fuel consumption are the next biggest hitters explaining 20.1% and 11.2%, respectively. Tables 4.9 and 4.10 show the regression results for HC and CO emissions. EIHC and EICO are the single most influential contributors to the variance of HC and CO emissions results, respectively.

Table 4.9 Estimated contributions of key uncertainties to variance of HC emissions

	Beta	Std. Err.	Contribution to Var.
Engine fuel consumption	0.041	0.00413	0.180%
Aerodynamic drag	0.056	0.00475	0.326%
Takeoff weight	0.031	0.00475	0.099%
Winds aloft	0.027	0.00412	0.074%
Ambient temperature at cruise	-0.074	0.00412	0.583%
Cruise altitude	0.005	0.00413	0.002%
Dispersion track	0.107	0.00413	1.20%
EIHC	0.963	0.00413	97.5%

$R^2 = .966$ Adjusted $R^2 = .966$ n=3000

$F(8,2991) = 7133.9$ p<0.0001 Std. Error of estimate: .18397

Table 4.10 Estimated contributions of key uncertainties to variance of CO emissions

	Beta	Std. Err.	Contribution to Var.
Engine fuel consumption	-0.086	0.00393	0.747%
Aerodynamic drag	-0.117	0.00453	1.37%
Takeoff weight	-0.080	0.00452	0.634%
Winds aloft	-0.058	0.00393	0.337%
Ambient temperature at cruise	-0.294	0.00393	8.65%
Cruise altitude	0.127	0.00393	1.61%
Dispersion track	0.171	0.00393	2.95%
EICO	0.914	0.00393	83.7%

$R^2 = .969$ Adjusted $R^2 = .969$ n=3000

$F(8,2991) = 7881.4$ p<0.0001 Std. Error of estimate: .17531

4.6 UNCERTAINTY ROLL-UP FOR EMISSIONS BELOW 3000 FEET

Table 4.11 shows the key uncertainties for a Monte Carlo simulation of NOx, HC and CO emissions below 3000 ft. Those uncertainties that impact LTO performance and emissions indices are included as discussed above.

Table 4.11 Key input uncertainties for emissions results below 3000 ft

Parameters	Uncertainty estimates	Approximated distribution
Ambient temperature	±10 K (1σ)	Normal
Winds aloft	±12.5 m/s (1σ)	Normal
Aerodynamic drag	±14% (1σ)	Normal
Engine fuel consumption	±11% (1σ)	Normal
Takeoff weight	±13% (1σ)	Normal
Rate of climb/descent + speed	+30% of flight time (1σ)	Normal (one sided)
Takeoff throttle setting	-10% (1σ)	Normal (one sided)
EINOx	24% (1σ)	Normal
EIHC	55% (1σ)	Normal
EICO	26% (1σ)	Normal

Based on these inputs, 3000 Monte Carlo runs were performed for the 11 aircraft types flown on OAG trajectories. The standard deviations for NOx, HC and CO were 71.2%, 85.0% and 37.3%, respectively. The differences between the nominal and the mean were -3.1%, -1.9% and -3.4% for NOx, HC and CO emissions results, respectively. In order to quantify the unique contribution of the key uncertainties to these emissions results, a regression was performed among the standardized input and output values of the Monte Carlo simulation.

Table 4.12 Estimated contributions of key uncertainties to variance of NOx emissions below 3000 ft

	Beta	Std. Err.	Contribution to Var.
Ambient temperature	-0.145	0.00985	6.38%
Winds aloft	-0.193	0.00985	11.3%
Aerodynamic drag	0.289	0.00985	25.4%
Engine fuel consumption	0.163	0.00985	8.03%
Takeoff weight	0.131	0.00949	5.16%
Rate of climb/descent + speed	0.235	0.00990	16.7%
Takeoff throttle setting	0.013	0.00985	0.0525%
EINOx	0.298	0.00990	27.0%

R^2= .823 Adjusted R^2= .821 n=3000

$F_{(8,2991)}$=1814.8 p<0.0001 Std. Error of estimate: .23627

Table 4.12 shows the regression results for NOx emissions. EINOx is the biggest hitter accounting for 27% of the variance. Drag and the LTO procedure (as modeled by the rate of climb/descent plus flight speed) are the next biggest hitters explaining 25.4% and 16.7% of the variance, respectively.

Table 4.13 Estimated contributions of key uncertainties to variance of HC emissions below 3000 ft

	Beta	Std. Err.	Contribution to Var.
Ambient temperature	-0.210	0.00738	5.08%
Winds aloft	-0.069	0.00739	0.557%
Aerodynamic drag	-0.046	0.00739	0.244%
Engine fuel consumption	0.009	0.00738	0.00986%
Takeoff weight	-0.008	0.00739	0.00811%
Rate of climb/descent + speed	0.398	0.00739	18.4%
Takeoff throttle setting	-0.025	0.00738	0.0718%
EIHC	0.809	0.00739	75.7%

R^2= .892 Adjusted R^2= .892 n=3000

$F_{(8,2991)}$=2055.2 p<0.0001 Std. Error of estimate: .18614

Tables 4.13 and 4.14 show the regression results for HC and CO emissions. EIHC and EICO are the most influential contributors to the variance of HC and CO emissions below 3000 ft. The LTO procedure (as modeled by the rate of climb/descent plus flight speed) also accounts for a significant portion of the remaining variance.

Table 4.14 Estimated contributions of key uncertainties to variance of CO emissions below 3000 ft

	Beta	Std. Err.	Contribution to Var.
Ambient temperature	-0.328	0.00673	11.3%
Winds aloft	-0.089	0.00673	0.833%
Aerodynamic drag	-0.050	0.00674	0.267%
Engine fuel consumption	0.012	0.00673	0.0152%
Takeoff weight	-0.031	0.00672	0.102%
Rate of climb/descent + speed	0.626	0.00673	41.2%
Takeoff throttle setting	-0.040	0.00673	0.164%
EIHC	0.663	0.00673	46.1%

R^2= .911 Adjusted R^2= .910 n=3000

$F_{(8,2991)}$=2523.4 p<0.0001 Std. Error of estimate: .15937

4.7 CHAPTER SUMMARY AND CONCLUSIONS

The previous chapter and this chapter presented an assessment of parametric and model uncertainties in SAGE. On average, the aggregate-level composite fuel burn results showed about -6% difference from reported fuel burn data. It should be noted that many of the uncertainties produce a shift in the mean of the output distribution because of the non-linear nature of many of the relationships. For example, the uncertainties in fuel burn account for most of the -6% mean shift suggested by the error compared to airline data.

In addition to the comparisons to reported data, a sensitivity analysis followed by Monte Carlo simulations confirmed the most significant uncertainties contributing to the variance of fuel burn and emissions results. The analyses showed that the uncertainties in engine and aerodynamic performance have the largest impact on system errors, accounting for around 60-70% of total variance in full-mission fuel burn results. The uncertainties in winds aloft and take-off weight explain another 20-25%. Since the uncertainty in ambient temperature during cruise is relatively very small, its impact on full-mission fuel burn results is minimal.

Ambient temperature has a greater impact on fuel burn results below 3000 ft where aircraft emissions have a greater impact on local air quality. LTO procedures, which consist of engine throttle setting, rate of climb/descent and flight speed, are the most influential uncertainties that drive the variance in SAGE fuel burn results below 3000 ft.

For both global and local emissions, it has been shown that the emissions indices are the most influential uncertainties for the variance in SAGE outputs. The direction of mean shift in the emissions results is consistent with that of the fuel burn results. That is, the NOx, HC and CO emissions tend to produce underestimates from SAGE. The degree of underestimation is two to three times greater for full mission emissions and

roughly the same for emissions below 3000 ft when compared to the magnitude of mean shift in fuel burn results.

CHAPTER 5

APPLICATIONS TO POLICY SCENARIOS

The ICAO's Committee on Aviation Environmental Protection (CAEP) is primarily responsible for monitoring the aviation industry's emissions and noise reduction efforts and seeking further options to mitigate the impacts of aviation on community noise, local air quality and the global atmosphere. Over the years, CAEP has set aircraft engine certification standards and phase-outs of noisy aircraft. In its most recent meeting (CAEP/6), increasing the stringency of NOx emissions standards was one of the issues under consideration. In 2001, CAEP also specifically recommended use of operational practices to reduce aircraft emissions [ICAO, 2001]. In this regard, there is high interest in using SAGE to analyze some of the important technological and operational options for aviation emissions reduction.

This chapter analyzes three aviation policy options. The first is more stringent engine certification standards and their impact on fleet-level emissions. The other two are Continuous Descent Approach (CDA) procedures and derated take-off procedures, which are operational practices. CDA was developed as a means to reduce the community noise impact of aircraft on approach [Clarke et al., 2004] and has not previously been evaluated as to its emissions benefits. Derated take-off procedures are used very frequently by airlines to reduce the maintenance costs by reducing the amount of time the engines are operating at the high temperatures characteristic of full throttle take-offs. While the airline industry uses derated take-off procedures commonly, the procedures are not included in the accounting when emissions fees are calculated at many European airports. Thus there is interest in evaluating the emissions impacts of these procedures.

5.1 ANALYSIS OBJECTIVES

For each policy alternative, fuel burn, emissions and associated uncertainties are analyzed by employing the research version of SAGE. The objectives are to:

- Estimate the fuel burn and emissions benefits of the representative policy options
- Estimate the uncertainty in the prediction of the difference in global aviation emissions between:
    1) a baseline scenario and an increased NOx certification standards scenario
    2) a baseline scenario and a CDA scenario
    3) a baseline scenario and a derated take-off scenario

5.2 GENERAL APPROACH
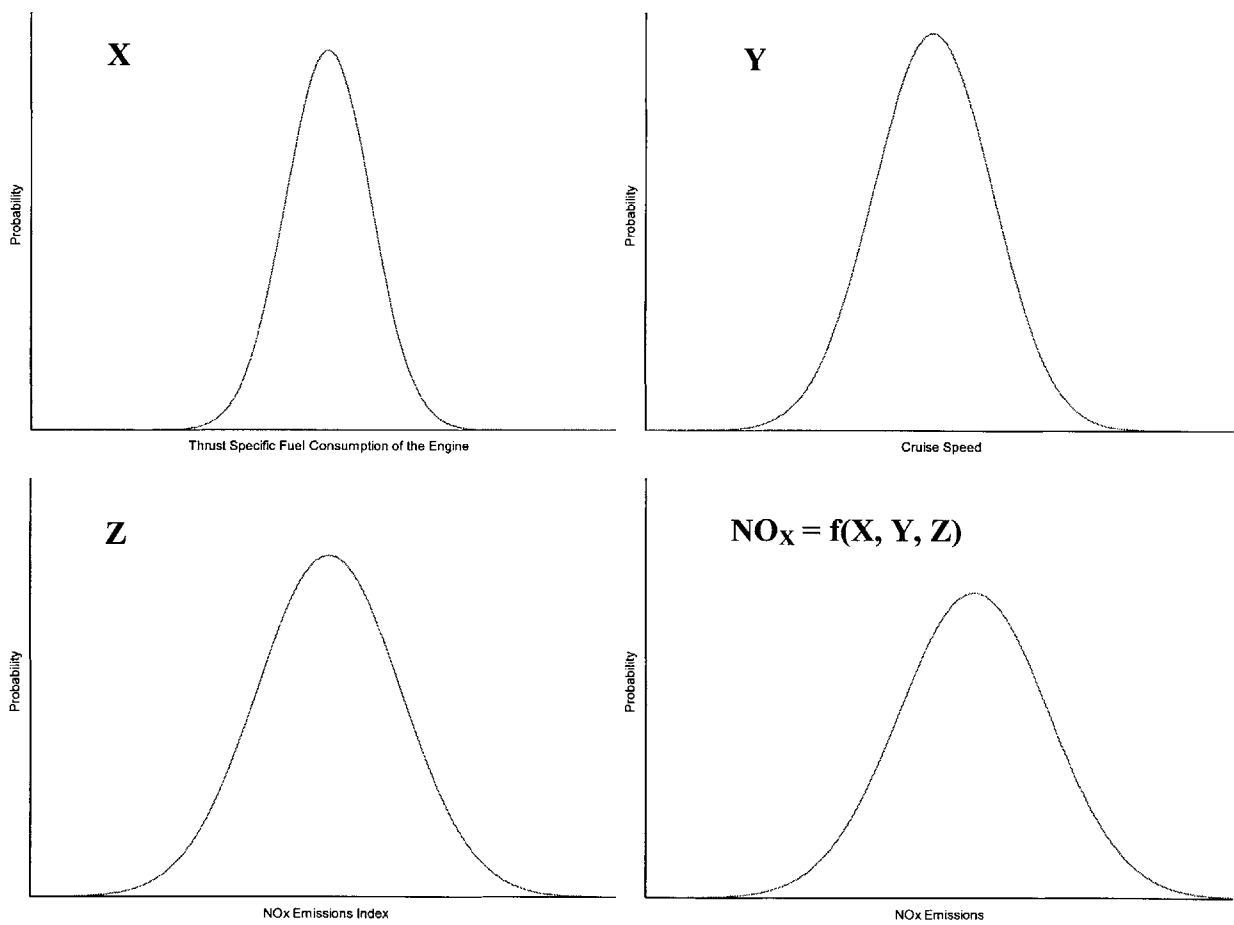
Figure 5.1 Flight-by-flight NO_X output as a function of input variables and uncertainties

102

To consider the difference in emissions between two scenarios where many of the component uncertainties are common, we employ a statistical approach introduced below. The following example illustrates the general approach to quantify the uncertainty in the SAGE prediction of the difference in aviation emissions between a baseline scenario and a more stringent NOx certification standards scenario.

The uncertainty in NO_X output is caused by a number of influential parameters. To simplify the illustration, we take three representative parameters with uncertainties—1) specific fuel consumption (SFC) of the engine, 2) cruise speed and 3) NO_X emissions index (EINOx). The NO_X emission is then a function of these three input variables as shown graphically in Figure 5.1. However, in the modeling presented in the first case study of this chapter, 7 key input and modeling uncertainties are considered.

When we evaluate the change in NO_X ($NO_{X\_}$delta) from no stringency (baseline) to 5% stringency scenario, it is important to account for the uncertainty associated with the estimated $NO_{X\_}$delta. Figure 5.2 shows two NO_X emissions scenarios where the mean NO_X output goes down from no stringency to 5% stringency. If the input uncertainties (i.e. SFC, cruise speed and $EINO_X$) were unrelated from one scenario to the other, then the uncertainty in $NO_{X\_}$delta would be simply estimated by

$$\sigma_{NO_X\_delta} = \sqrt{\sigma^2_{NO_X\_5\%} + \sigma^2_{NO_X\_baseline}} \cdot$$
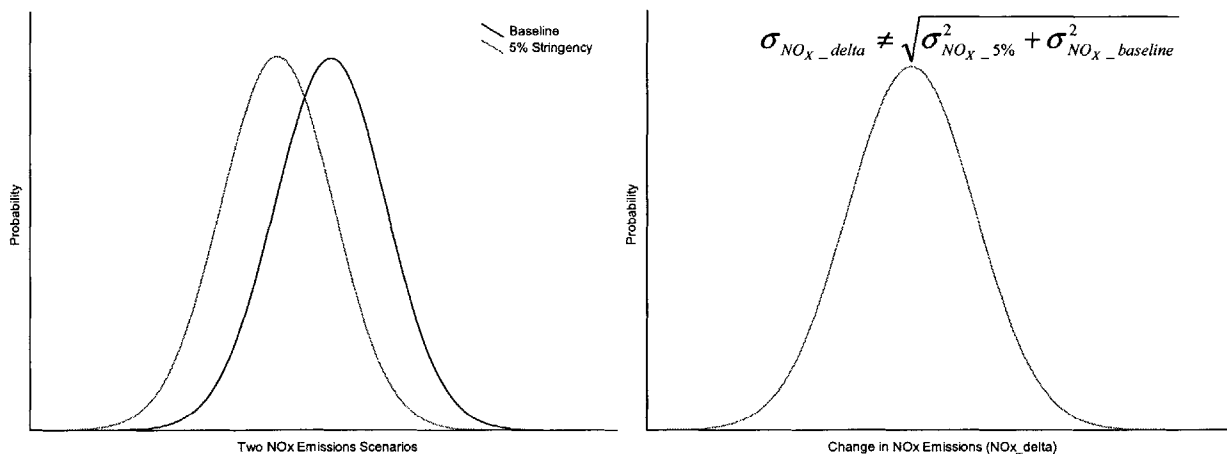
Figure 5.2 Uncertainties in the difference between two scenarios

However, the above equation does not hold when some uncertainties are common from one scenario to the other. We apply the same SFC and cruise speed in both baseline and 5% stringency scenarios while only different $EINO_x$ values are applied to account for the increased stringency on NO_x emissions. In other words, SFC and cruise speed are common uncertainties because it is assumed that the same aircraft types are operated the same way on the same routes for both baseline and 5% stringency scenarios. However, $EINO_x$ is not a common uncertainty because emissions performance (i.e. combustor technology) is improved from baseline to 5% stringency. The uncertainties associated with the new combustor will be different from those with the old combustor. This is why we vary $EINO_x$ uncertainty independently between the two scenarios.

To determine the uncertainty in NO_x_delta we employ a Monte Carlo simulation. Each run consists of a set of random input values. The input values are determined based on the probability distributions specified from above. For each run, the same input values are applied to both baseline and 5% stringency if the uncertainties are common between the two scenarios as illustrated by the green diamonds and hollow circles in Figures 5.3a and 5.3b. Otherwise, independent input values are selected for the two scenarios based on their unique probability distributions as illustrated in Figures 5.3c and 5.3d. These inputs are then run for baseline and 5% stringency scenarios, respectively, and the change in NO_x emissions (e.g. NO_x_delta) is plotted. When this is repeated multiple times, a distribution for NO_x_delta is obtained as shown in Figure 5.3e. This output contains information about the model behavior and the impact of the parameter values assumed.
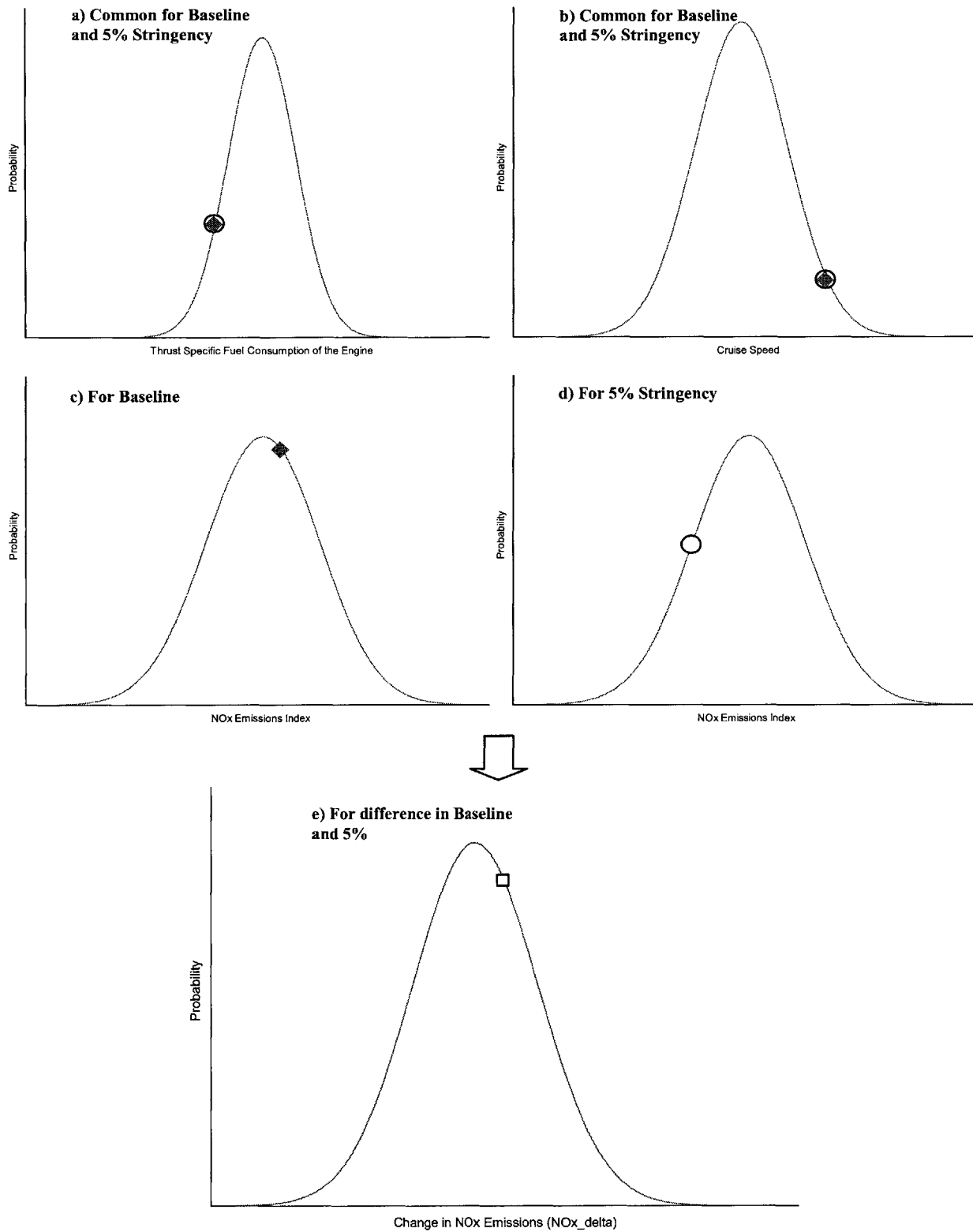
Figure 5.3 Monte Carlo simulation for assessing uncertainties in change in flight-by-flight NOx

5.3 CASE STUDY I: INCREASED NOx CERTIFICATION STANDARDS

5.3.1 Analysis Overview

The analysis is based on comparisons of two fleets of aircraft: baseline and scenario. The baseline is the Forecasting and Economic Support Group (FESG[10])-developed 2002 fleet and corresponding operations. The scenario is a fleet composed of the baseline aircraft except that all aircraft-engine combinations not meeting a particular stringency level are replaced with new aircraft-engine combinations as exemplified in Table 5.1. Only changes in equipment and operations were modeled. No other effects (e.g. a fuel burn penalty) were assumed.

Table 5.1 A sample output from NO_x stringency results for scenario year 2020

FESG Aircraft	FESG Engine	Year of Implementation	Stringency	NOx per Cycle (kg)
737-7	CFM56-7B24	Baseline	0%	133369
	CFM56-7B24_TL5b	2008	15%	112670
A330-3	CF6-80E1A3	Baseline	0%	589243
	CF6-80E1A3_TL2	2008	15%	504327

A Monte Carlo simulation was used to estimate the uncertainty in the prediction of the difference in fleet NOx between the baseline and stringency scenarios. The aircraft types of B727-200, B737-800, B757-200, B767-200, B767-300, B777-200, A300-600, DC10, MD80, MD90 and F100 were included in the simulation. These aircraft types were assumed to represent the NOx emissions characteristics and associated uncertainties in the FESG fleet in part because they represent a good mix of small versus large aircraft and old versus new aircraft. Also, the uncertainty assessment provided in Chapter 4 Section 3.3.1 has shown that these aircraft provide uncertainty estimates that are representative of the SAGE fleet.

The procedure for performing the analysis is shown below.

---

[10] FESG is a sub-group of United Nations' Intergovernmental Panel on Climate Change (IPCC) and is responsible for forecasting economic scenarios related to climate change.

- $NO_X\_delta = NO_X\_TL - NO_X\_baseline$ (where TL denotes technology level) was estimated 2,000 times. For each of the 2000 simulations key input uncertainties were varied randomly using a Monte Carlo simulation to represent the uncertainty in these parameters.

- With the exception of $EINO_X$, the key uncertainties (engine performance, aerodynamic performance, take-off weight, flight speed, winds aloft, ambient temperature and cruise altitude) were randomly varied <u>but applied identically</u> for both $NO_X\_baseline$ and NO_X_TL in formulating NO_X_delta. This is because these uncertainties remain the same between the baseline and TL scenarios.

- $EINO_X$ was randomly varied with 1σ uncertainty of $\pm 24\%$ (see Chapter 3 Section 3.4.3) in $NOx\_baseline$. As a conservative estimate, the TL combustors were assumed to have the same $\pm 24\%$ variability. Therefore for each run, the $EINO_X$ values were drawn from two independent random distributions with $\pm 24\%$ variability as illustrated in the previous section (see Figures 5.3c and 5.3d).

The variance (σ^2) in flight-by-flight NO_X_delta was calculated for the population of 2000 flights for the 11 aircraft types. This uncertainty was applied to the NOx results of each aircraft-engine combination in the FESG fleet's TL scenario. The uncertainty in the NOx results was then propagated analytically to arrive at an estimate for the uncertainty in the difference in fleet total NOx emissions. The uncertainty was propagated by assuming that the difference in NOx for each of the flights for each of the aircraft-engine combination is an independent random variable. Therefore the propagated uncertainty is estimated using the square root of the sum of squared σ's of only those aircraft-engine combinations that are replaced due to the stringency option considered. That is,

$$\sigma_{NO_X\_delta\ for\ entire\ fleet} = \sqrt{\sigma^2_{NO_X\_delta\ 737-7\ CFM56-7B24} + \sigma^2_{NO_X\_delta\ A330-3\ CF6-80E1A3} + \cdots}.$$

Ninety five percent confidence intervals based on the $\sigma_{NOx\_delta\ for\ entire\ fleet}$ are then added to the scenario plots. Note that this uncertainty in part originates from the performance of an aircraft-engine combination (e.g. the curve fitting uncertainty in EI) – not the flight-by-flight effects (e.g. aging, or engine-to-engine variability). Thus by taking advantage

of the averaging of the uncertainties over many flights of the same aircraft-engine combination, one does not get the conservative estimate. To get a conservative estimate, one could propagate the uncertainty only up to the type of aircraft-engine and then weight the results by the number of flights. This increases the $\sigma_{NOx\_delta\ for\ entire\ fleet}$. The question of uncertainty propagation to the fleet level is a fairly complex problem which goes beyond the scope of this thesis. For the purpose of this study, a few test cases have shown that the conservative $\sigma_{NOx\_delta\ for\ entire\ fleet}$ has a small impact on the outcome of the mean difference tests below. Therefore, it is still possible to resolve a small difference between two NOx scenarios, using the paired Monte Carlo approach here.

Twice the calculated uncertainty in $\sigma_{NOx\_delta\ for\ entire\ fleet}$ serves as the 95% confidence interval. From these, one can tell the likelihood that the scenario values (NO_x reductions) will be statistically significant relative to the known modeling and input uncertainties in SAGE.

5.3.2 Results and Discussion

Figure 5.4 shows a result from the Monte Carlo simulation for NO_x_delta for the aforementioned 11 aircraft types. The calculated standard deviation in NOx_delta on a flight-by-flight basis is ±45% (1σ). The flight-by-flight uncertainties in NO_x_TL and $NO_x\_baseline$ are 42% and 40%, respectively. If it were assumed that all of the input and modeling uncertainties were independent (versus being applied identically to both the baseline and the stringency scenario), then the propagated uncertainty is 58% (i.e. the square root of the sum of the squared 42% and 40%). As discussed previously, because many of the uncertainties are common between NO_x_TL and $NO_x\_baseline$, the estimated uncertainty in NOx_delta from the Monte Carlo simulation is smaller.
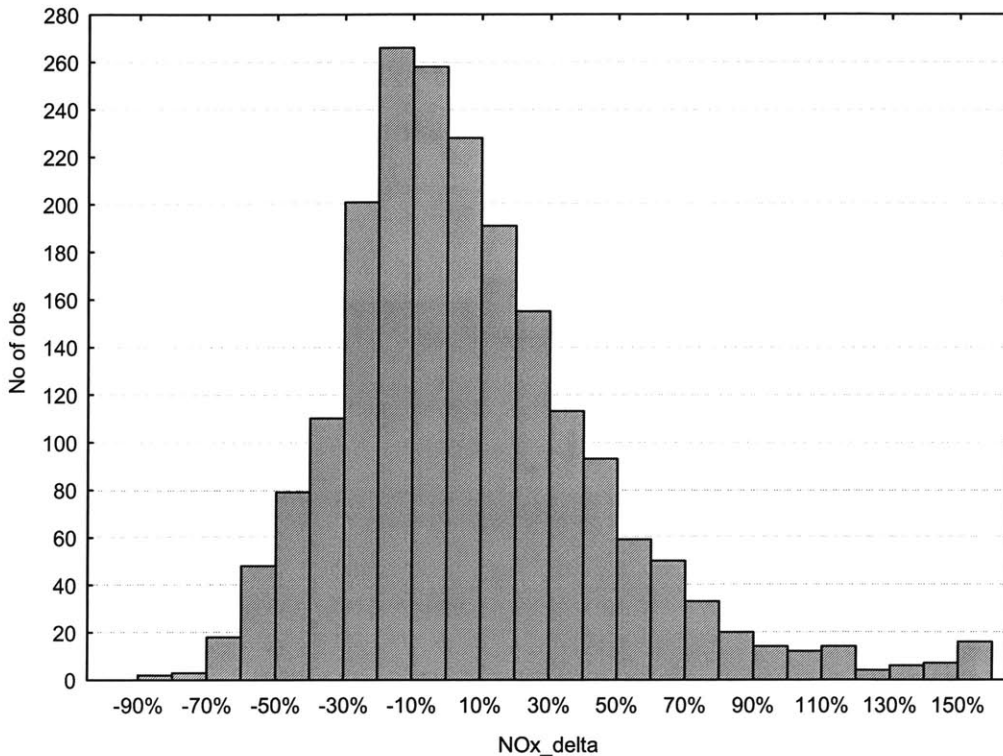
Figure 5.4 Monte Carlo simulation results for NO_X_delta (% change from baseline)

This uncertainty (±45%) in flight-by-flight NO_X_delta is propagated for the entire fleet for each combination of stringency level and implementation year. As a result, the propagated uncertainties range from 9% to 14% of the estimated NO_X_delta for various stringency levels and implementation years. Based on this information, 95% confidence intervals are attached to the scenario plots as shown in Figure 5.5. They show the range in which the scenario values can be interpreted with statistical significance given known input and modeling uncertainties. Both the 2008 and 2012 implementation of each of the stringency levels results in reductions in NOx that are statistically different from zero based on the 95% confidence intervals.

In addition, the confidence intervals show that some scenario estimates may not be statistically different from each other given knowledge of the uncertainties inherent in the modeling tool. For example, Figure 5.5 shows that for the 2008 implementation, the 20% stringency may not achieve more reduction in NO_X than the 15% stringency does as indicated by the uncertainty bars. To address this more rigorously, a t-test was

conducted to see if the 15% and 20% stringency scenarios were statistically different from each other. It was confirmed that even at 99% confidence level, the 15% and 20% stringency scenario values were statistically the same. Table 5.2 shows t-test results for implementation years 2008 and 2012.
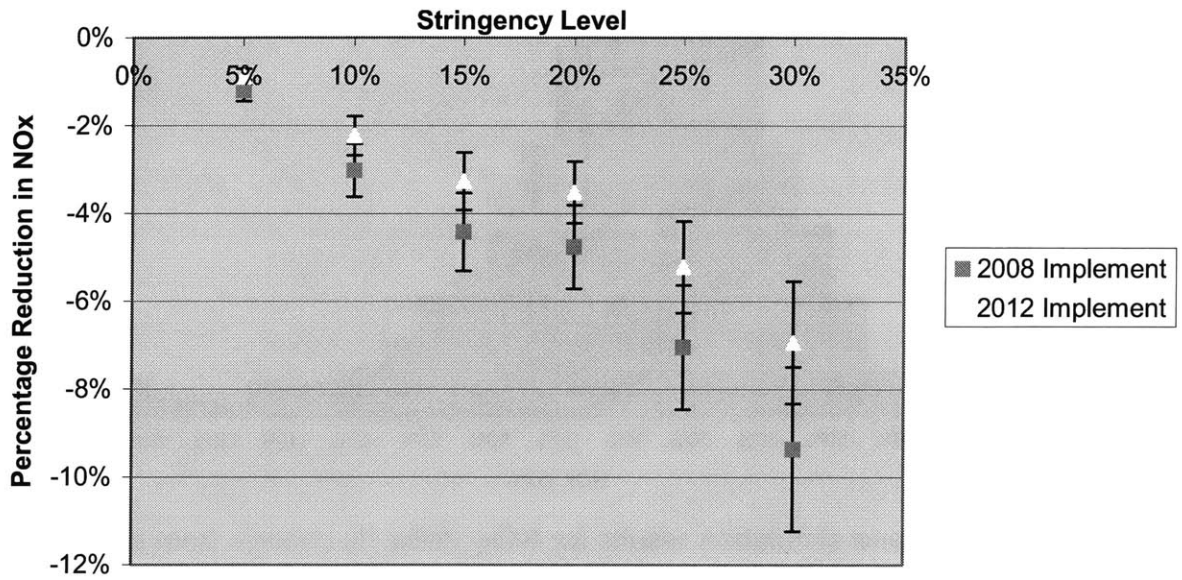
Figure 5.5 NO_X stringency scenario for year 2020

Table 5.2 t-test results for testing the difference between 15% and 20% scenarios for each implementation year

	2008 Implement	2012 Implement
Sample size, n	413	413
$t_n(.005)$	2.33	2.33
t-statistics calculated	0.464	0.339

Separate t-tests are required for analyzing other scenario pairs. One interesting example is testing the difference between 2008 and 2012 implementation years at each stringency level. Table 5.3 shows that the scenario estimates of the two implementation years are not statistically different for the stringency levels of 5% to 15%, as indicated by the calculated t-statistics being smaller than $t_n(.025)$, the significance t value at 95% confidence.

110

Table 5.3 t-test results for testing the difference between 2008 and 2012
implementation for each stringency level

Stringency level	Sample size, n	$t_n(.025)$	t-statistics calculated
5%	377	1.65	0.402
10%	390	1.65	1.03
15%	392	1.65	1.53
20%	413	1.65	1.69
25%	420	1.65	2.57
30%	434	1.65	3.54

Although the absolute uncertainty in flight-by-flight NOx predictions from SAGE is estimated to be 40% (1σ) (see Chapter 4 Section 4.5), it is well within the current capabilities of SAGE to distinguish between the various NO_x stringency options considered. It is estimated that the uncertainty (95% confidence) in the difference between the baseline and the NOx stringency scenarios ranges from 9% to 14% of the predicted difference.

Both the 2008 and 2012 implementation of each of the stringency levels results in reductions in NOx that are statistically different from zero based on 95% confidence. Although, the reductions in NOx generally increase with increasing stringency levels, statistical tests indicate that the scenario estimates of some stringency levels and implementation years are not statistically different from each other.

5.4 CASE STUDY II: CONTINUOUS DESCENT APPROACH (CDA)

5.4.1 Background
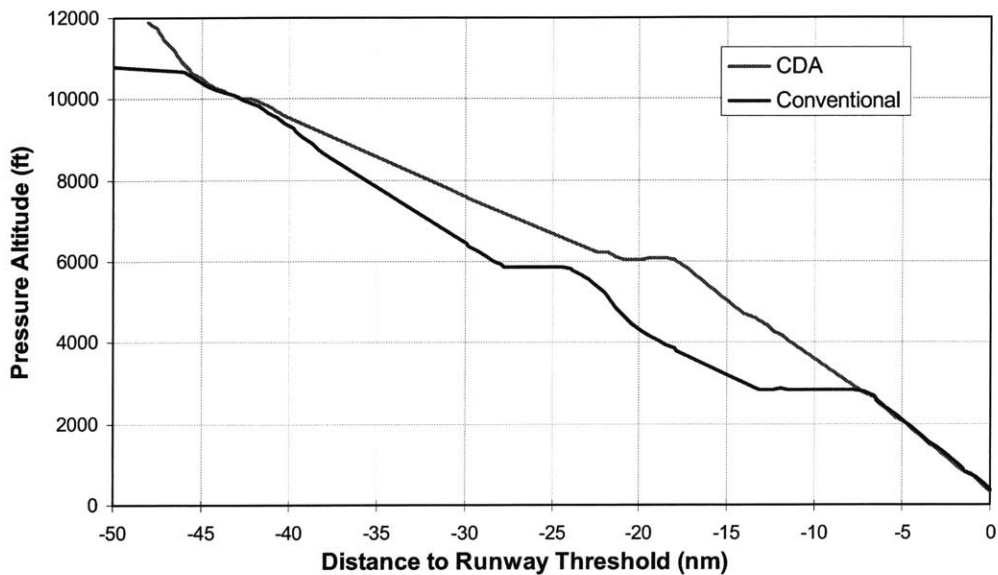
Figure 5.6 Conventional approach and Continuous Descent Approach

As a measure to address aircraft noise issues, a continuous descent approach (CDA) procedure is examined. In a conventional approach, the airplane is brought down in stages—descending and leveling off several times before landing—with the final level flight segment being only 3,000 ft above the elevation at the airport. Each time the airplane descends to an intermediate altitude and levels off, thrust must be applied to maintain level flight. Increasing thrust increases noise impact on the ground as well as fuel consumption. The CDA procedure addresses both the thrust and low-altitude level flight issues by keeping the planes higher longer and then bringing them down in a continuous descent. Figure 5.6 shows an example of both approaches. A two-segment CDA with a constant flight path angle (FPA) initial segment (-2.5 °) followed by a -3 ° instrument landing system (ILS) glide slope is shown. The altitude profile for a conventional step-down approach, with the aircraft descending from 11,000 ft to 3,000 ft, followed by a level-flight segment before intercepting the 3 ° ILS glide slope, is also shown [Clarke *et al.*, 2004].

The utility of this procedure was evaluated through a flight demonstration test where the noise impact of the CDA and the conventional approach were measured at seven different locations in Floyds Knobs, Indiana. The results proved that the CDA provides

consistent noise reduction. There were statistically significant differences at all seven measurement sites between the CDA and the conventional approach over the testing period. In fact, the observed reductions of between 3.9 and 6.5 dBA are very significant given the fact that a 3 dBA difference represents a 50% reduction in acoustic energy and is noticeable to the human ear. Given the subsequent analysis showing that the 50 DNL contour at Louisville would shrink by 7% if all aircraft were to perform the CDA, it is clear that adoption of the CDA at major airports would provide much needed relief for residents in communities near airports [Clarke et al., 2004].
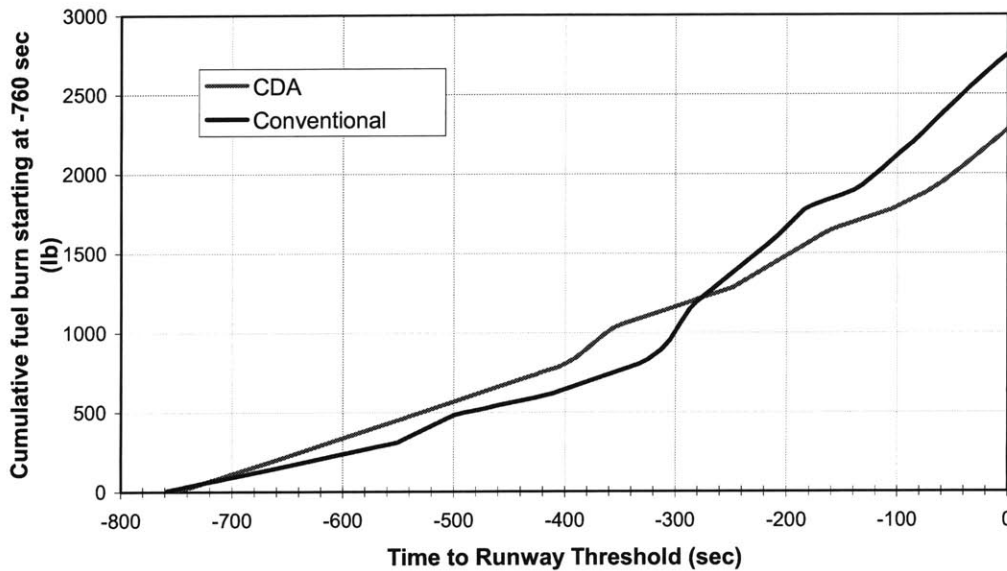
Figure 5.7 Cumulative fuel consumption of conventional approach and Continuous Descent Approach (from 11,000 ft to the ground; B767 at Louisville)

The reduced thrust levels of the CDA procedure lead to lower fuel consumption. Figure 5.7 shows that the CDA procedure burns about 20% less fuel than the conventional approach does on aggregate from 11,000 ft to the ground. This would translate to about 1% of typical full mission fuel burn of the B767. For this reason, there is high interest in estimating the emissions benefit from a procedure change using the CDA. This study entails use of SAGE for estimating the fuel burn and emissions benefits of the CDA procedure. The focus is on quantifying the uncertainties in the estimated CDA benefits.

5.4.2 Analysis Overview

For conventional approaches, actual trajectory, wind, ambient temperature and aircraft weight information for five aircraft types is available from the CFDR information of a major airline. For each aircraft type, the data for six flights are available and used to represent the actual flight profiles of conventional approaches. The CFDR data are then fed into SAGE for calculating aircraft performance and fuel burn. This allows for asserting the differences between true profiles and CDA when almost all of the uncertainties are removed except for those in the performance module of SAGE.

To model the CDA procedure, airplanes are flown on a 3 ° glide slope with SAGE. Indeed, this is the standard approach procedure employed in SAGE, so the analysis also provides an assessment of the uncertainties in fuel burn and emissions associated with this idealized model of approach procedures.

A thousand random performance models were flown on each of the CDA versus CFDR trajectories. This was done in a paired fashion as described in Sections 5.2 and 5.3.1, applying the same performance to each trajectory, calculating the difference in fuel burn and emissions, and then moving on to a new randomly selected performance.

5.4.3 Results and Discussion

Figure 5.8 shows a result for the B737-800 based on the thousand performance model runs. For the descent segment from 3000 ft above the elevation of the airport to the ground, the average fuel burn reduction is 30.4%. The 2σ interval for the mean is ±8.21%.

737-800 = 1000*0.1*normal(x, 0.3038, 0.103)
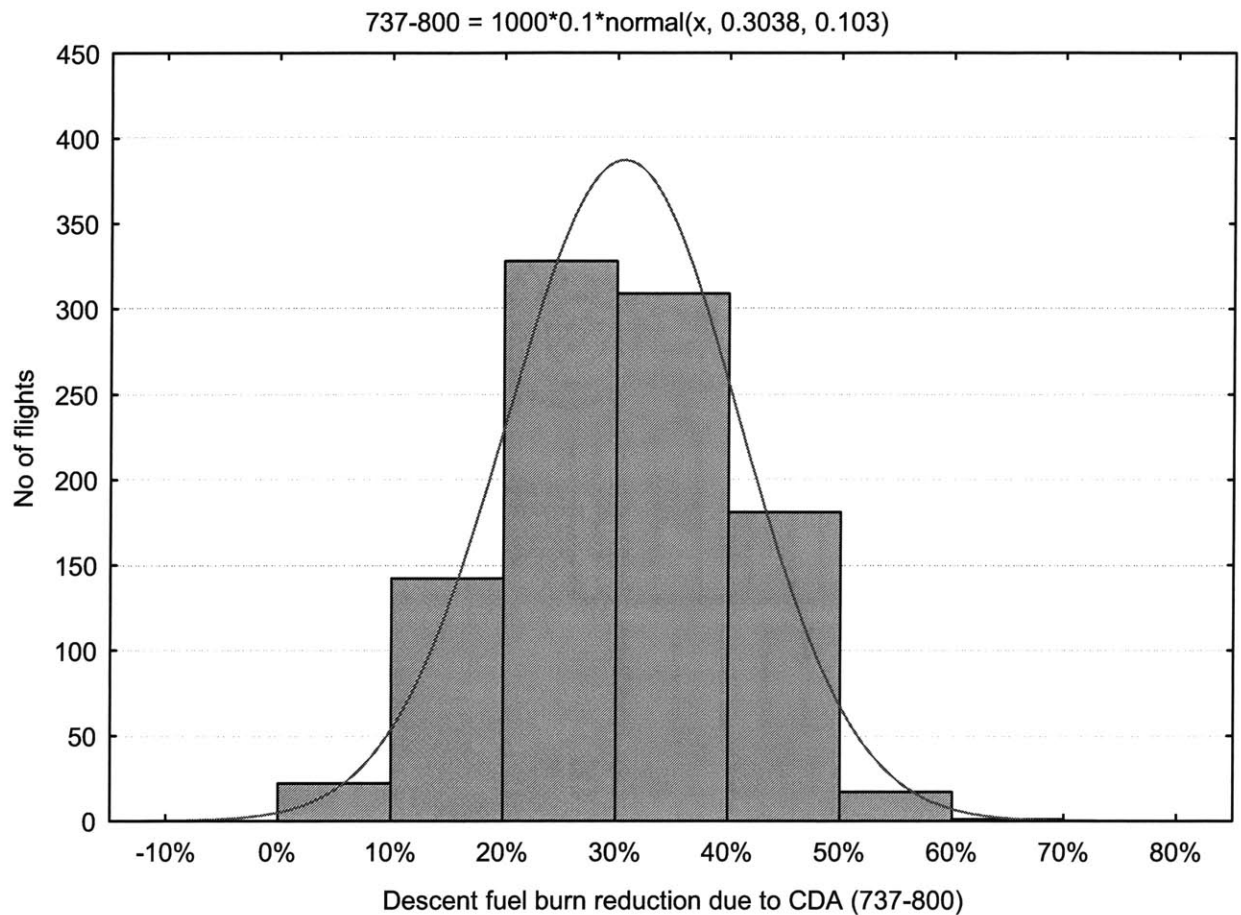
Figure 5.8 Continuous Descent Approach's impact on B737-800 descent fuel burn

The results for all aircraft types in this study are summarized in Figure 5.9. For all six aircraft types, the fuel burn savings of the CDA procedure are estimated to be around 30%.[11] Note that the large variability (indicated by 2σ confidence intervals) of the estimated fuel burn benefits originates from several factors. For each aircraft type, differences in airport runway configurations, landing procedures, aircraft weight and ambient conditions are the primary sources of the variability. Due to these uncertainties, the confidence intervals on the fuel burn savings estimates are quite large. Work is ongoing to obtain a larger sample of CFDR data for a unique set of airport/runway and flight date/time. By removing several sources of uncertainty this way, it will be possible to estimate the CDA benefits with higher confidence.

---

[11] These results are based on SAGE-modeled fuel burn values. For the descent segments (e.g. 3,000 ft to the ground), SAGE over-predicts reported fuel burn by 8% on average with 42% standard deviation. See Figure 3.17 for details.
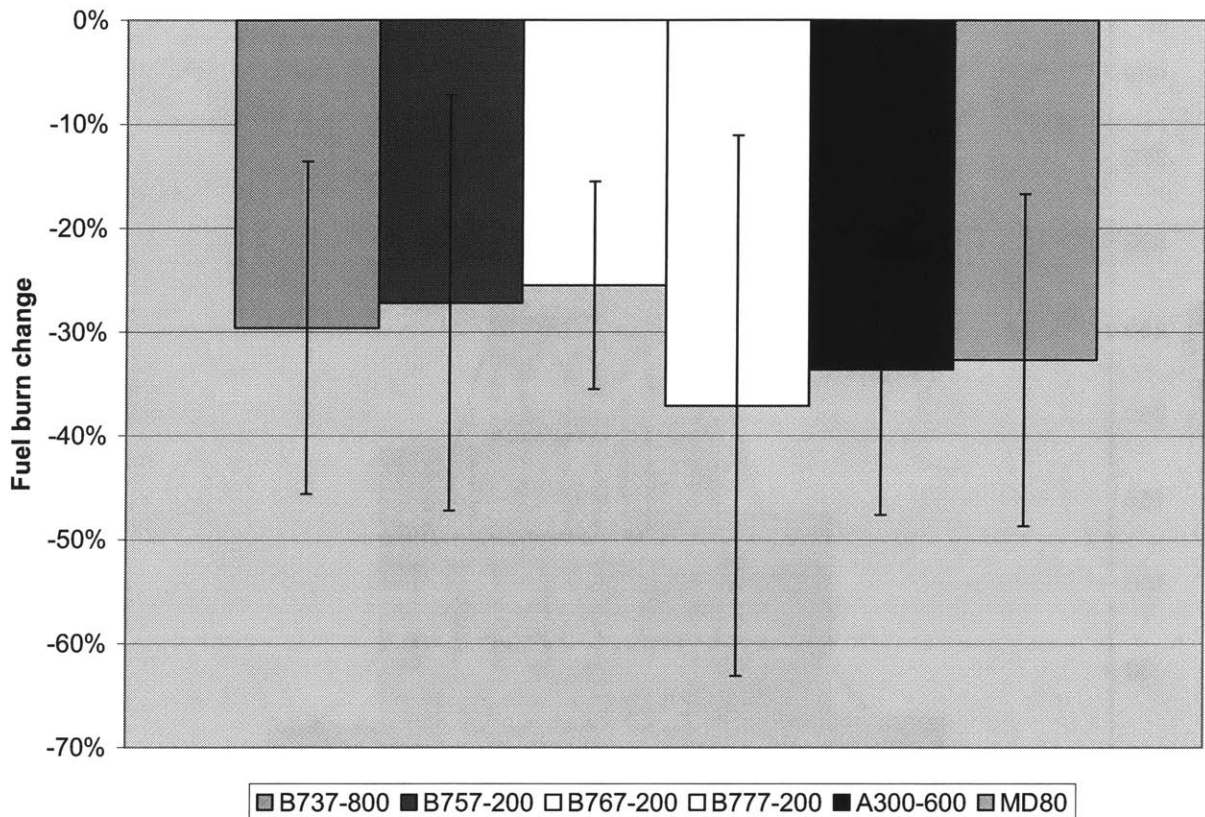
Figure 5.9 Fuel burn reductions due to Continuous Descent Approach (landing segment below 3000 ft to the ground shown)

Figure 5.10 shows percent changes in emissions produced by the six aircraft types of the above. Both the conventional and CDA profiles were flown in SAGE, and the uncertainties in the difference in emissions between the two procedures were estimated. Since the CDA procedure utilizes a reduced throttle setting, which causes the NOx emissions production rate to decrease, total NOx decreases by about 30-50%. The HC and CO emissions production rates sharply increase and outweigh the reductions in fuel burn. Therefore, total HC and CO increase by 20-70%. The large 2σ ranges of the estimated changes are due to the high uncertainty associated with the emissions indices modeled in SAGE in addition to the small number of flights tested for this case study. To examine the emissions scenarios of the CDA procedure for more aircraft types on an airport level, further work is planned.
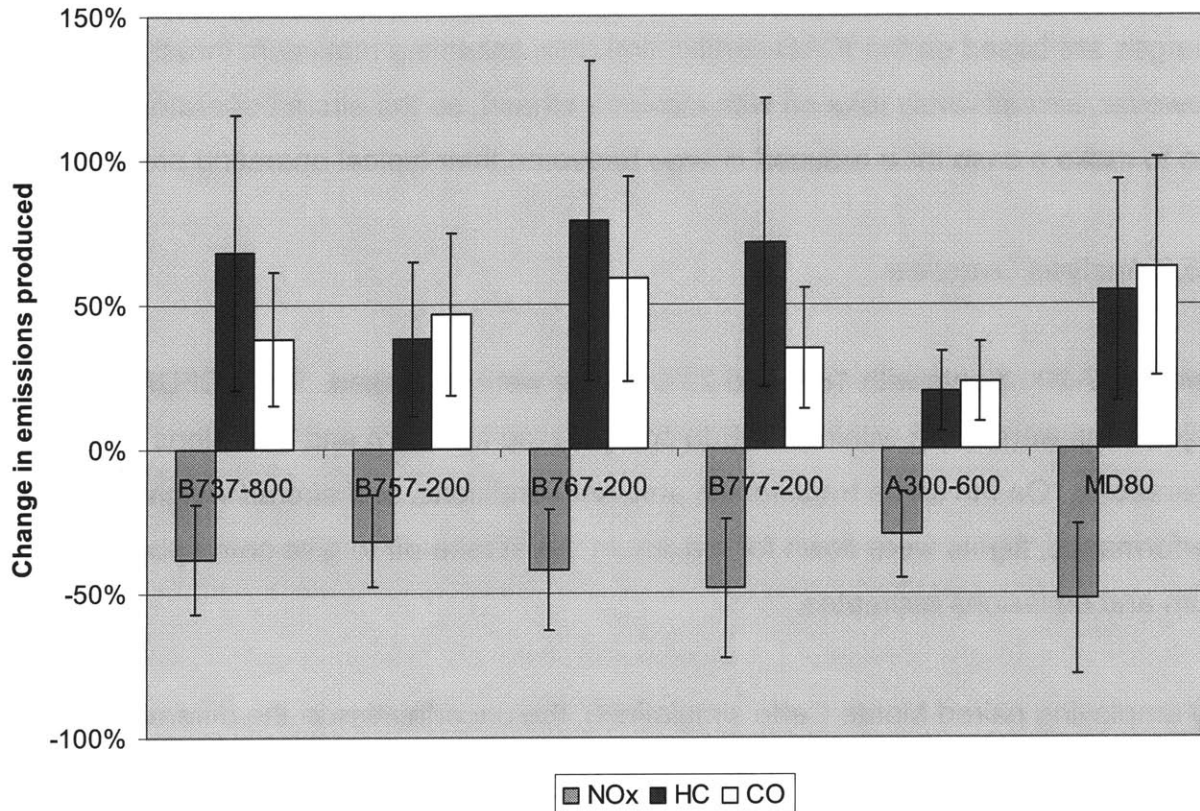
Figure 5.10 Emissions impacts of Continuous Descent Approach (landing segment from 3000 ft to the ground shown)

5.5 CASE STUDY III: DERATED TAKE-OFF

5.5.1 Background

Many aircraft operators currently utilize derated take-off power for various reasons including operating cost savings (through decreased wear and tear on engine parts and thus increased engine life) and noise abatement. The amount of derate possible is limited by such factors as take-off weight, runway length and weather conditions [Hall *et al.*, 2003].

Derated take-off can also result in reduced NOx emissions because of the lower fuel flow rate and NOx production rate. This is particularly of high interest to aircraft

operators as they are asked to pay emissions charges at some European airports. The charges are based on the ICAO certification data assuming maximum thrust take-off. However, aircraft rarely take off with maximum thrust, so the aircraft operators would like to make a case for a reduced charge based on their typical operating procedures.

5.5.2 Analysis Overview

Two B777-200 flights with 18% and 23% derate were assessed. Their CFDR trajectories were flown within SAGE to compute the fuel burn and emissions of derate operations. On the same trajectories, ambient conditions, and aircraft weight and performance, flights were flown for maximum thrust take-off to give corresponding fuel burn and emissions estimates.

By employing paired Monte Carlo simulations, the uncertainties in the difference in fuel burn and emissions between the two scenarios (i.e. derate versus maximum thrust) were assessed. For each pair of take-off procedures, 1000 comparisons were run with randomly chosen technology performance for the B777-200 with a mean given by BADA and a standard deviation given by the estimated uncertainty in the technology performance specification (see Chapter 3). Then the average of these 1000 different comparisons was taken. All other major uncertainties were removed by using the winds, ambient conditions and aircraft weight given in the CFDR data for both the derated procedure and the full throttle procedure.

5.5.3 Results and Discussion

Figures 5.11 and 5.12 show percent changes in fuel burn[12] and emissions due to derate operations below various mixing height[13] altitudes for the take-off segment only. Derated take-off uses more fuel than maximum thrust take-off does because it takes

---

[12] These results are based on SAGE-modeled fuel burn values. For the take-off segments (e.g. the ground to 3,000 ft), SAGE over-predicts reported fuel burn by 10% on average with a standard deviation of 12%. See Figure 3.16 for details.
[13] The mixing height is the height below which emissions are important for local air quality and can vary from location to location and from day to day.

longer to climb with derate. HC and CO emissions increase roughly 1% for each 2% of derate due to the increased time-to-climb and increased EIHC and EICO outweighing the reduced fuel burn rate. Tables 5.4 and 5.5 show the elapsed time from take-off to a given mixing height altitude. On the other hand, NOx emissions are reduced roughly 1% for each 2% of derate due to the reduced EINOx and reduced fuel burn rate outweighing the increased time-to-climb.
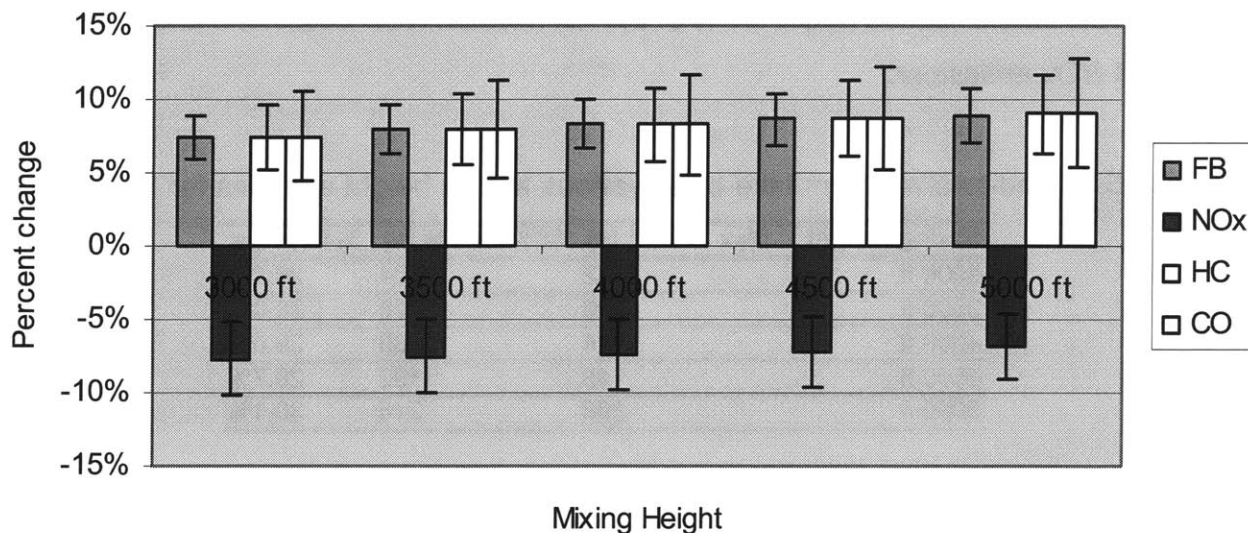
Figure 5.11 Fuel burn and emissions impact of 18% derate for the take-off segment only
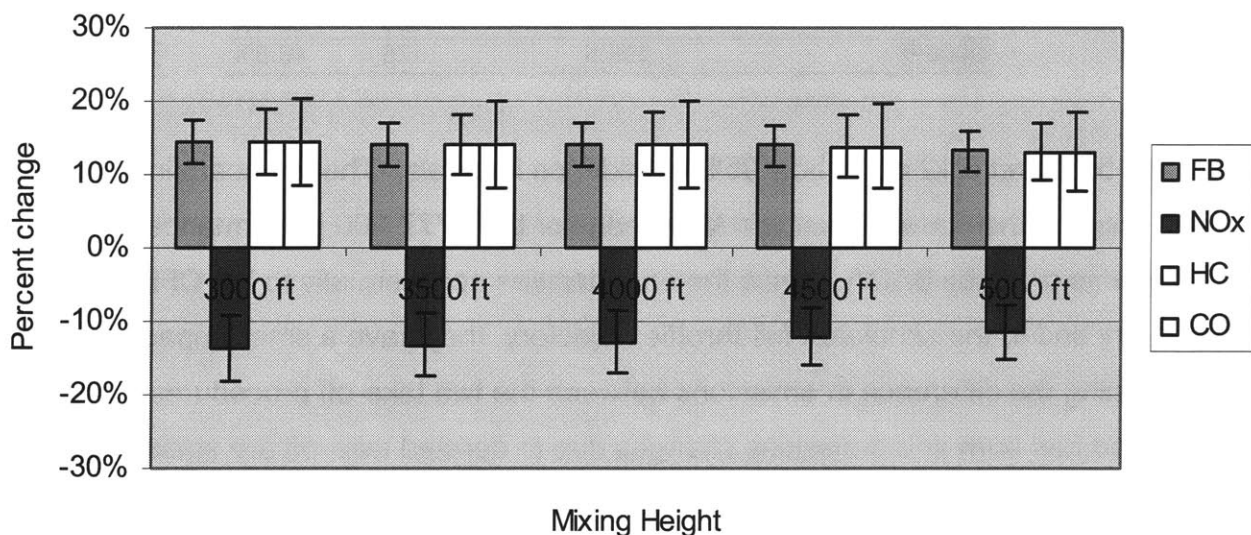
Figure 5.12 Fuel burn and emissions impact of 23% derate for the take-off segment only

Note that these results are only for the take-off segment. For the flights examined in this analysis, the take-off segment NOx emissions comprise about 5-10% of the full mission results and 80-90% of the full LTO results. For the HC and CO emissions, the take-off segment emissions comprise about 2-5% of the full mission results and 40-60% of the full LTO results. Based on this, the emissions reduction results above can be approximately translated in terms of the full mission and LTO results. For instance, the 18% derate would reduce about 3-7% of the full mission NOx emissions and 65-70% of the LTO NOx emissions.

Table 5.4 Time-to-climb from take-off to various mixing height altitudes for 18% derate

Mixing Height	Max Thrust (s)	18% Derate (s)	% Change
3000 ft	82	104	26.8%
3500 ft	100	128	28.0%
4000 ft	124	160	29.0%
4500 ft	148	192	29.7%
5000 ft	166	216	30.1%

Table 5.5 Time-to-climb from take-off to various mixing height altitudes for 23% derate

Mixing Height	Max Thrust (s)	23% Derate (s)	% Change
3000 ft	80.5	128	59.0%
3500 ft	86.5	136	57.2%
4000 ft	92.5	144	55.7%
4500 ft	104.5	160	53.1%
5000 ft	118.5	176	48.5%

Figures 5.11 and 5.12 also show 95% confidence intervals. These uncertainty levels are a result of the current uncertain knowledge of the B777-200 performance coefficients given by BADA. Since the uncertainties apply equally to the CFDR derated trajectory and to the simulated full-throttle trajectory, they have a small impact on determining the difference in emissions between the two take-off procedures. The estimated fuel burn and emissions changes due to derated take-off are statistically significant relative to the given uncertainty in the aircraft performance coefficients of SAGE.

The way in which derated take-off impacts fuel burn and emissions is the same among various studies [Yamartino et al., 2004; Hall et al., 2003]. However, different operating conditions and underlying assumptions result in a varying degree of emissions benefits associated with derated take-off. It is necessary to define the most standard full throttle take-off and derated take-off procedures and synchronize the key operating conditions (e.g. take-off weight and ambient conditions) between them. This way, it will be possible to assess the emissions benefits of derated take-off on a fleet level with higher confidence.

5.6 CHAPTER SUMMARY AND CONCLUSIONS

Three policy options have been analyzed in this chapter. Increased NOx stringency, the CDA procedure and the derated take-off procedure were modeled and their impacts on fuel burn and emissions were estimated. Note that the increased NOx stringency analysis was more relevant for assessing global emissions whereas the CDA and derated take-off procedures were mainly for evaluating emissions below 3000 ft. For the case of increased NOx stringency, its effects on reducing NOx emissions would be enhanced during take-off (i.e. below 3000 ft). It is because the rate of NOx emissions production is higher during take-off where the engine power setting is highest. On the other hand, increased NOx stringency may not have as strong an effect on reducing NOx emissions during descent as the CDA procedure does because descent thrust settings are usually lowest.

The analyses showed that the considered policy options would reduce NOx emissions but with trade-offs. One or all of fuel burn, HC and CO emissions would increase with reduced NOx emissions. Nonetheless airlines are willing to make such trade-offs as NOx emissions are considered more important than the other emissions species when airports impose emissions charges.

When one considers which of these technological and operational options is more effective for mitigating emissions impacts, a more detailed analysis on emissions and

associated costs should be conducted. For example, the CDA procedure would require advanced air traffic control systems both on board and at the control tower. This is an added cost to implementing the CDA procedure, which makes it difficult to compare the net benefits between technology and operations.

The results of this chapter do not support any policy decisions in one way or another. Rather, they were intended to test policy concepts with a focus on quantifying the uncertainty in the SAGE prediction of the difference in aviation emissions between a baseline scenario and a policy scenario. Although large uncertainties exist in aircraft performance and trajectories on a flight-by-flight basis, one can use SAGE to distinguish very small differences in emissions (a percent or less) for different policy options. For this, a paired Monte Carlo technique was introduced to analyze the difference in emissions between two scenarios where many of the component uncertainties are common. The statistical significance in the modeled scenario results was determined via this approach.

CHAPTER 6

CONCLUSIONS AND FUTURE WORK

This thesis focused on developing, assessing and applying the SAGE model to evaluate global aircraft fuel consumption and emissions, and to examine technological and operational measures to mitigate these emissions. Uncertainties of the model were analyzed in detail and carefully accounted for in the policy options considered. In doing so, this thesis provided a basis for understanding model uncertainty and fidelity. It assessed both random and bias errors of the model and demonstrated how they affect policy scenario outcomes. Future work to understand when one may or may not use the methodology and the results presented is also discussed below.

6.1 SUMMARY

In SAGE Version 1, the aircraft performance, fuel burn and emissions of CO_2, H_2O, NOx, HC and CO were modeled at each point on a flight mission. The most influential modeling assumptions were use of standard day ambient temperature, not correcting for winds aloft, uncertain aerodynamic and engine performance, and simplified assumptions about aircraft take-off weight and flight speed. Additional uncertainties associated with the use of OAG-based flight trajectories and the emissions estimation method were also important.

Chapter 3 and Chapter 4 presented an assessment of parametric and model uncertainties in SAGE. On average, the aggregate-level composite fuel burn results showed about -6% difference from reported fuel burn data. A statistical analysis showed that this mean shift was a combined contribution of the key uncertainties above.

In addition to the comparisons to reported data, a sensitivity analysis followed by Monte Carlo simulations confirmed the most significant uncertainties contributing to the variance of fuel burn and emissions results. The analyses showed that the

uncertainties in engine and aerodynamic performance had the largest impact on system errors, accounting for around 60-70% of the total variance in full-mission fuel burn results. The uncertainties in winds aloft and take-off weight explained another 20-25%. LTO procedures, which consist of engine throttle setting, rate of climb/descent and flight speed, were the most influential uncertainties that drove the variance in SAGE fuel burn results below 3000 ft. For emissions, it was shown that the emissions indices were the most influential uncertainties for the variance in SAGE outputs. Note that these are the key uncertainties associated with the use of the SAGE model for decision-making as well.

Three policy options were analyzed in Chapter 5. More stringent NOx certification standards, Continuous Descent Approach procedures and derated take-off procedures were modeled. The uncertainty in the SAGE prediction of the difference in aviation emissions between a baseline scenario and a policy scenario was quantified. Although large uncertainties exist in aircraft performance and trajectories on a flight-by-flight basis, it was possible to use SAGE to distinguish very small differences in emissions (a percent or less) for different policy options.

The considered 5% to 30% increases in NOx certification standards resulted in 1% to 9% reductions in the fleet-level NOx emissions. The uncertainty ranged from 9% to 14% at 95% confidence. Given this uncertainty in the modeling tool, it was not possible to distinguish a difference between 2008 and 2012 implementation years for 5-15% stringencies at a 95% confidence level.

The CDA procedures achieved around 30% reduction in fuel burn and as much as 50% reduction in NOx for landing segments below 3000 ft. HC and CO emissions increased 20-70% as a result of the higher emissions production rate at reduced engine throttle settings. Derated take-off used more fuel than maximum thrust take-off did because it takes longer to climb with derate. HC and CO emissions increased roughly 1% for each 2% of derate due to the increased time-to-climb and increased EIHC and EICO outweighing the reduced fuel burn rate. On the other hand, NOx emissions were

reduced roughly 1% for each 2% of derate due to the reduced EINOx and reduced fuel burn rate outweighing the increased time-to-climb.

6.2 CONCLUSIONS

In this thesis, the key uncertainties and their impacts on the variance and mean shift of the output error were assessed. The influence of random errors (i.e. component uncertainties) on the policy scenario results was quantified. Note, however, that those bias errors due to the effects of unscheduled and canceled flights were not addressed. Such unscheduled and canceled flights are expected to be a major source of bias error, which is to be better addressed in further research.

Although large uncertainties existed in aircraft performance and trajectories on a flight-by-flight basis, it was possible to use the SAGE model to distinguish small differences in emissions (a percent or less) for different policy options. To generalize this methodology for analyzing policy options under conditions of uncertainty, fleet averaging effects are important. Even though flight-by-flight uncertainties are large, their impacts get reduced when fleet-level fuel burn and emissions are considered.

In this context, a sensitivity study of fleet fuel burn and emissions with varying levels of component uncertainties would be valuable. For example, in the case of increased NOx stringency scenarios, one could examine what level of improvements in model uncertainty would be needed to distinguish between the implementation years for the 5-15% stringency options. This could help to guide model development resources and explain to what extent addressing the model development items would contribute to reducing uncertainty with respect to the ultimate decision-making. Once such mapping is complete between component uncertainties and fleet-level uncertainties, it might be even possible to estimate the confidence intervals on the policy scenario results without going through time-consuming Monte Carlo simulations.

Another important question is when the application of uncertainty analysis along with SAGE model results may or may not be relied upon for decision-making. It should be noted, however, that such reliability depends on the context. In the NOx stringency case, it might be possible to quote a statistically significant difference between 2008 and 2012 implementation years for 5-15% stringencies if one were to lower the confidence level to 90% or even less. The implication of using 90% confidence as opposed to 95% confidence is that there is higher likelihood for the scenario results to be incorrect. It is, therefore, the choice of the policy maker as to how certain he or she desires to be in order to make a policy decision under conditions of uncertainty.

For the other two policy analyses, it is still unclear to what extent these case studies can be used to make decisions concerning system-wide CDA or derated take-off procedure implementation. Acquiring data and designing analyses on a fleet level are required. In this regard, the results presented are only specific to the particular policy options considered. A contribution of this thesis is to articulate how uncertainties of the SAGE model should be treated for decision-making via a statistical approach that can be generalized.

6.3 SUGGESTED MODEL IMPROVEMENTS

The following are recommended for future development of SAGE:

- Wind and temperature databases: The ISA assumes only averaged weather conditions for the entire world over many years. Hence, both the seasonal and regional variations from standard day winds and temperatures should be modeled to higher fidelity. Work is ongoing to have gridded weather data into SAGE.

- Aerodynamic coefficients: Proper dependence on altitude and flight speed should be modeled.

- Adjust cruise C_{D0} by an appropriate correction factor (see Chapter 3 Section 3.4.2) when substituting it for C_{D0} for other modes.
- Drag coefficients at take-off, climb-out, approach and landing are currently missing for several major aircraft types (e.g. A300 and MD11). Use the latest BADA (version 3.5) for added/updated drag coefficients.
- Work is ongoing to revise the BADA aerodynamic model to account for transonic drag rise.

- Landing gear extension height
  - Conduct additional examination to lower the current height (3000 ft) to 1500-2000 ft in order to avoid getting excessively large drag caused by the landing gear.

- Thrust reduction coefficients
  - Examine if descent thrust coefficients (C_{TDES_LOW}, C_{TDES_AP} and C_{TDES_LD}) cause excessively low thrust values for part of descent segments.

- Fuel flow coefficients: Fuel flows at low engine power settings (e.g. idle and taxi) are not well predicted because the BADA minimum fuel flow model is only a function of altitude.
  - Work is ongoing to introduce proper dependence of fuel flow on both flight altitude and Mach number.
  - Use the latest BADA (version 3.5) for added/updated fuel flow coefficients.

- LTO components
  - For descent profiles, cut all ETMS points below 3000 ft and replace them with OAG-based trajectory points.
  - Compare SAGE LTO profiles to more CFDR data. Consider developing a module for a statistical choice of landing profiles.

- Cruise speed and cruise altitude
    - For flights on less than 500 NM stage, raise cruise altitude and lower cruise speed. Perform additional work to determine the exact magnitude of this adjustment.
    - Conduct additional research for implementing step climbs and cruise speed variations (routing optimization) for OAG flights.

- Other uncertainty assessment
    - Compare SAGE emissions results to measured data.
    - Compare SAGE turboprop results to CFDR data.

- Generalization of the CDA and derate studies
    - Obtain more CFDR data for a unique selection of airport/runway and flight date/time to separate aircraft-to-aircraft differences from other uncertainties such as airport-to-airport differences.
    - Develop a Monte Carlo simulation capability in the research version of SAGE.
    - Conduct a parametric study on important variables such as mixing height and throughput volume.
    - Develop emissions scenarios for a fleet or an airport.

6.4 FINAL REMARKS

A key word for engineering systems today is *sustainability*. In this context, four major elements of *sustainable air transportation* would be—1) increased mobility for people around the world, 2) profitable industry growth, 3) protection of the environment and 4) continuous improvement in safety and security.

For protection of the environment, it is important to stabilize, reduce or even eliminate conventional greenhouse gas emissions. To do so, we must consider not only the technological/operational solutions and economic costs but where aviation stands in

relation to society. Currently, there is not a strong public demand to reduce aircraft emissions. For the cases of aircraft noise or automobile emissions, a clear demonstration of health damages followed by strong public pressure to reduce the environmental nuisances have led to dramatic improvements in both technologies and the way the engineering systems are operated. However, people's awareness about aircraft emissions is relatively low today. There are also very large scientific uncertainties about the potential effects of jet engine emissions discharged at altitude.

Therefore, it will be important to continue to advance atmospheric science of jet engine emissions and raise general public awareness about aviation's impacts on local air quality and the global atmosphere. Such efforts along with modeling and assessments of various emissions reduction options will be another step toward sustainable air transportation.

REFERENCES

Babikian R., Lukachko S.P., and Waitz I.A., "Historical Fuel Efficiency Characteristics of Regional Aircraft from Technological, Operational, and Cost Perspectives," *Journal of Air Transport Management*, V 8(6), 389-400, 2002.

Baughcum S.L., Tritz T.G., Henderson S.C., and Pickett D.C., *Scheduled Civil Aircraft Emission Inventories for 1992: Database Development and Analysis*, NASA CR 4700, April 1996.

Bishop D.E. and Miller J.F., *Update of Aircraft Profile Data for the Integrated Noise Model Computer Program*, U.S. Department of Transportation, DOT-VNTSC-FAA-91-4, 1992.

Boeing, Current Market Outlook 2004, The Boeing Company, Seattle, United States, 2004.

CAEP, "Guidance on the Use of LTO Emissions Certification Data for the Assessment of Operational Impacts," CAEP/6, IP5, Montreal, Canada, 2004.

Cipra B., "Revealing Uncertainties in Computer Models," *Science*, 287: 960-961, February 2000.

Clarke John-Paul B., Ho N.T., Ren L., Brown J.A., Elmer K.R., Zou K, Hunting C., McGregor D.L., Shivashankara B.N., Tong Kwok-On, Warren A.W., and Wat J.K., "Continuous Descent Approach: Design and Flight Test for Louisville International Airport" *Journal of Aircraft*, Vol.41 No.5, 2004.

Cumpsty N.A., *Jet Propulsion: A Simple Guide to the Aerodynamic and Thermodynamic Design and Performance of Jet Engines*, New York, NY, USA: Cambridge University Press, 1997.

Daggett D.L., Sutkus Jr. D.J., DuBois D.P., and Baughcum S.L., *An Evaluation of Aircraft Emissions Inventory Methodology by Comparisons With Reported Airline Data*, The Boeing Commercial Airplane Group, NASA, NASA CR-1999-209480, September 1999.

Dobbie L. and Eran-Tasker M., "Measures to Minimize Fuel Consumption Appear to Be of Greatest Importance to Airlines," *ICAO Journal*, No. 4, 2001.

Eurocontrol, "User Manual for the Base of Aircraft Data (BADA)," Revision 3.3, France, December 2000.

FAA, "FAA Aerospace Forecasts Fiscal Years 2004-2015," FAA-APO- 04-1, Office of Aviation Policy & Plans, U.S. Department of Transportation, March 2004.

FAA, *SAGE Detailed System Architecture and Design Specification*, Office of Environment and Energy, United States Federal Aviation Administration, Washington, D.C. July 2002.

Flathers II G.W., "A Comparison of FAA Integrated Noise Flight Profiles with Profiles Observed at Seattle-Tacoma Airport," FAA-EE-82-10, December 1982.

FR 58, EPA, "Control of Air Pollution from Aircraft and Aircraft Engines: Proposed Amendments to Standards," Federal Register, pp. 12615-12634, United States, 1978.

FR 251, EPA, "Emissions Standards and Test Procedures," Federal Register, pp. 58461-58474, United States, 1982.

FR 155, DOT, "Fuel Venting and Exhaust Emission Requirements for Turbine Engine Powered Airplanes; Final Rule," Federal Register, pp. 32856-32866, United States, 1990.

Frings G., Exhaust Emission Characteristics and Variability for Maintained General Electric CF6-50 Turbofan Engines, FAA Report No. FAA-CT-80-36, Final Report, 1980.

Gunston B., *Jane's Aero-Engines*, Jane's Information Group, Alexandria, Virginia, 1998.

Hall C.T., Mondoloni S.L., and Thrasher T.G., "Estimating the Impact of Reduced Thrust Takeoff on Annual NOx Emissions at Airports", CSSI, Inc., Paper #69800, Washington, D.C. 2003.

Hupe J., "Experts Reformulating Strategy for Alleviating Aviation's Impact on the Environment," *ICAO Journal*, No. 4, 2001.

ICAO, "2001 Annual Civil Aviation Report," Int. Civil. Aviat. Organ. *ICAO Journal*, V 57(6) July/August: 12-20. 2002.

ICAO, International Civil Aviation Organization, *ICAO Engine Exhaust Emissions Data Bank*, November 2000.

IPCC, Climate Change 2001: Mitigation, Intergovernmental Panel on Climate Change, Report of Working Group III, 2001.

Jacoby H.D. and Prinn R.G., *Uncertainty in Climate Change Policy Analysis*, Joint Program on the Science and Policy of Global Change, MIT, Report No. 1, Cambridge, Massachusetts, December 1994.

Lee J.J., *Historical and Future Trends in Aircraft Performance, Cost, and Emissions*, SM Thesis, Massachusetts Institute of Technology, September 2000.

Lee J.J., Lukachko S.P., and Waitz I.A., "Aircraft and Energy Use," invited chapter in the *Encyclopedia of Energy*, Academic Press/Elsevier Science, San Diego California, March 2004.

Lee J.J., Lukachko S.P., Waitz I.A., and Schafer A., "Historical and Future Trends in Aircraft performance, Cost and Emissions. *Annual Review of Energy and the Environment*, 26:167-200, 2001.

Lukachko S.P. and Waitz I.A., "Effects of Engine Aging on Aircraft NOx Emissions," *ASME 97-GT-386*. ASME/IGTI Turbo Expo, Orlando, United States, June 1997.

Oberkampf W.L., Helton J.C., Joslyn C.A., Wojtkiewicz S.F., and Ferson S., "Challenge Problems - Uncertainty in System Response Given Uncertain Parameters", Reliability Engineering and System Safety, Vol. 85, Issue 1, July 2004.

Malwitz, A., "Analysis of Unscheduled and Cancelled Flights," Volpe National Transportation Systems Center, October 2004.

Mantis G.C., "Quantification and Propagation of Disciplinary Uncertainty via Bayesian Statistics", PhD Thesis, Georgia Institute of Technology, August 2002.

Miller B., *Aircraft Emissions Reductions through Operational Improvements*, SM Thesis, Massachusetts Institute of Technology, June 2001.

Morgan M.G. and Henrion M., *Uncertainty: A Guide to Dealing with Uncertainty in Quantitative Risk and Policy Analysis*, Cambridge University Press, New York, 1990.

Long D., Lee D.A., Johnson J.P., Gaier E.M., and Kostiuk P.F., *Modeling Air Traffic Management Technologies with a Queuing Network Model of the National Airspace System*, NASA Contractor Report 208988, United States, 1998.

Padilla C.E., *Optimizing Jet Transport Efficiency: Performance, Operations, and Economics*, McGraw-Hill, New York, 1996.

Penner J.E., Lister, D.H., Griggs, D.J., Dokken, D.J. and McFarland, M. (eds.), *Aviation and the Global Atmosphere: A Special Report of the Intergovernmental Panel on Climate Change*. Cambridge Univ. Press, Cambridge, United Kingdom, 1999.

Personal communication with a major US carrier, Discussion on step climbs, 2003a.

Personal communication with a major US carrier, Discussion on derated take-off, 2003b.

Personal communication with a major industry partner, Cruise fuel burn comparison for 7 aircraft types, 2003c.

RCEP. *The Environmental Effects of Civil Aircraft in Flight*, Royal Commission on Environmental Pollution, Special Report. United Kingdom, 2002.

Rogers H.L., Lee D.S., Raper D.W., de Forster P.M., Wilson C.W. and Newton P.J., The Impacts of Aviation on the Atmosphere, QinetiQ report number QINETIQ/FST/CAT/TR021654, 2002.

SAE, *SAE AIR 1845*, Society of Automotive Engineers A-21 Committee, Warrandale, Pennsylvania, 1986.

Schafer A. and Victor D., "Global Passenger Travel: Implications for CO_2-Emissions," *Energy-The International Journal*. 24(8): 657-79. 1999.

Taylor J., *An Introduction to Error Analysis: The Study of Uncertainties in Physical Measurements*, 2nd ed. University Science Books, Sausalito, California, 1997.

USDOT, United States Department of Transportation. Bureau of Transportation Statistics. Form 41 Schedule P5.2 and T2. 1968-2002. Washington, DC, 2002.

Waitz I.A., Lukachko S.P., and Lee J.J., "Military Aviation and the Environment: Historical Trends and Comparison to Civil Aviation" AIAA *Journal of Aircraft*, Vol. 41 No. 6, November–December 2004 (Tentative). .

Webster M.D., *Analysis of Uncertainty in Large Models with Application to Climate Policy*, SM Thesis, Massachusetts Institute of Technology, 1996.

Yamartino R.J., Builtjes P., and Stern R., Status of the Current Level of Development and Understanding in the Field of Modeling Pollutant Dispersion at Airports, Freie Universität Berlin, Institut für Meteorologie, UFOPLAN-Ref. No. 203 41 253/01, Berlin, Germany, July 2004.

APPENDIX A-1 – SAGE Inventory of Commercial Jet & Turboprop Global Activity for Calendar Year 2000

Regions*		Distance (nm)	Fuel Burn (Tg)	CO (Tg)	HC (Tg)	NOx (Tg)	CO2 (Tg)	H2O (Tg)	SOx (Tg)
Africa to Africa	Ground	4.27E+06	5.38E-02	1.23E-03	3.46E-04	4.27E-04	1.70E-01	6.66E-02	4.30E-05
	Ground to 3000 ft	6.80E+06	1.07E-01	4.39E-04	1.01E-04	2.12E-03	3.38E-01	1.33E-01	8.60E-05
	3000 ft and Above	1.74E+08	1.54E+00	3.47E-03	6.53E-04	2.25E-02	4.86E+00	1.91E+00	1.23E-03
	Total	1.85E+08	1.70E+00	5.14E-03	1.10E-03	2.51E-02	5.37E+00	2.10E+00	1.36E-03
Africa to Other	Ground	6.08E+06	9.82E-02	2.30E-03	4.55E-04	1.87E-03	3.10E-01	1.22E-01	7.90E-05
	Ground to 3000 ft	1.03E+07	2.48E-01	9.34E-04	1.49E-04	6.67E-03	7.83E-01	3.07E-01	1.98E-04
	3000 ft and Above	4.79E+08	6.00E+00	1.25E-02	1.61E-03	1.00E-01	1.89E+01	7.42E+00	4.80E-03
	Total	4.96E+08	6.34E+00	1.58E-02	2.21E-03	1.09E-01	2.00E+01	7.85E+00	5.08E-03
Asia to Asia	Ground	1.84E+07	3.59E-01	7.73E-03	1.23E-03	2.07E-03	1.13E+00	4.44E-01	2.87E-04
	Ground to 3000 ft	2.92E+07	8.07E-01	2.76E-03	3.52E-04	1.95E-02	2.55E+00	9.98E-01	6.46E-04
	3000 ft and Above	7.19E+08	9.81E+00	1.61E-02	1.98E-03	1.74E-01	3.10E+01	1.21E+01	7.85E-03
	Total	7.67E+08	1.10E+01	2.66E-02	3.56E-03	1.95E-01	3.46E+01	1.36E+01	8.78E-03
Asia to Other	Ground	9.03E+06	1.79E-01	4.39E-03	8.46E-04	8.79E-04	5.66E-01	2.22E-01	1.44E-04
	Ground to 3000 ft	1.49E+07	4.95E-01	1.70E-03	2.57E-04	1.28E-02	1.56E+00	6.12E-01	3.96E-04
	3000 ft and Above	9.96E+08	1.59E+01	2.63E-02	3.32E-03	2.60E-01	5.01E+01	1.96E+01	1.27E-02
	Total	1.02E+09	1.66E+01	3.24E-02	4.42E-03	2.74E-01	5.22E+01	2.05E+01	1.32E-02
Australia & Oceania to Australia & Oceania	Ground	5.28E+06	4.57E-02	1.07E-03	3.58E-04	3.91E-04	1.44E-01	5.65E-02	3.70E-05
	Ground to 3000 ft	7.29E+06	1.01E-01	3.89E-04	7.40E-05	1.89E-03	3.17E-01	1.24E-01	8.00E-05
	3000 ft and Above	1.61E+08	1.09E+00	2.82E-03	4.40E-04	1.64E-02	3.45E+00	1.35E+00	8.75E-04
	Total	1.73E+08	1.24E+00	4.27E-03	8.71E-04	1.87E-02	3.91E+00	1.53E+00	9.92E-04
Australia & Oceania to Other	Ground	1.16E+07	1.71E-01	3.51E-03	6.34E-04	1.37E-03	5.41E-01	2.12E-01	1.37E-04
	Ground to 3000 ft	1.83E+07	3.84E-01	1.33E-03	2.07E-04	8.40E-03	1.21E+00	4.74E-01	3.07E-04
	3000 ft and Above	6.75E+08	7.85E+00	1.52E-02	2.28E-03	1.26E-01	2.48E+01	9.71E+00	6.28E-03
	Total	7.05E+08	8.41E+00	2.00E-02	3.12E-03	1.36E-01	2.65E+01	1.04E+01	6.73E-03
Eastern Europe to Eastern Europe	Ground	2.17E+06	3.41E-02	1.40E-03	4.23E-04	1.57E-04	1.08E-01	4.22E-02	2.70E-05
	Ground to 3000 ft	3.84E+06	7.48E-02	8.36E-04	1.74E-04	1.07E-03	2.36E-01	9.25E-02	6.00E-05
	3000 ft and Above	1.42E+08	1.46E+00	9.70E-03	1.02E-03	1.62E-02	4.59E+00	1.80E+00	1.16E-03
	Total	1.48E+08	1.56E+00	1.19E-02	1.62E-03	1.75E-02	4.93E+00	1.93E+00	1.25E-03
Eastern Europe to Other	Ground	5.03E+06	8.76E-02	2.42E-03	4.87E-04	8.52E-04	2.76E-01	1.08E-01	7.00E-05
	Ground to 3000 ft	8.40E+06	2.11E-01	1.05E-03	1.85E-04	4.99E-03	6.66E-01	2.61E-01	1.69E-04
	3000 ft and Above	4.01E+08	4.66E+00	1.27E-02	1.65E-03	7.14E-02	1.47E+01	5.76E+00	3.73E-03
	Total	4.14E+08	4.96E+00	1.62E-02	2.33E-03	7.72E-02	1.56E+01	6.13E+00	3.97E-03

* Regions were defined for SAGE analysis purposes and to some extent relate to the areas of influence for ICAO regional offices.

Regions		Distance (nm)	Fuel Burn (Tg)	CO (Tg)	HC (Tg)	NOx (Tg)	CO2 (Tg)	H2O (Tg)	SOx (Tg)
Middle East to Middle East	Ground	2.92E+06	5.50E-02	1.20E-03	2.32E-04	3.34E-04	1.74E-01	6.81E-02	4.40E-05
	Ground to 3000 ft	5.38E+06	1.30E-01	5.19E-04	1.00E-04	3.15E-03	4.09E-01	1.60E-01	1.04E-04
	3000 ft and Above	1.29E+08	1.48E+00	3.64E-03	5.50E-04	2.62E-02	4.67E+00	1.83E+00	1.19E-03
	Total	1.37E+08	1.67E+00	5.36E-03	8.83E-04	2.96E-02	5.25E+00	2.06E+00	1.33E-03
Middle East to Other	Ground	3.56E+06	7.00E-02	1.78E-03	3.91E-04	8.28E-04	2.21E-01	8.66E-02	5.60E-05
	Ground to 3000 ft	6.45E+06	1.84E-01	8.21E-04	1.69E-04	4.67E-03	5.79E-01	2.27E-01	1.47E-04
	3000 ft and Above	3.46E+08	4.24E+00	1.07E-02	1.48E-03	6.82E-02	1.34E+01	5.25E+00	3.39E-03
	Total	3.56E+08	4.50E+00	1.33E-02	2.04E-03	7.37E-02	1.42E+01	5.56E+00	3.60E-03
North America & Caribbean to North America & Caribbean	Ground	1.43E+08	1.85E+00	4.12E-02	7.59E-03	1.46E-02	5.85E+00	2.29E+00	1.48E-03
	Ground to 3000 ft	1.93E+08	3.32E+00	1.20E-02	1.88E-03	6.36E-02	1.05E+01	4.11E+00	2.66E-03
	3000 ft and Above	6.86E+09	5.19E+01	1.37E-01	1.96E-02	6.86E-01	1.64E+02	6.41E+01	4.15E-02
	Total	7.20E+09	5.70E+01	1.90E-01	2.91E-02	7.64E-01	1.80E+02	7.05E+01	4.56E-02
North America & Caribbean to Other	Ground	1.92E+07	3.37E-01	7.25E-03	1.36E-03	2.26E-03	1.06E+00	4.17E-01	2.69E-04
	Ground to 3000 ft	3.01E+07	8.11E-01	2.73E-03	4.23E-04	1.97E-02	2.56E+00	1.00E+00	6.48E-04
	3000 ft and Above	1.82E+09	2.53E+01	4.63E-02	6.21E-03	4.08E-01	7.98E+01	3.13E+01	2.02E-02
	Total	1.87E+09	2.64E+01	5.63E-02	7.99E-03	4.30E-01	8.34E+01	3.27E+01	2.12E-02
South America to South America	Ground	2.45E+06	3.10E-02	6.34E-04	1.14E-04	1.22E-04	9.77E-02	3.83E-02	2.50E-05
	Ground to 3000 ft	4.08E+06	5.77E-02	2.43E-04	3.60E-05	9.12E-04	1.82E-01	7.13E-02	4.60E-05
	3000 ft and Above	7.90E+07	5.73E-01	1.39E-03	2.16E-04	7.59E-03	1.81E+00	7.08E-01	4.58E-04
	Total	8.56E+07	6.61E-01	2.26E-03	3.66E-04	8.62E-03	2.09E+00	8.18E-01	5.29E-04
South America to Other	Ground	5.93E+06	8.56E-02	1.96E-03	3.72E-04	4.30E-04	2.70E-01	1.06E-01	6.90E-05
	Ground to 3000 ft	9.54E+06	1.84E-01	7.42E-04	1.22E-04	3.53E-03	5.81E-01	2.28E-01	1.47E-04
	3000 ft and Above	3.05E+08	3.33E+00	7.85E-03	1.10E-03	5.08E-02	1.05E+01	4.12E+00	2.66E-03
	Total	3.21E+08	3.60E+00	1.06E-02	1.59E-03	5.47E-02	1.14E+01	4.45E+00	2.88E-03
Western Europe & North Atlantic to Western Europe & North Atlantic	Ground	3.72E+07	4.77E-01	9.64E-03	1.18E-03	6.85E-03	1.51E+00	5.90E-01	3.82E-04
	Ground to 3000 ft	5.67E+07	8.72E-01	3.55E-03	4.06E-04	1.72E-02	2.75E+00	1.08E+00	6.98E-04
	3000 ft and Above	1.28E+09	1.10E+01	2.44E-02	2.80E-03	1.74E-01	3.48E+01	1.36E+01	8.82E-03
	Total	1.38E+09	1.24E+01	3.76E-02	4.39E-03	1.98E-01	3.90E+01	1.53E+01	9.90E-03
Western Europe & North Atlantic to Other	Ground	1.72E+07	2.89E-01	6.64E-03	1.18E-03	2.77E-03	9.11E-01	3.57E-01	2.31E-04
	Ground to 3000 ft	2.70E+07	6.98E-01	2.46E-03	3.95E-04	1.81E-02	2.20E+00	8.63E-01	5.58E-04
	3000 ft and Above	1.54E+09	2.06E+01	4.25E-02	5.75E-03	3.34E-01	6.51E+01	2.55E+01	1.65E-02
	Total	1.59E+09	2.16E+01	5.16E-02	7.33E-03	3.55E-01	6.82E+01	2.67E+01	1.73E-02

Calendar Year 2000		Distance (nm)	Fuel Burn (Tg)	CO (Tg)	HC (Tg)	NOx (Tg)	CO2 (Tg)	H2O (Tg)	SOx (Tg)
Global Totals	Ground	2.94E+08	4.23E+00	9.44E-02	1.72E-02	3.62E-02	1.33E+01	5.23E+00	3.38E-03
	Ground to 3000 ft	4.31E+08	8.68E+00	3.25E-02	5.03E-03	1.88E-01	2.74E+01	1.07E+01	6.95E-03
	3000 ft and Above	1.61E+10	1.67E+02	3.73E-01	5.07E-02	2.54E+00	5.26E+02	2.06E+02	1.33E-01
	Total	1.68E+10	1.80E+02	4.99E-01	7.29E-02	2.77E+00	5.67E+02	2.22E+02	1.44E-01

Note: All fuel burn and emissions units are in Tg where 1 Tg = 10^{12}g.

APPENDIX A-2 – SAGE Inventory of Commercial Jet & Turboprop Global Activity for Calendar Year 2001

Regions*		Distance (nm)	Fuel Burn (Tg)	CO (Tg)	HC (Tg)	NOx (Tg)	CO2 (Tg)	H2O (Tg)	SOx (Tg)
Africa to Africa	Ground	4.14E+06	5.05E-02	1.10E-03	2.98E-04	4.07E-04	1.59E-01	6.24E-02	4.00E-05
	Ground to 3000 ft	6.86E+06	1.03E-01	4.05E-04	8.40E-05	1.94E-03	3.24E-01	1.27E-01	8.20E-05
	3000 ft and Above	1.66E+08	1.36E+00	3.04E-03	5.99E-04	1.96E-02	4.29E+00	1.68E+00	1.09E-03
	Total	1.77E+08	1.51E+00	4.55E-03	9.81E-04	2.20E-02	4.78E+00	1.87E+00	1.21E-03
Africa to Other	Ground	5.55E+06	8.59E-02	1.94E-03	3.59E-04	1.73E-03	2.71E-01	1.06E-01	6.90E-05
	Ground to 3000 ft	9.51E+06	2.21E-01	8.12E-04	1.21E-04	5.92E-03	6.98E-01	2.74E-01	1.77E-04
	3000 ft and Above	4.19E+08	5.12E+00	1.06E-02	1.32E-03	8.57E-02	1.62E+01	6.33E+00	4.10E-03
	Total	4.35E+08	5.43E+00	1.34E-02	1.80E-03	9.33E-02	1.71E+01	6.71E+00	4.34E-03
Asia to Asia	Ground	1.59E+07	3.01E-01	6.61E-03	1.06E-03	1.78E-03	9.50E-01	3.73E-01	2.41E-04
	Ground to 3000 ft	2.71E+07	7.28E-01	2.48E-03	3.13E-04	1.77E-02	2.30E+00	9.01E-01	5.83E-04
	3000 ft and Above	6.43E+08	8.73E+00	1.44E-02	1.70E-03	1.57E-01	2.75E+01	1.08E+01	6.98E-03
	Total	6.86E+08	9.76E+00	2.35E-02	3.07E-03	1.76E-01	3.08E+01	1.21E+01	7.81E-03
Asia to Other	Ground	8.12E+06	1.60E-01	3.81E-03	7.02E-04	7.77E-04	5.05E-01	1.98E-01	1.28E-04
	Ground to 3000 ft	1.42E+07	4.65E-01	1.53E-03	2.20E-04	1.19E-02	1.47E+00	5.75E-01	3.72E-04
	3000 ft and Above	8.56E+08	1.35E+01	2.23E-02	2.89E-03	2.21E-01	4.25E+01	1.67E+01	1.08E-02
	Total	8.79E+08	1.41E+01	2.77E-02	3.82E-03	2.34E-01	4.45E+01	1.74E+01	1.13E-02
Australia & Oceania to Australia & Oceania	Ground	4.91E+06	4.44E-02	1.03E-03	3.19E-04	3.80E-04	1.40E-01	5.49E-02	3.60E-05
	Ground to 3000 ft	7.17E+06	1.03E-01	3.87E-04	6.90E-05	1.95E-03	3.25E-01	1.27E-01	8.20E-05
	3000 ft and Above	1.55E+08	1.08E+00	2.62E-03	4.04E-04	1.70E-02	3.41E+00	1.34E+00	8.65E-04
	Total	1.67E+08	1.23E+00	4.03E-03	7.93E-04	1.94E-02	3.88E+00	1.52E+00	9.83E-04
Australia & Oceania to Other	Ground	1.13E+07	1.66E-01	3.43E-03	5.76E-04	1.42E-03	5.25E-01	2.06E-01	1.33E-04
	Ground to 3000 ft	1.83E+07	3.80E-01	1.30E-03	1.93E-04	8.36E-03	1.20E+00	4.70E-01	3.04E-04
	3000 ft and Above	6.56E+08	7.51E+00	1.37E-02	1.98E-03	1.22E-01	2.37E+01	9.29E+00	6.01E-03
	Total	6.86E+08	8.05E+00	1.84E-02	2.75E-03	1.32E-01	2.54E+01	9.96E+00	6.44E-03
Eastern Europe to Eastern Europe	Ground	2.09E+06	2.89E-02	9.81E-04	3.34E-04	1.47E-04	9.12E-02	3.58E-02	2.30E-05
	Ground to 3000 ft	3.68E+06	6.17E-02	5.68E-04	1.30E-04	9.00E-04	1.95E-01	7.63E-02	4.90E-05
	3000 ft and Above	1.24E+08	1.25E+00	6.87E-03	7.71E-04	1.51E-02	3.94E+00	1.55E+00	1.00E-03
	Total	1.30E+08	1.34E+00	8.42E-03	1.24E-03	1.61E-02	4.23E+00	1.66E+00	1.07E-03
Eastern Europe to Other	Ground	4.73E+06	7.81E-02	2.02E-03	4.10E-04	7.48E-04	2.47E-01	9.67E-02	6.30E-05
	Ground to 3000 ft	8.19E+06	1.98E-01	8.62E-04	1.51E-04	4.74E-03	6.26E-01	2.45E-01	1.59E-04
	3000 ft and Above	3.65E+08	4.29E+00	1.03E-02	1.39E-03	6.74E-02	1.35E+01	5.30E+00	3.43E-03
	Total	3.78E+08	4.56E+00	1.32E-02	1.95E-03	7.29E-02	1.44E+01	5.65E+00	3.65E-03

* Regions were defined for SAGE analysis purposes and to some extent relate to the areas of influence for ICAO regional offices.

Regions		Distance (nm)	Fuel Burn (Tg)	CO (Tg)	HC (Tg)	NOx (Tg)	CO2 (Tg)	H2O (Tg)	SOx (Tg)
Middle East to Middle East	Ground	2.71E+06	5.12E-02	1.21E-03	1.89E-04	2.75E-04	1.62E-01	6.34E-02	4.10E-05
	Ground to 3000 ft	5.13E+06	1.26E-01	5.27E-04	7.90E-05	3.06E-03	3.99E-01	1.56E-01	1.01E-04
	3000 ft and Above	1.19E+08	1.40E+00	3.08E-03	3.88E-04	2.51E-02	4.42E+00	1.73E+00	1.12E-03
	Total	1.27E+08	1.58E+00	4.82E-03	6.55E-04	2.84E-02	4.98E+00	1.95E+00	1.26E-03
Middle East to Other	Ground	3.14E+06	5.98E-02	1.49E-03	3.33E-04	7.02E-04	1.89E-01	7.39E-02	4.80E-05
	Ground to 3000 ft	5.81E+06	1.66E-01	6.98E-04	1.48E-04	4.26E-03	5.22E-01	2.05E-01	1.32E-04
	3000 ft and Above	3.01E+08	3.74E+00	9.33E-03	1.31E-03	6.11E-02	1.18E+01	4.63E+00	2.99E-03
	Total	3.10E+08	3.97E+00	1.15E-02	1.79E-03	6.61E-02	1.25E+01	4.91E+00	3.17E-03
North America & Caribbean to North America & Caribbean	Ground	1.35E+08	1.68E+00	3.78E-02	6.32E-03	1.41E-02	5.31E+00	2.08E+00	1.35E-03
	Ground to 3000 ft	2.07E+08	3.26E+00	1.26E-02	1.77E-03	6.13E-02	1.03E+01	4.03E+00	2.61E-03
	3000 ft and Above	6.21E+09	4.65E+01	1.12E-01	1.55E-02	6.50E-01	1.47E+02	5.76E+01	3.72E-02
	Total	6.55E+09	5.15E+01	1.63E-01	2.36E-02	7.26E-01	1.62E+02	6.37E+01	4.12E-02
North America & Caribbean to Other	Ground	1.84E+07	3.14E-01	6.82E-03	1.26E-03	2.34E-03	9.89E-01	3.88E-01	2.51E-04
	Ground to 3000 ft	3.07E+07	7.85E-01	2.67E-03	3.99E-04	1.87E-02	2.48E+00	9.70E-01	6.28E-04
	3000 ft and Above	1.57E+09	2.15E+01	3.77E-02	4.89E-03	3.51E-01	6.79E+01	2.66E+01	1.72E-02
	Total	1.62E+09	2.26E+01	4.72E-02	6.55E-03	3.72E-01	7.13E+01	2.80E+01	1.81E-02
South America to South America	Ground	1.95E+06	2.60E-02	5.78E-04	9.10E-05	9.40E-05	8.19E-02	3.21E-02	2.10E-05
	Ground to 3000 ft	3.63E+06	5.32E-02	2.39E-04	3.40E-05	8.46E-04	1.68E-01	6.58E-02	4.30E-05
	3000 ft and Above	7.40E+07	5.39E-01	1.33E-03	1.99E-04	7.10E-03	1.70E+00	6.67E-01	4.31E-04
	Total	7.96E+07	6.18E-01	2.15E-03	3.24E-04	8.04E-03	1.95E+00	7.64E-01	4.94E-04
South America to Other	Ground	5.64E+06	7.99E-02	1.79E-03	3.17E-04	3.73E-04	2.52E-01	9.88E-02	6.40E-05
	Ground to 3000 ft	9.52E+06	1.81E-01	6.99E-04	1.10E-04	3.46E-03	5.70E-01	2.24E-01	1.45E-04
	3000 ft and Above	2.91E+08	3.10E+00	7.13E-03	9.63E-04	4.71E-02	9.79E+00	3.84E+00	2.48E-03
	Total	3.07E+08	3.36E+00	9.62E-03	1.39E-03	5.10E-02	1.06E+01	4.16E+00	2.69E-03
Western Europe & North Atlantic to Western Europe & North Atlantic	Ground	3.67E+07	4.45E-01	9.15E-03	1.13E-03	6.85E-03	1.41E+00	5.51E-01	3.56E-04
	Ground to 3000 ft	5.43E+07	7.89E-01	3.35E-03	3.76E-04	1.57E-02	2.49E+00	9.76E-01	6.31E-04
	3000 ft and Above	1.17E+09	1.02E+01	2.24E-02	2.56E-03	1.63E-01	3.20E+01	1.26E+01	8.13E-03
	Total	1.26E+09	1.14E+01	3.49E-02	4.07E-03	1.86E-01	3.59E+01	1.41E+01	9.11E-03
Western Europe & North Atlantic to Other	Ground	1.59E+07	2.48E-01	5.82E-03	1.07E-03	2.83E-03	7.81E-01	3.06E-01	1.98E-04
	Ground to 3000 ft	2.54E+07	6.12E-01	2.25E-03	3.64E-04	1.58E-02	1.93E+00	7.57E-01	4.90E-04
	3000 ft and Above	1.31E+09	1.74E+01	3.43E-02	4.61E-03	2.88E-01	5.50E+01	2.16E+01	1.40E-02
	Total	1.35E+09	1.83E+01	4.24E-02	6.05E-03	3.06E-01	5.77E+01	2.26E+01	1.46E-02

Calendar Year 2001		Distance (nm)	Fuel Burn (Tg)	CO (Tg)	HC (Tg)	NOx (Tg)	CO2 (Tg)	H2O (Tg)	SOx (Tg)
Global Totals	Ground	2.76E+08	3.82E+00	8.56E-02	1.48E-02	3.50E-02	1.21E+01	4.73E+00	3.06E-03
	Ground to 3000 ft	4.36E+08	8.23E+00	3.14E-02	4.56E-03	1.76E-01	2.60E+01	1.02E+01	6.59E-03
	3000 ft and Above	1.44E+10	1.47E+02	3.12E-01	4.15E-02	2.30E+00	4.65E+02	1.82E+02	1.18E-01
	Total	1.51E+10	1.59E+02	4.29E-01	6.08E-02	2.51E+00	5.03E+02	1.97E+02	1.27E-01

Note: All fuel burn and emissions units are in Tg where 1 Tg = 10^{12}g.

APPENDIX A-3 – SAGE Inventory of Commercial Jet & Turboprop Global Activity for Calendar Year 2002

Regions*		Distance (nm)	Fuel Burn (Tg)	CO (Tg)	HC (Tg)	NOx (Tg)	CO2 (Tg)	H2O (Tg)	SOx (Tg)
Africa to Africa	Ground	4.35E+06	5.54E-02	1.11E-03	2.70E-04	3.17E-04	1.75E-01	6.86E-02	4.40E-05
	Ground to 3000 ft	6.90E+06	1.09E-01	4.06E-04	7.50E-05	2.06E-03	3.44E-01	1.35E-01	8.70E-05
	3000 ft and Above	1.71E+08	1.47E+00	3.12E-03	5.77E-04	2.16E-02	4.64E+00	1.82E+00	1.18E-03
	Total	1.82E+08	1.63E+00	4.64E-03	9.23E-04	2.40E-02	5.16E+00	2.02E+00	1.31E-03
Africa to Other	Ground	5.68E+06	9.14E-02	2.04E-03	3.77E-04	1.59E-03	2.88E-01	1.13E-01	7.30E-05
	Ground to 3000 ft	9.24E+06	2.28E-01	8.14E-04	1.31E-04	6.36E-03	7.20E-01	2.82E-01	1.82E-04
	3000 ft and Above	4.28E+08	5.38E+00	1.09E-02	1.44E-03	9.11E-02	1.70E+01	6.66E+00	4.31E-03
	Total	4.43E+08	5.70E+00	1.38E-02	1.94E-03	9.91E-02	1.80E+01	7.06E+00	4.56E-03
Asia to Asia	Ground	1.86E+07	3.48E-01	7.30E-03	1.06E-03	1.98E-03	1.10E+00	4.30E-01	2.78E-04
	Ground to 3000 ft	3.00E+07	8.22E-01	2.52E-03	2.86E-04	2.00E-02	2.59E+00	1.02E+00	6.57E-04
	3000 ft and Above	7.34E+08	9.55E+00	1.57E-02	1.77E-03	1.69E-01	3.01E+01	1.18E+01	7.64E-03
	Total	7.83E+08	1.07E+01	2.55E-02	3.12E-03	1.91E-01	3.38E+01	1.33E+01	8.58E-03
Asia to Other	Ground	9.56E+06	1.92E-01	4.47E-03	7.62E-04	9.53E-04	6.06E-01	2.38E-01	1.54E-04
	Ground to 3000 ft	1.57E+07	5.36E-01	1.69E-03	2.32E-04	1.45E-02	1.69E+00	6.63E-01	4.28E-04
	3000 ft and Above	9.47E+08	1.45E+01	2.31E-02	2.94E-03	2.45E-01	4.58E+01	1.80E+01	1.16E-02
	Total	9.73E+08	1.52E+01	2.93E-02	3.93E-03	2.60E-01	4.81E+01	1.89E+01	1.22E-02
Australia & Oceania to Australia & Oceania	Ground	4.72E+06	4.16E-02	9.34E-04	2.63E-04	3.14E-04	1.31E-01	5.15E-02	3.30E-05
	Ground to 3000 ft	6.46E+06	9.19E-02	3.30E-04	5.10E-05	1.67E-03	2.90E-01	1.14E-01	7.40E-05
	3000 ft and Above	1.28E+08	9.17E-01	2.19E-03	3.09E-04	1.45E-02	2.89E+00	1.13E+00	7.34E-04
	Total	1.39E+08	1.05E+00	3.46E-03	6.22E-04	1.65E-02	3.32E+00	1.30E+00	8.41E-04
Australia & Oceania to Other	Ground	1.09E+07	1.61E-01	3.18E-03	4.70E-04	1.52E-03	5.07E-01	1.99E-01	1.28E-04
	Ground to 3000 ft	1.70E+07	3.57E-01	1.15E-03	1.58E-04	8.19E-03	1.12E+00	4.41E-01	2.85E-04
	3000 ft and Above	6.16E+08	7.25E+00	1.25E-02	1.70E-03	1.22E-01	2.29E+01	8.97E+00	5.80E-03
	Total	6.44E+08	7.77E+00	1.68E-02	2.33E-03	1.32E-01	2.45E+01	9.61E+00	6.21E-03
Eastern Europe to Eastern Europe	Ground	2.52E+06	3.75E-02	1.55E-03	4.88E-04	1.79E-04	1.18E-01	4.64E-02	3.00E-05
	Ground to 3000 ft	4.26E+06	7.84E-02	8.99E-04	1.94E-04	1.14E-03	2.47E-01	9.69E-02	6.30E-05
	3000 ft and Above	1.35E+08	1.37E+00	9.39E-03	1.02E-03	1.55E-02	4.32E+00	1.69E+00	1.10E-03
	Total	1.42E+08	1.48E+00	1.18E-02	1.70E-03	1.68E-02	4.68E+00	1.84E+00	1.19E-03
Eastern Europe to Other	Ground	5.26E+06	8.74E-02	2.42E-03	4.67E-04	8.29E-04	2.76E-01	1.08E-01	7.00E-05
	Ground to 3000 ft	8.64E+06	2.15E-01	1.04E-03	1.73E-04	5.19E-03	6.77E-01	2.65E-01	1.72E-04
	3000 ft and Above	3.80E+08	4.56E+00	1.24E-02	1.55E-03	7.11E-02	1.44E+01	5.64E+00	3.65E-03
	Total	3.94E+08	4.86E+00	1.59E-02	2.19E-03	7.71E-02	1.53E+01	6.01E+00	3.89E-03

* Regions were defined for SAGE analysis purposes and to some extent relate to the areas of influence for ICAO regional offices.

Regions		Distance (nm)	Fuel Burn (Tg)	CO (Tg)	HC (Tg)	NOx (Tg)	CO2 (Tg)	H2O (Tg)	SOx (Tg)
Middle East to Middle East	Ground	2.81E+06	5.33E-02	1.16E-03	1.81E-04	2.73E-04	1.68E-01	6.59E-02	4.30E-05
	Ground to 3000 ft	5.12E+06	1.27E-01	5.10E-04	8.10E-05	3.13E-03	4.02E-01	1.58E-01	1.02E-04
	3000 ft and Above	1.08E+08	1.31E+00	3.04E-03	4.08E-04	2.40E-02	4.14E+00	1.62E+00	1.05E-03
	Total	1.16E+08	1.49E+00	4.71E-03	6.70E-04	2.74E-02	4.71E+00	1.85E+00	1.19E-03
Middle East to Other	Ground	3.34E+06	6.43E-02	1.65E-03	3.56E-04	4.94E-04	2.03E-01	7.96E-02	5.10E-05
	Ground to 3000 ft	5.76E+06	1.68E-01	7.54E-04	1.59E-04	4.29E-03	5.30E-01	2.08E-01	1.34E-04
	3000 ft and Above	3.01E+08	3.74E+00	9.70E-03	1.38E-03	6.12E-02	1.18E+01	4.63E+00	3.00E-03
	Total	3.10E+08	3.98E+00	1.21E-02	1.90E-03	6.60E-02	1.25E+01	4.92E+00	3.18E-03
North America & Caribbean to North America & Caribbean	Ground	1.30E+08	1.54E+00	3.46E-02	5.11E-03	1.49E-02	4.87E+00	1.91E+00	1.24E-03
	Ground to 3000 ft	1.79E+08	2.88E+00	9.99E-03	1.28E-03	5.94E-02	9.10E+00	3.57E+00	2.31E-03
	3000 ft and Above	6.24E+09	4.52E+01	1.05E-01	1.31E-02	6.80E-01	1.43E+02	5.59E+01	3.61E-02
	Total	6.55E+09	4.96E+01	1.49E-01	1.95E-02	7.54E-01	1.57E+02	6.14E+01	3.97E-02
North America & Caribbean to Other	Ground	2.00E+07	3.46E-01	7.35E-03	1.24E-03	2.39E-03	1.09E+00	4.28E-01	2.77E-04
	Ground to 3000 ft	3.24E+07	8.48E-01	2.82E-03	4.00E-04	2.09E-02	2.68E+00	1.05E+00	6.79E-04
	3000 ft and Above	1.57E+09	2.15E+01	3.79E-02	4.89E-03	3.59E-01	6.77E+01	2.65E+01	1.72E-02
	Total	1.63E+09	2.27E+01	4.80E-02	6.54E-03	3.83E-01	7.15E+01	2.80E+01	1.81E-02
South America to South America	Ground	2.31E+06	3.00E-02	6.29E-04	1.00E-04	1.18E-04	9.45E-02	3.71E-02	2.40E-05
	Ground to 3000 ft	4.11E+06	6.11E-02	2.39E-04	3.70E-05	1.10E-03	1.93E-01	7.56E-02	4.90E-05
	3000 ft and Above	8.01E+07	5.99E-01	1.42E-03	2.24E-04	8.56E-03	1.89E+00	7.40E-01	4.79E-04
	Total	8.66E+07	6.90E-01	2.29E-03	3.61E-04	9.78E-03	2.18E+00	8.53E-01	5.52E-04
South America to Other	Ground	5.89E+06	8.32E-02	1.80E-03	3.13E-04	3.96E-04	2.63E-01	1.03E-01	6.70E-05
	Ground to 3000 ft	9.00E+06	1.78E-01	6.69E-04	1.09E-04	3.60E-03	5.60E-01	2.20E-01	1.42E-04
	3000 ft and Above	2.88E+08	3.10E+00	7.09E-03	9.57E-04	4.84E-02	9.78E+00	3.83E+00	2.48E-03
	Total	3.03E+08	3.36E+00	9.55E-03	1.38E-03	5.24E-02	1.06E+01	4.16E+00	2.69E-03
Western Europe & North Atlantic to Western Europe & North Atlantic	Ground	3.62E+07	4.29E-01	8.60E-03	1.06E-03	6.31E-03	1.35E+00	5.31E-01	3.44E-04
	Ground to 3000 ft	5.36E+07	7.66E-01	3.13E-03	3.61E-04	1.51E-02	2.42E+00	9.48E-01	6.13E-04
	3000 ft and Above	1.13E+09	9.24E+00	2.09E-02	2.47E-03	1.48E-01	2.92E+01	1.14E+01	7.39E-03
	Total	1.22E+09	1.04E+01	3.26E-02	3.89E-03	1.69E-01	3.29E+01	1.29E+01	8.35E-03
Western Europe & North Atlantic to Other	Ground	1.61E+07	2.54E-01	5.84E-03	1.04E-03	2.88E-03	8.02E-01	3.14E-01	2.03E-04
	Ground to 3000 ft	2.56E+07	6.30E-01	2.23E-03	3.59E-04	1.69E-02	1.99E+00	7.80E-01	5.04E-04
	3000 ft and Above	1.36E+09	1.82E+01	3.60E-02	4.81E-03	3.02E-01	5.75E+01	2.26E+01	1.46E-02
	Total	1.40E+09	1.91E+01	4.41E-02	6.21E-03	3.22E-01	6.03E+01	2.36E+01	1.53E-02

Calendar Year 2002		Distance (nm)	Fuel Burn (Tg)	CO (Tg)	HC (Tg)	NOx (Tg)	CO2 (Tg)	H2O (Tg)	SOx (Tg)
Global Totals	Ground	2.78E+08	3.82E+00	8.46E-02	1.36E-02	3.54E-02	1.20E+01	4.72E+00	3.06E-03
	Ground to 3000 ft	4.12E+08	8.10E+00	2.92E-02	4.08E-03	1.84E-01	2.55E+01	1.00E+01	6.48E-03
	3000 ft and Above	1.46E+10	1.48E+02	3.10E-01	3.96E-02	2.38E+00	4.67E+02	1.83E+02	1.18E-01
	Total	1.53E+10	1.60E+02	4.24E-01	5.72E-02	2.60E+00	5.04E+02	1.98E+02	1.28E-01

Note: All fuel burn and emissions units are in Tg where 1 Tg = 10^{12}g.